2013-07-18

Critical and Steady-Flow Analysis of a High Performance Automotive Exhaust Port

Jeremy Decker
University of Miami, jeremyddecker@gmail.com

UNIVERSITY OF MIAMI

CRITICAL AND STEADY-FLOW ANALYSIS OF A HIGH PERFORMANCE AUTOMOTIVE EXHAUST PORT

By

Jeremy Dallas Decker

A DISSERTATION

Submitted to the Faculty
of the University of Miami
in partial fulfillment of the requirements for
the degree of Doctor of Philosophy

Coral Gables, Florida

August 2013

UNIVERSITY OF MIAMI

A dissertation submitted in partial fulfillment of
the requirements for the degree of
Doctor of Philosophy

CRITICAL AND STEADY-FLOW ANALYSIS OF A HIGH PERFORMANCE AUTOMOTIVE EXHAUST PORT

Jeremy Dallas Decker

Approved:

Michael R. Swain, Ph.D. Associate Professor of Mechanical & Aerospace Engineering	M. Brian Blake, Ph.D. Dean of the Graduate School
Singiresu S. Rao, Ph.D. Professor of Mechanical & Aerospace Engineering	Jizhou Song, Ph.D. Assistant Professor of Mechanical & Aerospace Engineering
Matthew N. Swain, Ph.D. President Analytical Technologies Incorporated Miami, Florida	

DECKER, JEREMY DALLAS (Ph.D, Mechanical Engineering)

Critical and Steady-Flow Analysis of a High Performance Automotive Exhaust Port (August 2013)

Abstract of a dissertation at the University of Miami.

Dissertation supervised by Professor Michael Swain.
No. of pages in text (126)

During the early phase of the exhaust process of an internal combustion engine, gas exits under high pressure as critical flow. Conversely, exhaust ports are often physically tested under steady, low pressure airflow and inconsistences frequently occur between test results and engine performance. Modifications are often made using traditional intake port improvement techniques that may have a negative impact on high pressure, compressible flow within the port. This research focused on the question of whether downstream exhaust port geometry can negatively affect port efficiency during low valve lift, critical flow. Typical engine analysis assumes critical flow through the entire valve curtain area with no downstream effects on flow rates or coefficients.

A chamber was constructed to use compressed gases to test the critical flow performance of two Chevy SB2.2 cylinder head ports. A Weld Tech ported cylinder head was chosen based on discussions with port designers indicating the final design was modified to increase port volume and diameter which increased engine performance, but resulted in reduced flow under low pressure, steady airflow. One port was modified to decrease port volume and increase steady flow coefficients to mimic these conditions as described by designers. Then, compressed carbon dioxide and nitrogen were used as testing fluids to investigate the low lift critical flow performance of the original and

modified ports. These results were compared to those obtained from steady flow, low pressure testing using air. The use of the products of lean hydrogen combustion was also investigated, but ultimately deemed infeasible with the envisioned testing apparatus.

Through modifications the port volume was reduced 4.7% and steady, low pressure flow coefficients were improved by 7.2% at 0.050" valve lift and 6.1% at 0.100" valve lift compared to the original port. These improvements were mostly gained through pressure recovery. Using the compressed gas chamber, the measured effective critical flow coefficients averaged over 20 to 90 lb/in^2 were decreased 2.8% and 3.2% at 0.050" lift using nitrogen and carbon dioxide, respectively. At 0.100" lift, the effective critical flow coefficients averaged over 20 to 70 lb/in^2 were decreased 0.1% and 0.14% using nitrogen and carbon dioxide, respectively. Critical flow coefficient results indicated a dependence on upstream pressure and downstream port geometry, which could contribute to the inconsistencies in steady flow testing and engine performance. Engine Analyzer software was also used to demonstrate the benefits of increased exhaust flow path diameter on predicted power at high engine speeds and the beneficial translation to racing engines. These improvements were the result of reduced back pressure, increased scavenging, and decreased pumping losses.

Acknowledgements

I would like to thank my advisor, Dr. Michael Swain, without whom this research could not have been accomplished. I would also like to show my appreciation to my committee members for their support and helpful suggestions.

I would like to thank Dr. Matthew Swain for his support and guidance in project construction and data collection and analysis.

I would like to thank Angel Morciego and the college of engineering's machine shop support staff for assistance during project construction.

I would like to thank my parents and family for their love, support, and patience that has allowed me to achieve my goals in life.

Lastly, and most importantly, I would like to thank my wife, Renee, and faithful companions, Bo, Lucy, Rocco, Bailey, Hou, and Gator, for being there for me during the good times and bad times. Thank you.

TABLE OF CONTENTS

LIST OF FIGURES

LIST OF TABLES

NOMENCLATURE

This section presents and defines the symbols, acronyms, and variables used in the text, tables, and figures of this report. Some symbols used exclusively in the appendices are defined within and are not addressed here. Definitions are presented alphabetically.

Symbol/Acronym	Definition
a	Speed of sound
A	Area
a_1, a_2, a_3, a_4	Polynomial Fit Coefficients
Ar	Argon
BTU	British Thermal Unit
C	Orifice Flow Coefficient
C_{ef}	Effective Flow Coefficient
CFD	Computational Fluid Dynamics
CFM	Cubic Feet Per Minute (Flow Rate)
Cl_2	Diatomic Chlorine
cm	Centiimeter
CNC	Computer Numeric Controlled (Machining)
CO_2	Carbon Dioxide
c_p	Constant pressure specific heat
C_{th}	Thermal Mass
c_v	Constant volume specific heat
$\overline{D}_i$	Mean Absolute Deviation

E	Stored Energy
ºF	Degree Fahrenheit
f_{sc}	Scaling Factor
ft	Foot
f_{vm}	Voltage Multiplier
GM	General Motors
H_2	Diatomic Hydrogen
H_2O	Water (vapor)
He	Helium
Hg	Mercury
Hr.	Hour
IC	Internal Combustion
in	Inch
in.	Inch
L	Coil Inductance
lb	Pound-force
LB_{Fuel}	Mass of fuel for combustion
lbm	Pound-mass
lbmole	Pound-mole
LED	Light Emitting Diode
LHV	Lower heating value
m	Meter
$\dot{m}$	Mass flow rate

Ma	Mach number of moving fluid
mH	Millihenry
min	Minute
mm	Millimeter
MRC	Molar Rate of Combustion
MW	Molecular weight
n	Number of Data Points
N_2	Diatomic Nitrogen
N_2O	Nitrous Oxide
NMOS	Metal–Oxide–Semiconductor Field-Effect Transistor
n_p	Number of moles of products
NPT	National Pipe Thread
n_r	Number of moles of reactants
O_2	Diatomic Oxygen
P	Pressure of gas mixture
p_c	Cylinder pressure
p_e	Exhaust manifold pressure
P_f	Final pressure due to combustion
$PHPBE$	Pressure of the high pressure gases before expansion
$PLPBE$	Pressure of the low pressure gases before expansion
PVC	Polyvinyl Chloride
Q	Energy addition due to combustion
Q_f	Flow Rate

R_c	Coil Resistance
R	Gas constant of fluid
ºR	Degree Rankine
R_u	Universal gas constant
s	Second
T	Temperature of gas mixture
T_0	Initial gas temperature before combustion
T_c	Exhaust gas temperature
T_f	Final temperature due to combustion
TIG	Tungsten Inert Gas Welding
v	Fluid Velocity
V_{dc}	Voltage
V	Volume
$VHPAE$	Volume of the high pressure gases after expansion
$VHPBE$	Volume of the high pressure gases before expansion
$VLPAE$	Volume of the low pressure gases after expansion
$VLPBE$	Volume of the low pressure gases before expansion
VR	Volume Ratio, % volume in air
V_{Total}	Total volume of gases in mixture
x_i	Maximum Pressure of Ignition Test
$\bar{x}$	Mean Maximum Pressure
γ	Ratio of specific heats
Δp	Pressure Difference

Δt	Change in time
ΔT	Change in temperature due to combustion
ρ	Density
φ	Equivalence Ratio
Ω	Ohm

CHAPTER 1 - INTRODUCTION

The breathing capabilities of an internal combustion (IC) engine directly affect its ability to produce power. Engineers and designers will typically invest much of their resources to improve the efficiency of the intake and exhaust ports. Despite the many advances in Computational Fluid Dynamics (CFD), computer modeling has not been able to adequately describe these flows. The complexities associated with the geometry, compressibility, and turbulence have pushed inaccuracies outside the acceptable range. Designers of high performance ports are often trying to achieve improvements as little as 0.5-2% while errors using CFD often exceed 5-10%. Therefore, CFD has been utilized as a tool to gain insight into the general flow characteristics of the intake and exhaust systems, but is not seen as a critical design tool.

With the shortcomings of current CFD modeling capabilities, experimentation using physical models is essential to the development of effective high performance port designs. This is traditionally accomplished using a steady flow rig or flow bench. A known pressure drop (normally 28" H_2O or 1.01 lb/in^2) is placed across the valve opening and the resulting flow rates are measured for various valve lift values throughout the operating range. Experienced designers can examine measurements of flow rate vs. valve lift for the intake and quickly approximate the power capabilities of the cylinder head. Flow and lift values can also be used to calculate flow coefficients that give an indication of the efficiency of the valve/port combination and can be used for computer simulations involving cylinder filling/exhausting. These testing conditions are quite different than the intermittent, pulsating flow of an IC engine; however extensive

investigations have concluded that steady flow coefficients are effective when judging the air flow capabilities of intake valves in dynamic operating environments [7 & 20].

The steady, low pressure airflow testing described for intake valves often fails to adequately predict the performance of exhaust valves/ports. Inconsistences frequently occur where enhanced flow bench performance leads to decreased engine performance. This is a result of the considerably different exhaust port flow environment, which includes higher pressures, compressible flow, and products of combustion. Early gas exiting occurs under high pressure as critical, or choked, flow then transitions to sub-critical flow under lower pressure ratios. Normal practices are to ensure the exhaust port flow capabilities are at a minimum of 60-80% of the intake. This however does not ensure the most efficient geometry and can lead to larger than required valves/ports or a restrictive exhaust. Excessively large diameter exhaust valves leave less room in the cylinder head for the intake valves, while a restriction can significantly lower the capabilities of the engine regardless of intake flow improvements. Other general findings include maintaining a minimum area throughout the port or increasing exhaust port volume can often increase engine performance. It would be desirable to have improved methods of analysis specifically designed for exhaust ports during critical flow to understand these findings and produce more efficient port geometry. This would be of particular interest to high performance engine designers within the motorsports industry.

CHAPTER 2 - PROPOSED RESEARCH

The proposed research focuses on the question of whether downstream exhaust port geometry can affect port efficiency during low valve lift, critical flow. Traditional analysis assumes theoretical choked flow through the entire valve curtain area with no downstream geometry effects on flow rates or coefficients. With port geometry developed using low pressure, steady flow air rigs and intake port improvement techniques, pressure recovery past the valve could lead to reduced flow around portions of the valve curtain area.

Attempts will be made using two different methods to test port/valve efficiency during critical flow and the results of these efforts will be presented and compared. The success of a particular technique will be judged on its ability to decipher between a port that appears to have less flow capabilities on a steady flow rig, but actually performs better once placed on an engine. Critical flow and steady flow rigs will be designed and built for this and future studies.

The first proposed method involves combusting a fuel/air mixture within a chamber, then exhausting the mixture through a physical model of the exhaust port. In order to accomplish this task, the ignition properties of the chosen fuel will have to be researched and a study will be conducted in order to establish consistent ignition and repeatable pressure rises. This knowledge will then be used to establish an adequate fuel/air mixture to obtain the desired pressures and fluid properties. The second proposed method will use a pressurized gas or gas mixture possessing desirable properties to simulate the exhaust flow. Any flow results obtained from these methods will be compared to results from a steady flow, low pressure testing rig.

CHAPTER 3 - THEORY

3.1 General Flow Characteristics of an IC Engine

The primary function of an IC engine's intake and exhaust systems are to supply fresh air and fuel mixtures to the combustion chamber and to then exhaust combustion gases back into the atmosphere. Pulsating flow, introduction of fuel, and variations in pressure, temperature, and composition contribute to the complex behavior of the system. The basic components of the intake system may include a filter, carburetor/fuel injection system, intake manifold, and the intake side of the cylinder head which houses the intake port and valves. Typically, with the exception of forced induction, atmospheric air is pulled through the valve and into the chamber with each intake stroke of the piston. Pressure waves oscillate through the manifold and their interactions can be optimized to increase performance. The pressure within an intake system of a naturally aspirated engine typically does not deviate significantly from atmospheric pressure.

A representative exhaust system is composed of exhaust tubing, a header/manifold, silencer, emissions equipment, and the exhaust port and valve. Its operation is similar to the intake's. The piston ascends pushing combustion gases through the exhaust valve and into the manifold. Flow interactions between each cylinder and the exhaust exit can again be optimized to increase the system's overall performance. However, the flow conditions are considerably different than the intake's. Since its induction, the intake charge has been transformed into hot products of combustion with significantly different fluid properties. Exhaust valves typically open under high cylinder pressures causing gases to quickly exit through the valve and subsequent rapid drop in pressure. This is referred to as "blowdown". When the cylinder

to manifold pressure difference is large enough, the flow will become critical, or choked, and must be considered compressible. For cylinder pressures great enough to cause critical flow, any further decreases in the downstream pressure theoretically have no effect on the mass flow rate. Typically, the flow area used for analysis during blowdown is considered as the entire curtain area.

3.2 Compressible Flow Considerations

Once a fluid begins to travel at speeds comparable to its speed of sound, density variations can become significant. These variations are mainly due to changes in temperature and pressure and typically, a fluid is treated as "compressible" once the fluid's speed results in a Mach number, *Ma*, greater than 0.3:

$$Ma = \frac{v}{a} \tag{3.1}$$

where v is the fluid velocity and a is the fluid's speed of sound. Mach number can be considered as the ratio of inertial forces to elastic forces within a flow. The consideration of density variations will add complexities to the system and will alter the governing equations. Different fluid properties emerge and begin to more significantly dictate the fluid's behavior. One such property is the specific heat ratio, γ:

$$\gamma = \frac{c_p}{c_v} \tag{3.2}$$

where c_p is the constant pressure specific heat and c_v is the constant volume specific heat. The specific heat ratio of a fluid is primarily a function of temperature and gradually decreases with an increase in temperature. When large variations in temperature or pressure are present in a system, γ cannot be considered a constant.

The flow through an exhaust valve can become critical or choked when the ratio of cylinder pressure to exhaust manifold pressure falls below a value dependent upon the specific heat ratio:

$$\frac{p_e}{p_c} \leq \left(\frac{2}{\gamma+1}\right)^{\frac{\gamma}{\gamma-1}} \tag{3.3}$$

where p_e and p_c are the exhaust manifold and cylinder pressure respectively. When the flow becomes choked, this is referred to as the critical pressure ratio and for exhaust gas ($\gamma \approx 1.28$) this occurs at a ratio of approximately 0.549 as opposed to 0.528 for air ($\gamma \approx 1.40$). In theory, once the critical pressure ratio is reached further reductions in downstream pressure have no effect on the upstream flow, and mass flow is at its maximum. The dependence on γ can also be seen in the equation for mass flow rate per area:

$$\frac{\dot{m}}{A} = \frac{P_c}{\sqrt{RT_c}}\sqrt{\gamma}\left(\frac{2}{\gamma+1}\right)^{\left(\frac{\gamma+1}{2(\gamma-1)}\right)} \tag{3.4}$$

where $\dot{m}$ is the mass flow rate, A is the curtain area of the valve opening, R is the gas constant of the fluid, and T_c is the exhaust gas temperature. Pressure within the throat, or in this case the valve-to-valve seat opening, will remain at the critical value and downstream pressures will be achieved quickly upon exit through lateral expansion of the stream. It's important to note that these equations are the result of several simplifications, including the assumptions of one-dimensional flow of an isentropic, adiabatic, perfect gas, but can give insight into a flow's behavior and dependent properties [15, 23, 1, & 10]. With the high exhaust to cylinder pressure ratio present during the opening of the exhaust valve, the effects of compressible flow should not be

ignored. The testing of exhaust ports without addressing this could lead to substantial errors.

The simplistic concept of choked flow presented through Equations 3.3 and 3.4 has also been challenged for certain geometries. Ideally, once the critical pressure ratio has been met for a given upstream pressure a continued drop in downstream pressure has no effect on mass flow rate. However, several experimental studies have been completed and document changes in flow rate beyond the critical pressure [2, 12, 21, & 5]. In referenced study, Cunningham noted that for well-formed convergent nozzles the theoretical critical pressure ratio and experimental maximum flow ratio were nearly identical. Square edged orifices tested did not exhibit a maximum flow ratio and the flow rate continued to increase for pressure ratios below critical [2]. Similar observations have been made and attempts to explain this behavior have varied. The bulk of the explanations rely upon the movement and size of the vena contracta, the minimum flow area downstream of flow orifice (Figure 3.1). As pressure continues to drop below the critical pressure the vena contracta has been theorized to move towards the restriction and possibly increase in area. Therefore, the maximum mass flow rate cannot be assumed to be constant at pressure ratios below the critical pressure for all geometries and may depend on upstream and downstream geometry that effect the location and size of the minimum flow area. Simply assuming the valve-to-valve seat curtain area as the minimum flow area may not be accurate for complex port geometry.

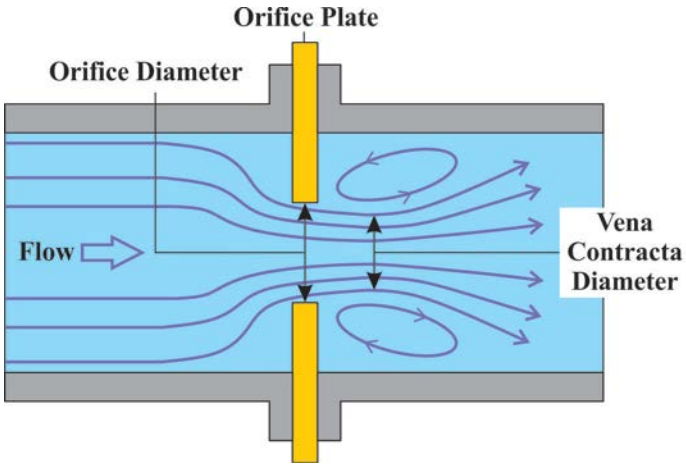

Figure 3.1 Flow through typical square-edged orifice.

Another source of discrepancies when using a steady flow, low pressure air rig originate from port improvement techniques used for intake geometries, which do not translate to improvements during blowdown. Localized pressure rises near the valve and valve seat during the high flow rates of blowdown may produce variations in the pressure ratio around portions of the circumference of the valve seat impeding flow. In fact, the techniques used to obtain better low lift flow capabilities for the intake port include efforts to increase these pressure rises near valve seat within the cylinder in order to have some pressure recovery. This technique can be successful for improving the intake port performance, but could reduce flow rates during blowdown and may explain occurrences when an exhaust port performs better with the addition of a larger bowl or maintaining a minimum port diameter despite suffering losses on a traditional flow bench.

Additional errors may result from compressible flow's dependence on the specific heat ratio when there are significant differences between the exhaust gases and test fluid. Possible improvements to experimental methods include changes in test fluid with a focus on specific heat ratios. Other dissimilarities within the fluid properties, such as viscosity could be addressed. However, estimation, prediction, and manipulation of such

properties would be more difficult. A complicated, expensive process to modify other fluid property would be far less desirable for a motorsports application and would not offer a feasible cost-effective alternative to current testing methods.

3.3 Current Testing Methods for Intake and Exhaust Ports

As mentioned, the most commonly used techniques for testing intake and exhaust ports involve steady flow air rigs, also known as flow benches. The refinement of port designs typically involve an initial evaluation of the port model, followed by a series of minor modifications. Material can be added or removed in an attempt to improve the flow characteristics. Each modification is followed by a reevaluation of the flow. The measured effect of the flow is noted and will inform further modifications. The task is long and tedious, but the reward is gains in air flow capacity, port efficiency, and power and/or torque [10]. In a typical flow bench setup (Figure 3.2) an air pump is used to create a pressure drop across the valve and port. Air flows through the test piece and into the plenum where the pressure difference is measured using a manometer. The most commonly used pressure difference is 28" H_2O (1.01 lb/in^2), but other values have been utilized. A radiused inlet is typically placed on the port entrance to provide smooth airflow into the test piece. It is often molded from clay, but for more consistent testing it can be machined from Plexiglas or polycarbonate to match the port entrance.
From the plenum, air then enters a pipe section which includes an orifice plate used to measure the flow rate. Beyond this measurement device, the flow is controlled by a system of valves. Usually a larger valve is used to make large scale changes to the pressure drop and in conjunction, a smaller valve is used for fine tuning.

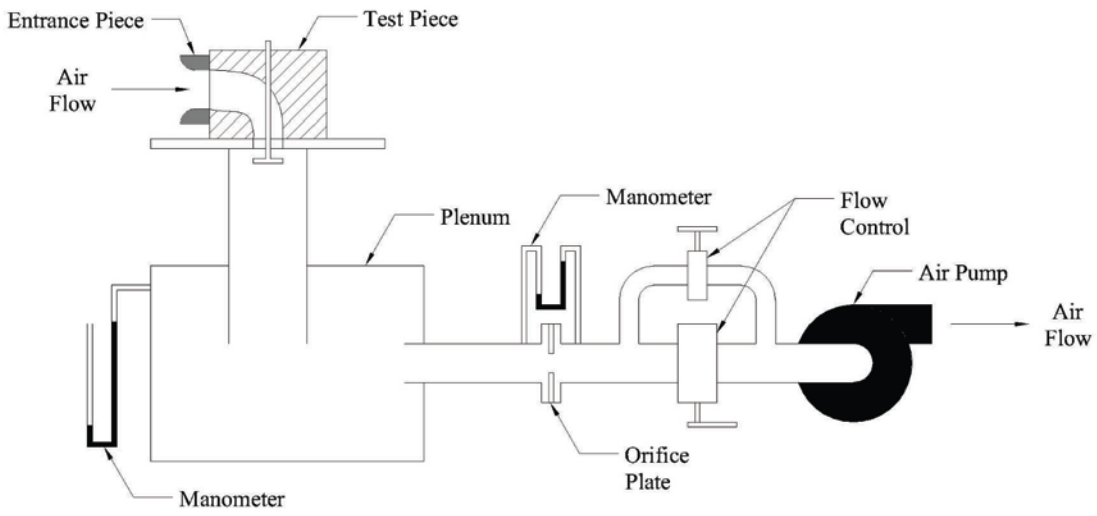

Figure 3.2 Typical Flow Bench Arrangement.

In practice, the air pump is turned on, the large valve is set, and the smaller valve is adjusted until the target pressure drop is maintained within the plenum. The pressure drop across the orifice plate is measured and used to calculate the flow rate. This procedure is repeated for multiple valve lifts often ranging from 0.050" to as much as 1.000". The range and increments are chosen based on the lift values of the camshaft being used. Specific flow bench setups may vary, but the overall ideals are typically the same as described.

The previous figure of the flow bench is an arrangement used to test intake ports. One method to modify the setup to test exhaust ports is to rotate the test piece and pull air through the valve in the opposite direction (Figure 3.3). A pipe section can be affixed to the test piece in order to simulate the cylinder. The testing procedure is the same as for testing intake port designs. With some flow benches this modification is unnecessary and the pumping direction can simply be reversed so that air is pushed out the intake port testing setup (Figure 3.2).

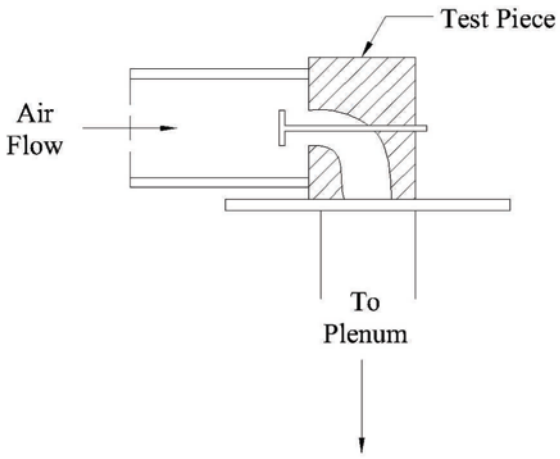

Figure 3.3 Modification to Flow Bench Configuration for Exhaust Port Evaluation.

3.4 Changes in Testing Conditions to Measure Blowdown

The working fluid used for experimental testing of exhaust valves/ports is typically room temperature air. As mentioned, one of the primary concerns with this is the significantly different fluid properties, specifically, the specific heat ratio, γ. Table 3.1 gives the specific heat ratio of air for different temperatures and the specific heat ratio of the products of combustion of a hydrocarbon using 100% theoretical air for a range of temperatures that may be seen in hot exhaust gases [9].

Specific Heat Ratio of Air		
Temp. (°R)	Temp. (°F)	γ
500	40.33	1.401
550	90.33	1.400
600	140.33	1.399
Specific Heat Ratio of Combustion Products of Hydrocarbon (100% air)		
Temp. (°R)	Temp. (°F)	γ
1500	1040.33	1.309
1600	1140.33	1.304
1700	1240.33	1.299
1800	1340.33	1.295
1900	1440.33	1.29
2000	1540.33	1.287
2100	1640.33	1.283
2200	1740.33	1.28

Table 3.1. Specific Heat Ratio of Low Pressure Air and Products of Combustion of Hydrocarbons.

A difference in specific heat ratio of approximately 9% exists when comparing air at 550°R and products of combustion at 1900°R. This difference could lead to deviations in flow bench behavior versus engine performance that would mislead investigators when looking for very fine improvements in exhaust port design.

Another potential source of error that can affect flow bench performance is the low pressure drops typically used for testing. As mentioned, 28" H_2O is the accepted norm and only represents a pressure drop of 1.01 lb/in^2. This pressure difference results in a ratio of p_e to p_c (Equation 3.3) of approximately 0.93, which is significantly higher than the ratio of approximately 0.53 required to produce the choked flow. Therefore, increasing the cylinder pressure and subsequently the pressure difference across the valve will capture the compressible nature of the blowdown process.

Two methods have been proposed to test the critical flow capabilities of an exhaust port taking the aforementioned information into account. The first method uses actual products of combustion at an elevated temperature and pressure to test the flow

characteristics of the port. A fuel/air mixture would be placed in a combustion chamber, ignited, and released through a model of the valve and port. The resulting pressure drop within the chamber would be measured using a high speed, in-cylinder combustion pressure sensor and the results then used to gauge the efficiency of the port to exhaust the gases. This would be repeated for different exhaust valve lift values with emphasis on the lower lifts (<0.100"), during which the majority of blowdown actually occurs.

The proposed ignition would occur within a stationary mixture making the use of liquid fuels problematic. Atomization would be difficult to initiate and even harder to maintain. Suspended fuel droplets would tend to condense and pool on the chamber floor. That would lead to the consideration of a gaseous fuel. Extensive research into the combustion and safety of hydrogen has been completed at the University of Miami under the direction of Dr. Michael Swain. Therefore it was chosen as the fuel, with specific interest in lean mixtures. The ignition properties of hydrogen are very interesting and quite different from more common fuels. These concerns will be addressed in subsequent sections.

The second method of testing improvements uses a compressed gas with fluid properties closer to those of combustion products. This eliminates the need for an ignition/combustion process. A survey of the properties of common gases identifies the components of combustion products that have the largest lowering effect on the value of specific heat ratio as water vapor and carbon dioxide (Table 3.2) [23 & 9]. Interestingly, room temperature carbon dioxide ($\gamma \approx 1.29$) and exhaust gases at 1900°R have very similar values of specific heat ratio. Therefore because of similarities described above and the availability and ease of handling, compressed carbon dioxide was chosen as an

alternative to combustion products. Compressed nitrogen ($\gamma \approx 1.40$) was also chosen in order to test the sensitivity of the process to fluid type.

Specific Heat Ratio of Common Gases (T = 68°F, P = 1 atm)

Gas	γ
H_2	1.41
He	1.66
H_2O	1.33
Ar	1.67
Dry Air	1.40
CO_2	1.29
N_2	1.40
O_2	1.40
N_2O	1.31
Cl_2	1.34

Table 3.2. Specific Heat Ratio of Common Gases at 1 atm and Room Temperature.

In this study, the two methods mentioned above have been investigated in order to establish their feasibility in the experimental testing of exhaust ports.

3.5 Use of Lean Hydrogen Combustion in Blowdown Testing

The use of hydrogen as an energy source has been and remains of much scientific interest. It has a high burning velocity, wide flammability range, high heating value per unit weight, and excellent flame stability [4]. The search for alternative fuel sources in recent years has only fueled this interest. Its ignition properties, especially for lean mixtures, are quite different than those of other fuel types.

The lean and rich limits of a fuel are the fuel concentration levels that bound the flammability limits for a given temperature and pressure. A mixture is considered lean if it contains more air or less fuel than a stoichiometric mixture. Inversely, a rich mixture will contain more fuel or less air than a stoichiometric mixture. Once a fuel-air mixture has been pushed above the rich limit or below the lean limit it will not sustain a flame.

The flammability limits vary for upward and downward propagating flames, due to convection assisting the flame travel. They are typically described as a percent volume in air:

$$\% \text{ volume in air, } VR_H = \frac{V_{Hydrogen}}{V_{Hydrogen} + V_{Air}} = \frac{V_{Hydrogen}}{V_{Total}} \tag{3.5}$$

Hydrogen's behavior is different than typical fuels, such as methane, which has upward propagation limits of 5.3% and 13.9% and limits of 5.8% and 13.6% for downward propagation. Hydrogen's rich limit is the same regardless of direction, 74%. For downward propagation the lean limit is 9.0%, but for upward propagation hydrogen has two lean limits. The first is the limit of a coherent flame, which is 9.0%. This is the leanest mixture that will burn completely. However, hydrogen is still ignitable down to 4.0%, but the flame is considered incoherent and ascends as separated globules. This lower limit is typically considered only for safety purposes.

This represents an exceptionally wide range in flammability limits [4]. Typically, fuels require an equivalence ratio, ϕ:

$$\phi = \frac{\left(\frac{Fuel}{Air}\right)}{\left(\frac{Fuel}{Air}\right)_{Stoichiometric}} \tag{3.6}$$

of approximately 0.5 for sustained combustion. For hydrogen, this lean limit is 0.1 for 4.0% by volume or 0.24 for 9.0%. Such a low equivalence ratio is achieved due to hydrogen's high diffusion rate. After ignition, hydrogen preferentially enters the combustion zone much quicker than air resulting in a higher concentration of hydrogen within the flame [16]. The upper limit of 74% corresponds to an equivalence ratio of 6.8, which is also well outside the range for most fuels [12].

For this study, a 7.0% VR was the lowest hydrogen concentration level feasible to alter the properties of the test mixture. Lower concentration levels have proven to ignite and burn less consistently causing variations in the resulting combustion gases [4]. Next, the properties of the resultant gases were predicted to estimate the concentration level needed to obtain the desired chamber pressure and fluid properties.

The first step to predicting the resultant gas composition, temperatures, and pressure is to setup the chemical balance of the combustion process:

For Lean Combustion ($\phi \leq 1$) Assuming Complete Combustion:

$$\phi H_2 + \frac{1}{2}\left(O_2 + 3.76N_2\right) \rightarrow \phi H_2O + 1.88N_2 + \left(\frac{1-\phi}{2}\right)O_2 \tag{3.7}$$

As mentioned earlier, water vapor and carbon dioxide are the main components that contribute to the lower specific heat ratio for hydrocarbon combustion products. The products of hydrogen combustion exclude carbon dioxide, but have a larger percentage of water vapor which results in similar values of γ. Next, the molar rate of combustion, *MRC*, is derived and is the ratio of the number of moles in the products to the number of moles in the reactants:

$$MRC = \frac{n_p}{n_r} = \frac{\phi + 4.76}{2\left(\phi + 2.38\right)} \tag{3.8}$$

where n_p and n_r are the number of moles of products and number of moles of reactants respectively. From this point, the simplest approach to the prediction of the final pressure and temperature due to a combustion process is to assume it happens instantaneously with a constant specific heat. First, the number of moles of reactant is calculated using the ideal gas law:

$$PV = n_R RT \Rightarrow n_R = \left(\frac{PV}{RT}\right)_{\text{Re}\,ac\,\text{tan}\,ts} \tag{3.9}$$

where P is the pressure of mixture, V is the volume of mixture and T is the temperature of mixture. The number of moles of the products can easily be calculated using the MRC and the number of moles of reactant:

$$n_p = (MRC)n_R = \left(\frac{\phi + 4.76}{2(\phi + 2.38)}\right)n_R \tag{3.10}$$

The energy addition to the system is calculated using:

$$Q = LHV(LB_{Fuel}) \tag{3.11}$$

where Q is the energy addition due to combustion, LHV is the lower heating value of the fuel ($LHV_{Hydrogen}$ = 51,608), and LB_{Fuel} is the mass of fuel. Next, the temperature change is predicted:

$$Q = \Delta T C_v n_p \Rightarrow \Delta T = \frac{Q}{c_v n_p} \tag{3.12}$$

where ΔT is the change in temperature due to combustion. The final temperature, T_f, and final pressure, P_f, are calculated using:

$$T_f = T_0 + \Delta T \tag{3.13}$$

$$P_f = \left(\frac{V}{n_p RT_f}\right)_{\text{Pr}\,oducts} \tag{3.14}$$

where T_0 is the initial temperature of mixture. The equations and steps for this estimation process are listed again in Appendix A.

A potentially significant source for error with this approach stems from assuming constant specific heat values. This process can be improved through iteratively using the beginning and final temperatures values to correct the average specific heat value being

used, but is still too simplified to give adequate results. Some initial calculations using this simplistic method were completed using the constants and properties given in Table 3.3 and the calculated final temperatures and pressures are shown in Figure 3.4. These results are compared with those using a more complex method described later.

In Table 3.3 MW represents the molecular weight and R_u represents the universal gas constant. One thing that should be noted is the use of a starting pressure of 14.7 lb/in^2, which is the standard atmospheric condition. In practice, it was decided that the chamber would be pumped down to a vacuum between each test and then the hydrogen air mixture would be allowed to enter at atmospheric pressure. Higher pressure can be utilized, but safety was considered paramount and following this procedure would produce the desirable changes in fluid properties with minimal combustion pressures.

Simplified Combustion Calculations
Properties and Constants

Description	Value	Units
$(MW)_{Air}$ =	28.95	lb/lbmole
$(MW)_{Hydrogen2}$ =	2	lb/lbmole
$(MW)_{Oxygen}$ =	16	lb/lbmole
$(MW)_{Nitrogen}$ =	14	lb/lbmole
$(LHV)_{Hydrogen2}$ =	51,608	BTU/lb
Specific Heat Ratio [5] =	1.41	-
Chamber Volume =	44.75	in^3
Initial Pressure, P_0 (abs) =	14.7	lb/in^2
Initial Temperature, T_0 =	75	°F
R_u =	1.9859	BTU/lbmole°R

Table 3.3. Properties and Constants Used in Simplified Combustion Calculations.

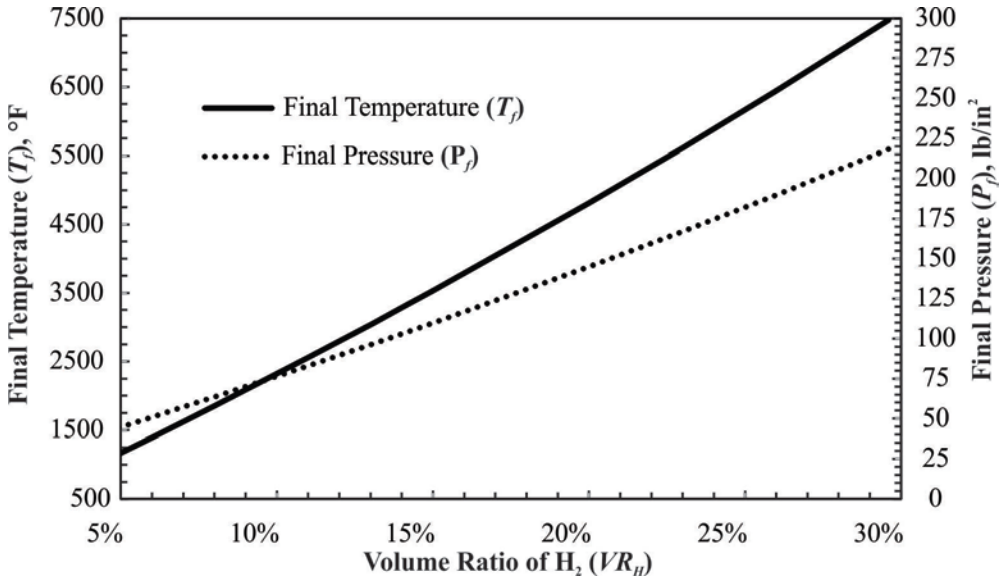

Figure 3.4 Estimated Final Pressure (Absolute) and Temperature Calculated Using Simplified Approach for a Range of Volume Ratios of H_2.

An improvement to these methods involves theoretically dividing the mixture into segments and simulating a stepped combustion process. Each segment is "burned" one at a time resulting in a high pressure division within the constant volume chamber. Then the high pressure segment is allowed to isentropically expand, compressing the other low pressure segments within the chamber:

$$VLPAE = \left(\frac{V_{Total}}{1 + \left(\frac{PHPBE}{PLPBE} \right)^{\frac{1}{\gamma_{ave}}} \left(\frac{VHPBE}{VLPBE} \right)} \right) \tag{3.15}$$

$$VHPAE = V_{Total} - VLPAE \tag{3.16}$$

where *VLPAE* is the volume of the low pressure gases after expansion, *VHPAE* is the volume of the high pressure gases after expansion, *VLPBE* is the volume of the low pressure gases before expansion, *VHPBE* is the volume of the high pressure gases before expansion, *PLPBE* is the pressure of the low pressure gases before expansion, *PHPBE* is

the pressure of the high pressure gases before expansion, γ_{ave} is the average ratio of specific heats for the mixture and V_{Total} is the total volume of gases in mixture. For each combustion and expansion process, a new value of specific heat is used based on the temperature from the previous steps. Further improvements are made within each combustion step by iterating to provide better estimation of average specific heat based on the starting and ending temperatures of each combustion stage. For each step, the temperature is used with curve fit equations to find the c_v value for the component gases. Then based on the number of moles of each gas type in each segment, an average c_v value is computed:

$$c_{v(ave)} = (c_v)_{H_2}\left(\frac{n_{H_2}}{n_{Total}}\right) + (c_v)_{H_2O}\left(\frac{n_{H_2O}}{n_{Total}}\right) + (c_v)_{N_2}\left(\frac{n_{N_2}}{n_{Total}}\right) + (c_v)_{O_2}\left(\frac{n_{O_2}}{n_{Total}}\right) \tag{3.17}$$

$$\gamma_{ave} = \frac{c_{v(ave)} + R_u}{c_{v(ave)}} \tag{3.18}$$

where n_{H_2} is the number of moles of hydrogen, n_{H_2O} is the number of moles of water vapor, n_{N_2} is the number of moles of nitrogen, n_{O_2} is the number of moles of oxygen, and n_{total} is the total number of moles in mixture. The average value of specific heat is used for subsequent iterations until convergence. The process for this segmented combustion and the individual equations for these modifications are fully outlined in Appendix A. Figure 3.5 illustrates the process of segmented combustion for 4 segments and a 7.0% VR.

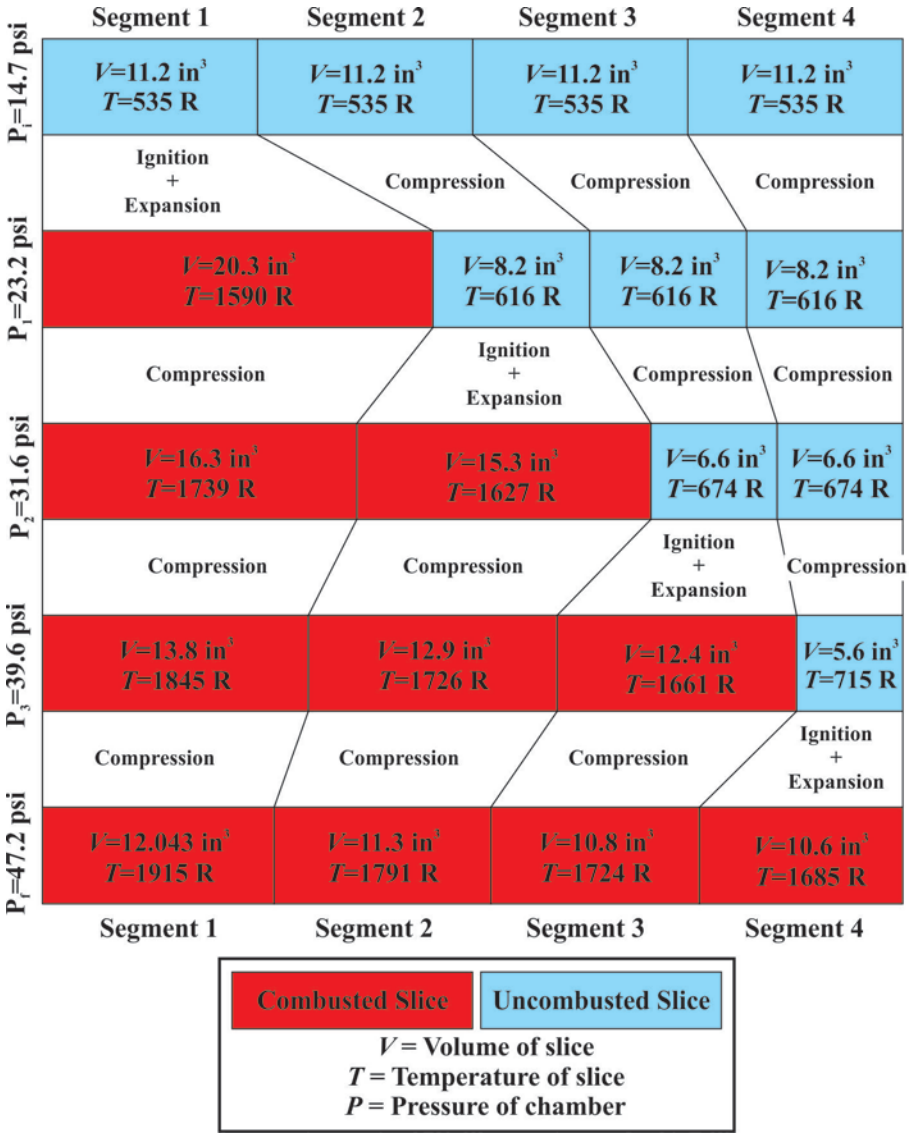

Figure 3.5. Illustration of segmented combustion process for 4 segments and a 7.0% VR.

This process is still an approximation, but is more complex than the initial estimation technique, especially as the number of combustion slices and iterations are increased. Therefore a computer program capable of making quick predictions for a variety of scenarios was created. The program was written in Fortan and is included in Appendix A. The predictions were calculated using the same constant values as used in the simplified approach (Table 3.3). The chamber volume was fixed at 44.75 in^3, but the final values of temperature, pressure, and specific heat are independent of the actual size.

The number of segments and iterations per segment were determined using a user specified convergence criteria, which is outlined in Appendix A. The final values of predicted pressure, temperature, and specific heat ratio assuming 100% combustion efficiency and no heat losses were calculated for several hydrogen volume ratios and compared to the simplified approach (Figure 3.6). The results of the segmented process are significantly different from those using the simplified calculation method, especially at higher equivalency ratios. Using this approach, a volume ratio of approximately 14-15% produces a specific heat ratio of approximately 1.29, which is similar to the products of combustion at 1900°R and also to carbon dioxide at room temperature. The calculated final pressure for these volume ratios is approximately 74 lb/in^2 and results in a chamber to atmospheric pressure ratio of over 5 which is more than adequate to achieve choked flow through the valve opening. Higher volume ratios may be required to offset the losses associated with incomplete combustion and heat losses, which have been neglected and are unavoidable.

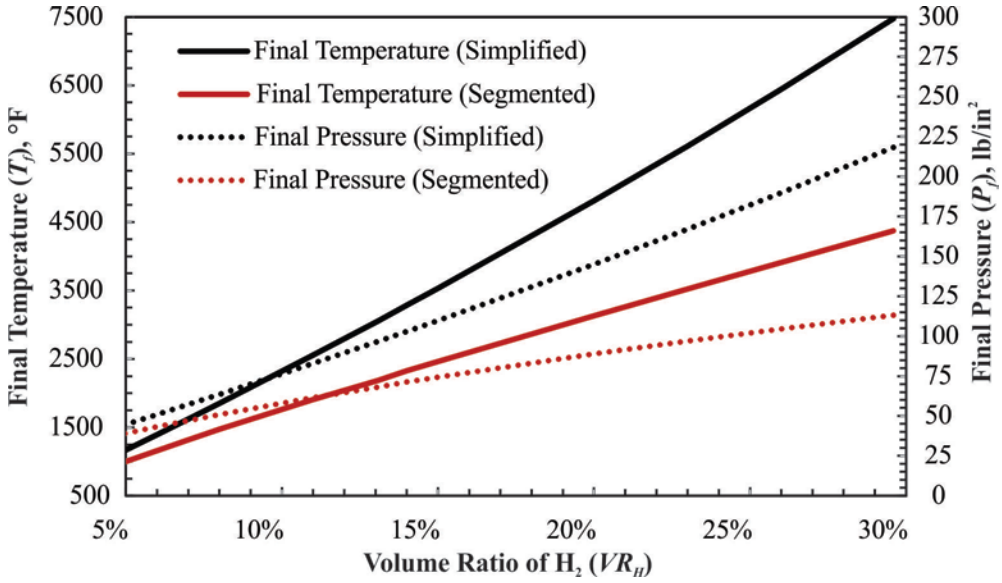

Figure 3.6. Estimated Final Pressure (Absolute) and Temperature Calculated Using a Segmented & Simplified Approach for a Range of Volume Ratios of H_2.

CHAPTER 4 - TASK 1: LEAN HYDROGEN IGNITION STUDY

The lean hydrogen ignition study was setup to determine the feasibility of using hydrogen combustion gases as an approximation to actual combustion gases. Of particular interest was the ability to produce repeatable ignition and subsequent pressure rises within a fixed volume chamber to be used as a test fluid for the simulation of exhaust port blowdown.

4.1 Experimental Apparatus and Setup

The experimental setup can be broken down into 4 general areas: fixed volume combustion chamber, ignition system, hydrogen delivery system, and data collection system.

4.1.1 Fixed Volume Combustion Chamber

The fixed volume chamber was constructed using 304 stainless steel. The design consists of a center pipe section with flanges welded to each end, end plates, and an aluminum stand. The pipe section was constructed from 4" nominal size pipe with an inside diameter of 4.026" and an outer diameter of 4.5". The flanges were machined from 6" wide by 0.5" thick bar stock. They each have an irregular pentagonal bolt pattern that matches the head bolt pattern of a small block Chevrolet engine. This allowed the use of standard head gaskets for sealing purposes and the ability to bolt a stock cylinder head directly onto the chamber for subsequent testing. Additional holes in the lower flange allow the chamber to be securely bolted to the stand. These three pieces were TIG welded to form the center section (Figure 4.1). After welding, the upper and lower faces were smoothed and flattened and the head bolt holes were tapped for 7/16-14 studs. The height of the chamber is 3.433" which gives a chamber volume of 44.75 in^3

with the addition of the gasket material. This is equal to the displacement of a single cylinder of a 358 in^3, 8 cylinder engine.

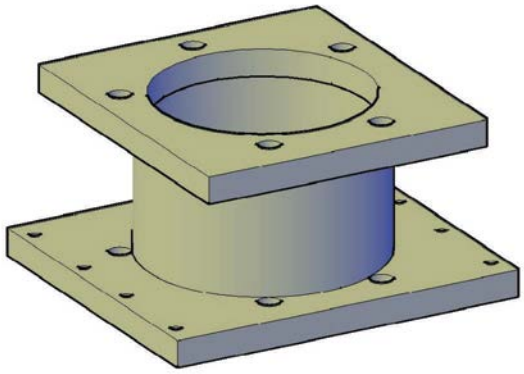

Figure 4.1. Center Section of Combustion Chamber

Two plates were machined from stainless steel and cap each end of the center section. The top plate (Figure 4.2) has 5 thru-holes drilled in the same bolt pattern as the center pipe section, which are used to secure it. The center hole was tapped M14X1.25 for the addition of a standard 14mm spark plug used for ignition testing. An additional hole in the plate was tapped 1/4" NPT and is used for gas delivery/instrumentation. The bottom plate (Figure 4.2) is similar to the top plate and has the same pentagonal thru-hole bolt pattern. The center hole accommodates a standard 14mm spark plug. The smaller hexagonal pattern was drilled and tapped M10X1.00 for an array of 10mm spark plugs. The final hole was tapped 1/4" NPT for hydrogen delivery.

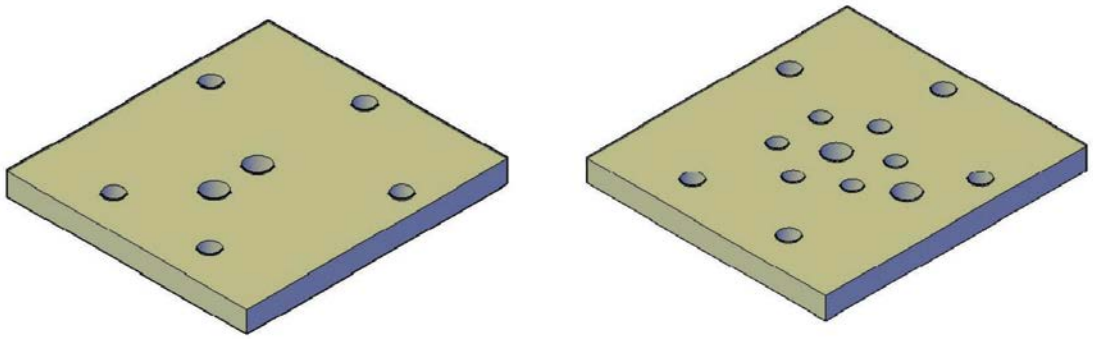

Figure 4.2. Top (Left) and Bottom (Right) Plates of Combustion Chamber.

Side plates are used to mount the chamber to a stand. Each side consists of 2 plates created from 0.5" thick 6061 aluminum (Figure 4.3). The two plates can be bolted together differently to rotate the chamber in different positions from a vertical position to horizontal in 15 degree increments. For the current testing the chamber remained in the vertical position (Figure 4.4).

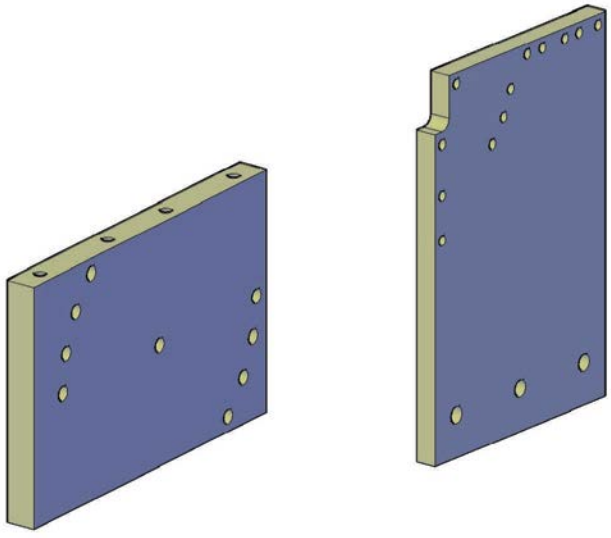

Figure 4.3. Side Support Plates for Combustion Chamber.

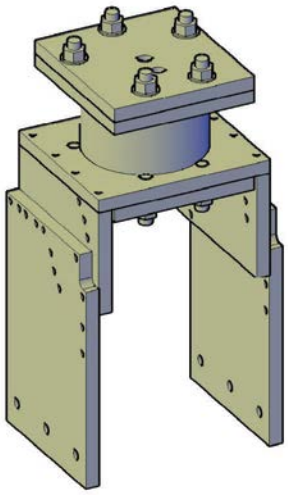

Figure 4.4. Combustion Chamber Assembly.

Bulk exhaust gasket material was used to seal the chamber's top and bottom plate to the center section. High temperature, liquid thread-locker and sealant was used to seal each stud.

4.1.2 Ignition System

The ignition system includes the battery, coil packs, spark plugs, spark plug wires, control system, and all necessary wiring. The system was heavily tested and underwent several design revisions to ensure consistent sparking. The battery that was used was a high performance 12V automotive battery and supplied all power for the project. It was fully charged each time data was taken to ensure consistent ignition energy.

For each ignition, there was a total of 8 spark plugs that could be used. Six 10mm NGK spark plugs (part # CR4HSB) were mounted in the bottom plate of the chamber. One additional 14mm spark plug (NGK, part # BR8HS) could be installed in both the top and bottom plate (Figure 4.2), however, the six 10mm plugs were deemed sufficient to ensure reliable ignition. The gaps on all spark plugs were set to 0.030" for each experiment. Each spark plug was connected to an Accel Super Stock Coil (part # 8140)

using Accel Superstock universal fit spark plug wires (part # 4041). The ignition energy stored in each coil was approximated using:

$$E = \frac{1}{2} L \left(\frac{V_{dc}}{R_c} \right)^2 \tag{4.1}$$

where E is the stored energy, V_{dc} is the supply voltage and L and R_c are the coil inductance and primary resistance respectively. Using a model 878 B&K LCR meter, the inductance and resistance of the coils was found to be 6.356 mH and 1.5 Ω respectively. This results in approximately 203 mJ of stored energy per coil.

The control system underwent several revisions in order to achieve consistent operation. The original design (Figure 4.5) utilized a heavy-duty momentary push button to initiate ignition and a LED light to indicate a closed ignition circuit. A condenser from a 74-78 Honda Accord/Civic was wired parallel to the switch. When the circuit is broken, the oscillations across the condenser reduces the arcing and burning of the contacts within the switch. This is the typical setup used for mechanical distributors to protect the points as well.

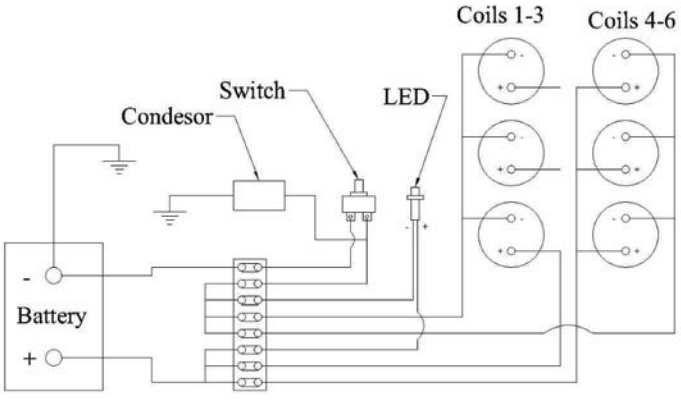

Figure 4.5. Simplified Schematic of Ignition Wiring Circuit Utilizing Momentary Switch.

However, the collapsing of the coils produced large sparking across the contacts within the switch and led to inconsistencies and the ultimate failure of the switch. The switch was replaced with a distributor containing ignition points for a Toyota 2TC 1.6L engine used in previous laboratory testing. This setup proved consistent and reliable while using 3 or less coils, but failed to do the same for more. This led to the design of a new control system that uses individual transistors to trigger each coil (Figure 4.6). This ignition system was constructed and used for the all remaining ignition tests (Figure 4.7, 4.8).

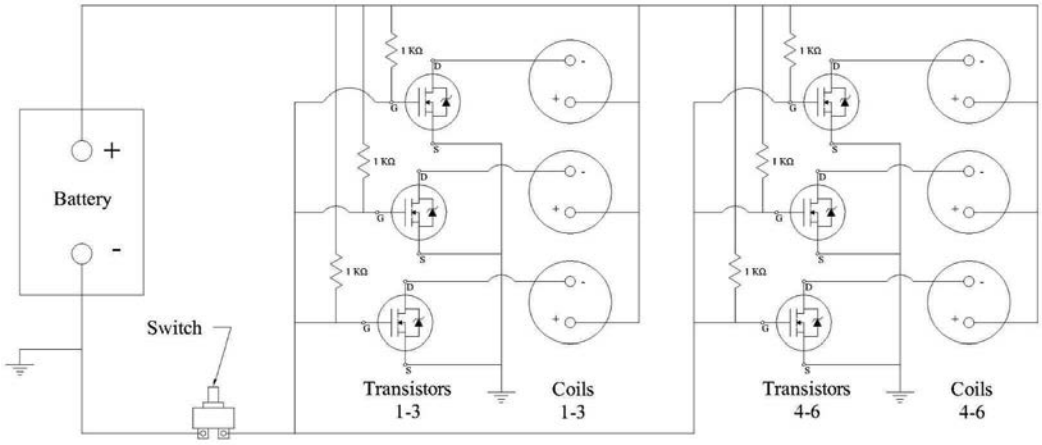

Figure 4.6. Simplified Schematic of Ignition Wiring Circuit Utilizing Tansistors.

The system uses six STMicroelectronics IRF540 NMOS transistors. The ability of these transistors to produce reliable ignitions was tested in a custom ignition system for a hydrogen-fueled engine previously developed in the IC engines laboratory.

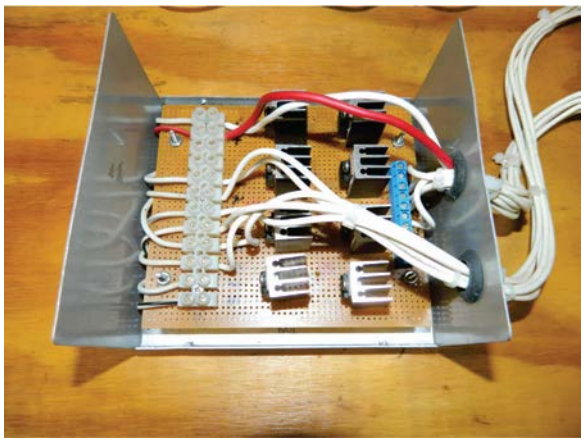

Figure 4.7. Ignition Box Transistor Setup.

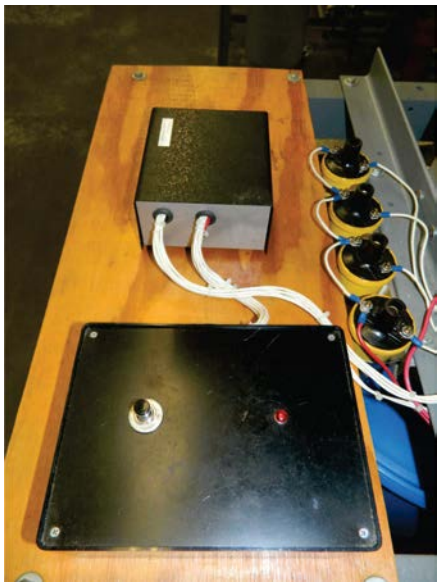

Figure 4.8. Ignition Box and Ignition Coils.

4.1.3 Hydrogen Delivery System

The delivery of the hydrogen-air mixture and exhausting of the combustions gases was executed using a combination of needle valves, stainless steel and rubber tubing, multiple pressure gauges, and a vacuum pump (Figure 4.9). All hard lines, fittings and valves were stainless steel and utilized Swage-lok fittings. The setup used Swage-lok valves and Wika pressure gauges.

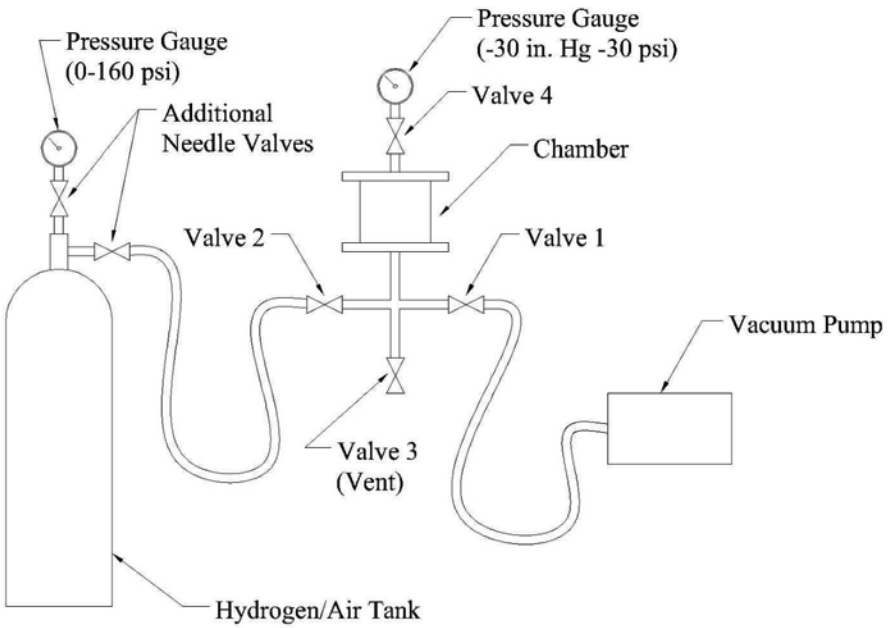

Figure 4.9. Delivery Setup for Hydrogen/Air Mixture.

Before ignition testing began, the chamber and associated tubing/fittings were tested for possible leaks. Pressurized air in conjunction with a vacuum pump was used to ensure the chamber could remain sufficiently sealed for pressures up to 120 lb/in^2 and a vacuum of 30 in Hg. The needle valves described above were used to isolate the chamber from the air supply or vacuum and pressure gauges were used to indicate if any leaks were present.

4.1.4 Data Collection System

Combustion pressures were measured using a piezoelectric high temperature transducer installed in a 14-mm spark plug and mounted in the center of the bottom plate (Figure 4.2). The spark plug was not used for ignition and was not attached to a coil. The pressure transducer was wired to a Fluke 192B ScopeMeter oscilloscope (Figure 4.10), which was used to digitally record the pressure rise.

Figure 4.10. Oscilloscope used for data collection.

4.2 Experimental Procedure

The combustion testing was completed as follows (references Figure 4.9 unless noted):

1. All valves are closed.
2. The valves attached to the hydrogen/air tank are opened to fill rubber supply tubing.
3. The valve to the vacuum pump and vacuum gauge (Valves 1 and 4) are opened and the vacuum pump is used to pump the chamber down to a vacuum.
4. The valve to the vacuum pump is closed (Valve 1) and Valve 2 is opened allowing the hydrogen-air mixture to fill the chamber to a pressure slightly above atmospheric.
5. Valve 2 is closed and the vent valve (Valve 3) is briefly opened to vent excess pressure to the atmosphere.
6. All valves except for those attached to the hydrogen air tank are closed

7. The data collection system is set to record with a change in pressure trigger.
8. Ignition is initiated and data is collected.
9. Valve 3 is opened to vent combustion gasses to atmosphere and is then closed.
10. Repeats steps 3-9 as needed to collect data.

4.3 Results and Discussion

Lean hydrogen ignition tests were completed with different VRs of hydrogen and air. Example output for four consecutive ignitions of 7.01% VR hydrogen-air (Figure 4.11) illustrates the difficulties of using ignited lean hydrogen to simulate consistent exhaust port testing conditions.

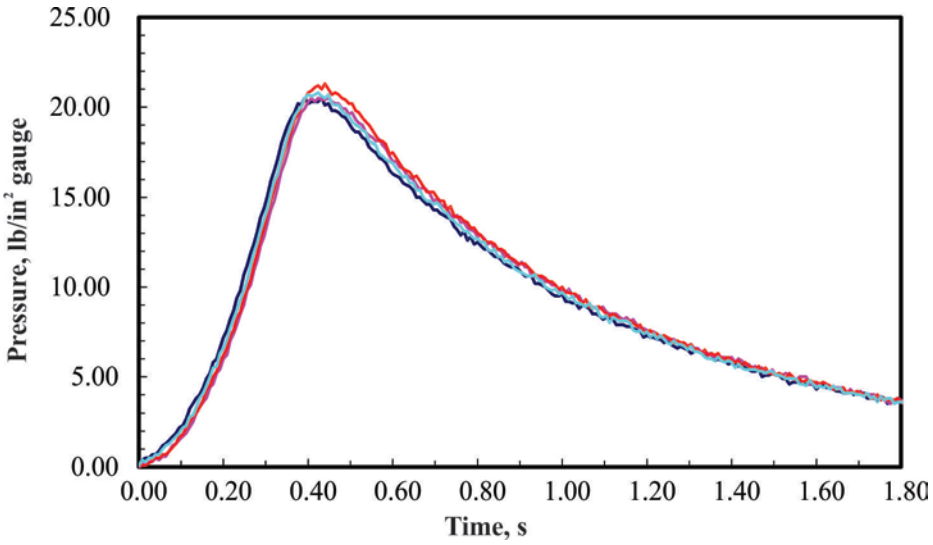

Figure 4.11. Observed pressure (gauge) vs. time for ignition of H_2-Air, VR = 7.01%

The four ignitions shown produced a mean maximum gauge pressure, $\bar{x}$, of 20.78 lb/in^2 with an mean absolute deviation, $\bar{D}_i$, of 0.275 lb/in^2:

$$\bar{x} = \frac{\sum_{i=1}^{n} x_i}{n} \tag{4.2}$$

$$D_i = \left| x_i - \bar{x} \right| \tag{4.3}$$

where x_i is the maximum pressure of an individual ignition test and n is the number of tests being analyzed. Even with a VR of 7.01%, these pressure rises are sufficiently consistent; however the peak values are considerably less than the predicted valued of 32.3 lb/in^2 and 42.3 lb/in^2 gauge pressure calculated using the segmented and simplified approaches described in Section 3.5. This would seem to indicate incomplete combustion and/or significant heat losses. With a lean hydrogen mixture below the coherent flame limit incomplete combustion may be a factor in the lower than expected maximum pressure. More importantly, the rapid pressure drop following the peak indicates significant heat losses to the chamber itself.

The magnitude of heat losses to the chamber walls can be investigated by calculating and comparing the thermal mass, C_{th}, of the chamber and internal gases, the total energy transfer required and subsequent temperature changes and the required convective heat transfer coefficient to produce the heat transfer rate. The thermal mass of the chamber is calculated using:

$$C_{th} = mc_p \tag{4.4}$$

where c_p is the constant pressure specific heat and m is the mass of the chamber. Similarly, the thermal mass of the gas mixture can be calculated using the combined mass and average constant volume specific heat of products of combustion, c_v. The total heat transfer required to cool the gases and produce the measured pressure drop was calculated using Equations 3.14 and 3.12. The subsequent, potential temperature drop in the chamber itself, $\Delta T_{chamber}$, can be calculated similarly:

$$\Delta T_{chamber} = \frac{Q}{C_p m} \tag{4.5}$$

The convective heat transfer coefficient, h, required to produce the temperature and pressure drop can be calculated using:

$$h = \frac{Q}{A\Delta T\Delta t} \tag{4.6}$$

Where ΔT is the temperature drop of the gas mixture, Δt is the estimated time of temperature drop, A is the chamber's internal surface area.

Using Equation 4.4, the thermal mass of the chamber is 0.918 BTU/ºR compared to 0.0003046 BTU/ºR calculated for the gas mixture using the curve fit method outlined in Appendix A to estimate c_v. The maximum temperature of the gas is estimated to be 754ºR and the change in temperature, ΔT, of the gas mixture during cooling is approximately 219ºR. The total heat transferred, Q, is 0.0667 BTU and would represent a chamber temperature drop of only 0.999ºR due to the large difference in C_{th}. Lastly, the required convective heat transfer coefficient, h, assuming a 2 second Δt, estimated using Figure 4.11, is calculated to be 0.402 BTU/Hr-ft^2-ºR. Therefore, it is reasonable to assume that heat transfer between the gases and chamber walls is significant and cannot be ignored. In fact, the rapid pressure drop that occurs following the peak pressure makes using heated combustion products impractical without maintaining a heated chamber. Due to these findings, the lean hydrogen ignition study was halted and the blowdown process was exclusively tested using pressurized room temperature gases. The properties used to calculate the above values are given in Table 4.1.

Constants and Properties (VR=7.01%)		
n_p =	6.40E-05	lbmol
m_{H20} =	7.80E-05	lbm
m_{N2} =	1.27E-03	lbm
m_{02} =	3.17E-04	lbm
Cv_{H2O} =	0.344	BTU/lbm°R
Cv_{N2} =	0.178	BTU/lbm°R
Cv_{O2} =	0.161	BTU/lbm°R
$V_{chamber}$ =	27.062	in^3
$m_{chamber}$ =	7.659	lbm
$Cp_{chamber}$ =	0.120	BTU/lbm°R
$A_{chamber}$ =	69.922	in^2

Table 4.1. Properties and Constants Used in Thermal Mass and Heat Transfer Calculations

4.4 Conclusions of Task 1

The combustion of lean hydrogen at atmospheric pressure was used to produce consistent pressure rises within a closed chamber. The heat losses to an ambient temperature chamber resulted in a rapid temperature and pressure decrease following combustion. The low thermal mass of the gas mixture combined with the three orders of magnitude higher thermal mass of the chamber results in a near constant chamber temperature as the gas rapidly cools. It is also reasonable to assume that the turbulence produced from the combustion process and any naturally occurring localized fluid movement from the rapid cooling is sufficient to produce the necessary convective heat transfer coefficients that result in the observed temperature change of the gas mixture. Therefore, the primary conclusion of Task 1 is that the products of combusted lean hydrogen-air mixtures are not practical as a testing fluid for the blowdown process simulated with the envisioned testing apparatus. Heat transfer losses between the combusted gases and the chamber could be reduced if the chamber itself was heated, but would add complexities to the system and reduce the likelihood of industry acceptance.

CHAPTER 5 - TASK 2: EXPERIMENTAL ANALYSIS OF HIGH PERFORMANCE EXHAUST PORT UTILIZING COMPRESSED GASES

To simulate the blowdown process that takes place within an IC engine, an experimental setup was constructed that uses compressed gas, a physical model, and a manual valve actuator. The system was designed to be durable, produce repeatable test results, and be able to measure differences in critical flow performance for different exhaust port geometries. The results from this portion of the study are later compared to more traditional steady flow test results.

5.1 Experimental Apparatus and Setup

The experimental apparatus consists of modified versions of the fixed volume combustion chamber, gas delivery system, and stand described in Section 4.1, additional pieces used for valve opening, and an exhaust port/valve test piece.

5.1.1 Modifications of Fixed Volume Combustion Chamber and Gas Delivery System

Preliminary experimentation utilizing the combustion chamber designed for the lean hydrogen ignition testing indicated the need for a lengthened testing duration. Therefore, an extension piece was created to increase the internal chamber volume. The extension has a top flange that bolts to the bottom of the original chamber using the irregular pentagonal bolt pattern used to secure the bottom plate (Figure 4.2). The extension body was constructed from 3" nominal size 304 stainless steel pipe with an internal diameter of 3.068" and an outer diameter of 3.5". A bottom flange was machined from 0.5" thick stainless steel bar stock and has one M14X1.25mm and one 1/4" NPT threaded hole for compressed gas delivery and data acquisition. The top

flange, pipe section, and bottom flange were TIG welded together and bolted to the bottom of the combustion chamber using 7/16” studs and hex nuts and sealed using bulk intake gasket material (Figure 5.1). The extension increases the chamber volume from 44.75 in^3 to 133.46 in^3.

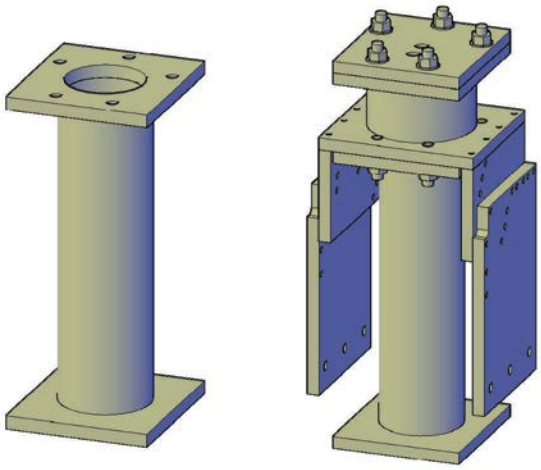

Figure 5.1. Combustion Chamber Volume Extension and Assembly.

Compressed gas is added to the chamber using a combination of needle valves, stainless steel and rubber tubing, multiple pressure gauges, and a pressure regulator (Figure 5.2). All hard lines, fittings and valves are stainless steel and use Swage-lok fittings. The setup uses Swage-lok valves and Wika pressure gauges. Once the chamber is charged, the valve within the test port is opened and the gas exits through the test piece and into the atmosphere.

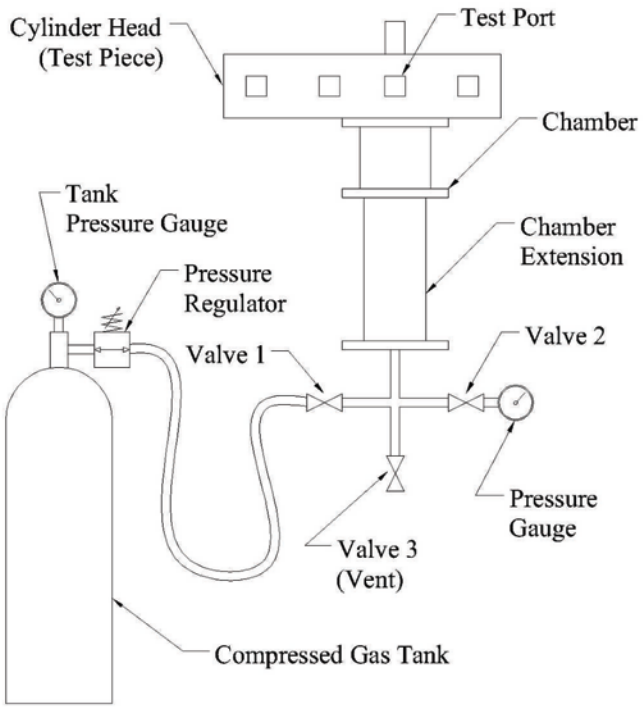

Figure 5.2. Delivery Setup for Compressed Gas.

5.1.2 Valve and Exhaust Port Test Piece

The cylinder head used for testing is a small block Chevrolet SB2.2 from a GM 12480011 casting. The intake and exhaust ports were designed and CNC machined by Weld Tech with a GP Tech 1 designation. It has 2.170" diameter intake valves and 1.625" exhaust valves. This particular head and design was chosen based on conversations with company employees and Weld Tech's product statement [22]:

> The exhaust port design is relatively straightforward with the exception of a fairly large bowl and a large venturi. Both act to further enhance the performance of the engine, but do not necessarily increase flow numbers.

This is the situation that an improved exhaust port analysis could help explain. The flow capabilities reported by Weld Tech for this exhaust port begin with a lift value of 0.200" (Figure 5.3); however the values of concern for blowdown are typically below 0.100". The port designed by Weld Tech was tested as well as an adjacent port that had some

alterations near the valve seat in order to decrease the port volume and improve traditional flow bench performance. These modifications involved adding automotive body filler, then sanding and contouring the material to the desired shape. To mimic the conditions reported by Weld Tech, the exhaust port underwent three progressive rounds of alterations. Each alteration focused on adding filler near the valve, past the valve seat to obtain some pressure recovery producing increased flow at low lift values on a steady flow, low pressure flow bench. Table 5.1 contains the measured pressure drops across the orifice plate for each alteration and Table 5.2 shows the calculated flow rates and port volumes. The flow rates were calculated using

$$CFM = 400\left(\frac{\Delta p}{6}\right)^{1/2} \tag{5.1}$$

where *CFM* is the flow rate in ft^3/min, and Δp is the pressure drop across the orifice in inches of water. The thin-plate orifice in the flow bench was calibrated to produce 400 CFM at 6 inches of pressure drop. The high flow rate capability of the orifice plate resulted in inaccuracies and pressure fluctuations when trying to read flow values at lifts below 0.100". The port with the last set of alterations (Alt. 3) was used as the modified port for all subsequent testing for Task 2 and Task 3. The port volume was decreased 4.7% from 116.5 cm^3 to 111.0 cm^3. This is likely not the exact geometry of the port described by Weld Tech, but has the same port volume and flow characteristics. The designations from here forward are GPTech1 (Figure 5.4) and GPTech1_mod1 (Figure 5.5).

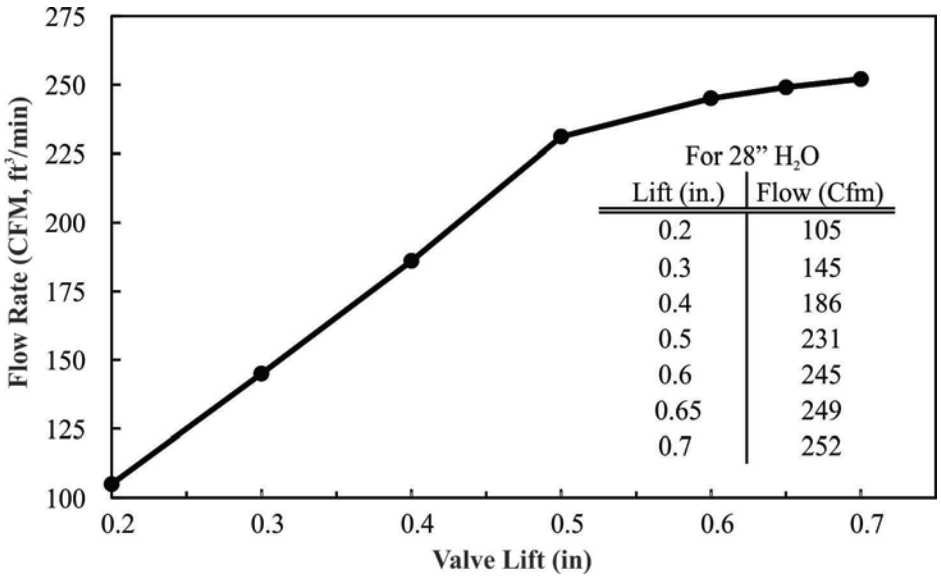

Figure 5.3. Flow Rates of GPTech 1 Exhaust Port as Reported by Weld Tech.

WeldTech GPTech1 Measured Pressure Differential

Lift	Original	Alt. 1	Alt. 2	Alt. 3
0.05"*	0.033"	0.033"	0.033"	0.033"
0.1"	0.11"	0.11"	0.12"	0.13"
0.2"	0.41"	0.42"	0.42"	0.43"
0.3"	0.80"	0.87"	0.90"	0.90"
0.4"	1.34"	1.37"	1.40"	1.40"
0.5"	1.78"	1.82"	1.88"	1.91"
0.6"	2.1"	2.14"	2.21"	2.25"
0.7"	2.31"	2.31"	2.33"	2.39"

*Measurements at 0.050" lift are inaccurate with 400 CFM orifice plate

Table 5.1. Pressure drops measured while flow testing alterations to GPTech1 port.

WeldTech GPTech1 Measured Flow Rates

	Original	Alt. 1	Alt. 2	Alt. 3	
Port Volume (cm3)	116.5	114.8	112.3	111.0	Alt 3
Lift	Flow Rates (ft³/min)				% Change
0.05"*	29.4	29.4	29.4	29.4	0.0%
0.1"	54.2	54.2	55.4	57.7	6.6%
0.2"	104.6	105.8	105.2	106.5	1.8%
0.3"	146.3	152.3	154.9	154.9	5.9%
0.4"	189.0	191.1	193.2	193.2	2.2%
0.5"	217.9	220.3	223.6	225.7	3.6%
0.6"	236.6	238.9	242.8	244.9	3.5%
0.7"	248.2	248.2	249.3	252.5	1.7%

*Measurements at 0.050" lift are inaccurate with 400 CFM orifice plate

Table 5.2. Flow performance and exhaust port volume for alterations to GPTech1 port.

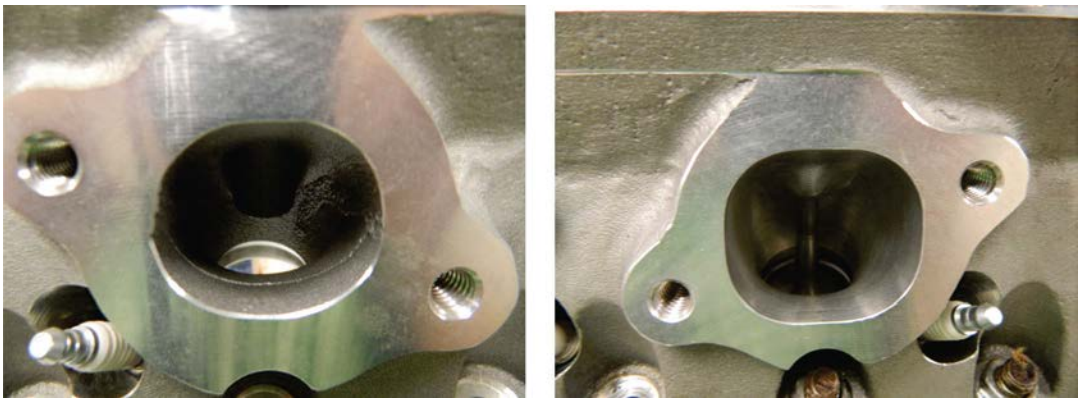

Figure 5.4. As Cast Port (Left) and Weld Tech GPTech 1 Port (Right).

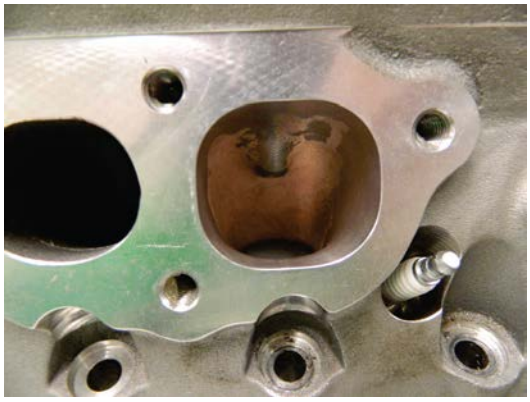

Figure 5.5. Modified Weld Tech GPTech 1 Port.

An exhaust exit piece was constructed from aluminum and details were shaped into it using automotive body filler (Figure 5.6B & C). The pipe has a 2.25" diameter and was filled and matched to the exhaust port exit and simulates the first 3.3125" inches of an exhaust header pipe allowing the flow to develop down its length before exiting. Measuring flow rates without this piece can produce inconsistent results. The exhaust valve used for all testing was a Del West titanium valve part no. DW-EV-1625-7T25 with a 5/16" valve stem as recommended by Weld Tech (Figure 5.6A).

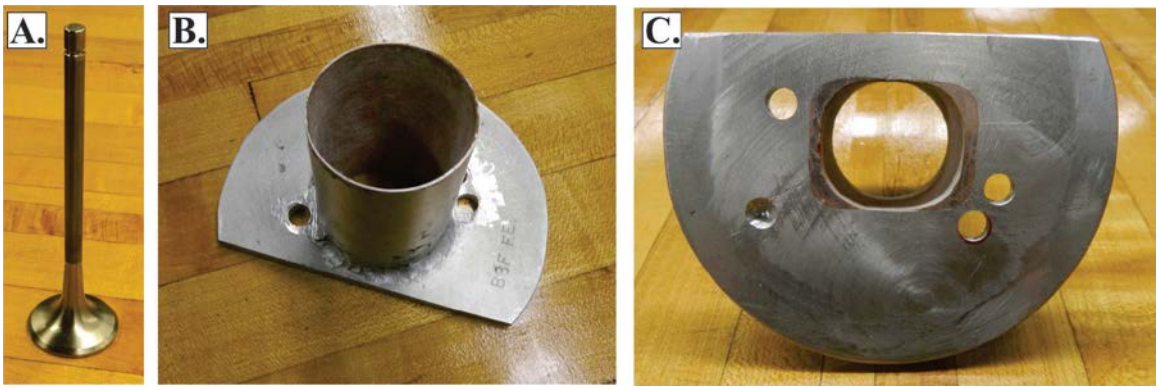

Figure 5.6. Exhaust Valve (A) and Exhaust Exit Piece (B & C).

5.1.3 Valve Actuation and Additional Hardware

A valve holder was designed, machined and assembled to ensure consistent valve lift (Figure 5.7A). A valve actuator was also constructed to manually open the valve to vent the compressed gas (Figure 5.7B). The actuator is bolted to the cylinder head using the rocker arm mounting holes and a lever arm is attached (Figure 5.8).

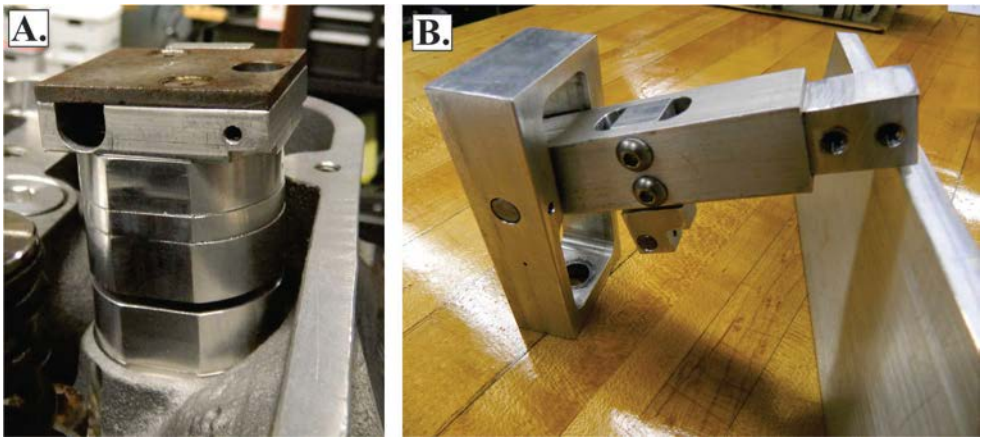

Figure 5.7. Exhaust Valve Holder (A) and Valve Actuator Assembly (B).

Figure 5.8. Exhaust Valve Holder and Valve Actuator Assembly on Cylinder Head.

5.1.4 Data Collection System

The pressure sensor used for the critical flow testing using compressed gas was an Omegadyne PX209-300G10V. The pressure range is 0-300 lb/in^2 with an output voltage of 0-10V. The sensor was wired to a Fluke 192B ScopeMeter oscilloscope (Figure 4.10), which was used to digitally record the pressure drop during the simulated blowdown.

5.1.5 Finished Experimental Setup

Figures 5.9 and 5.11 are photographs taken of the finished experimental setup for the compressed gas blowdown testing of exhaust ports. Figure 5.11 shows the use of a dial indicator to check the valve lift during testing.

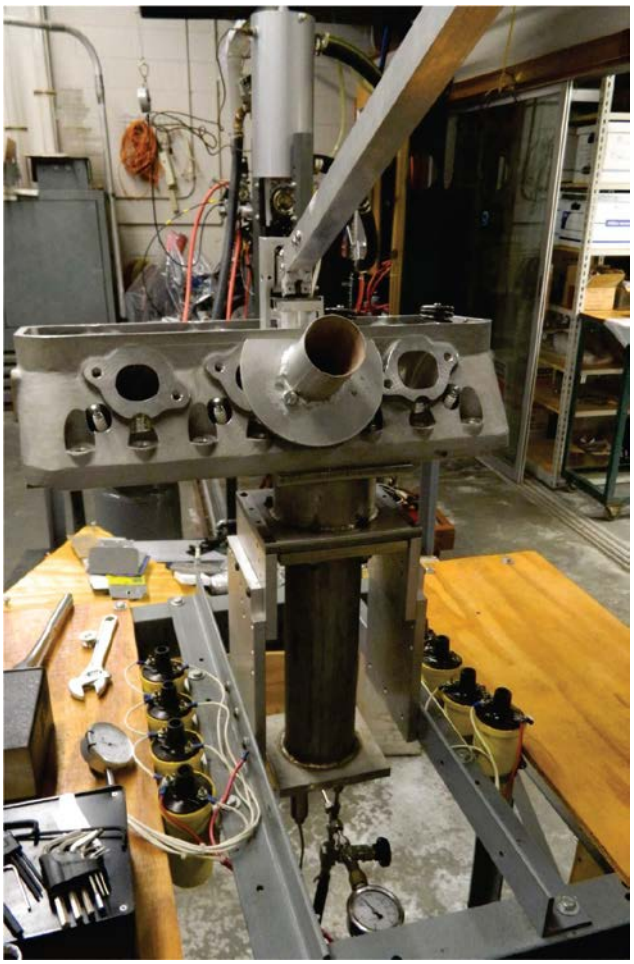

Figure 5.9. Final setup for compressed gas blowdown testing.

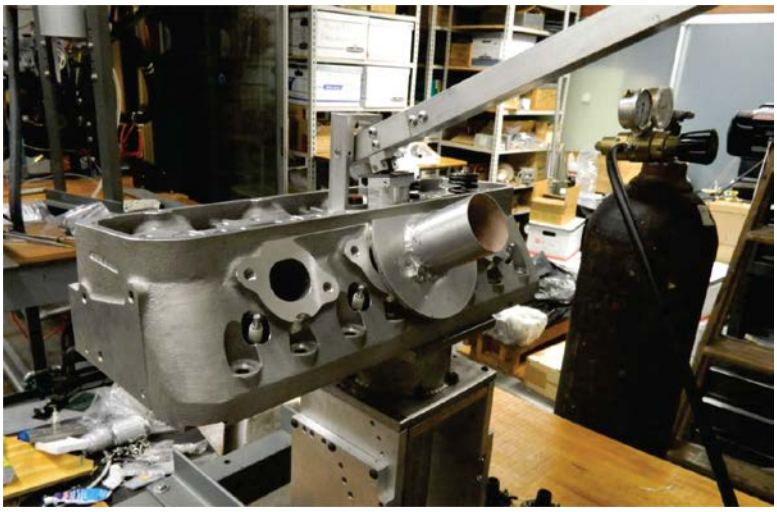

Figure 5.10. Final setup for compressed gas blowdown testing.

Figure 5.11. Setup using dial indicator to measure valve lift.

5.2 Experimental Procedure

The experimental blowdown testing was completed as follows (references Figure 5.2 unless noted):

1. All valves are closed except Valve 2 attached to the pressure gauge.
2. The valve (Valve 1) attached to the regulator on the compressed gas tank is opened, letting the chamber fill.
3. Once the chamber reaches the regulated pressure the valve attached to the regulator (Valve 1) is closed. The pressure can be checked using the attached gauge.
4. The data collection system is set to record using a pressure trigger point.
5. The exhaust port valve is rapidly opened initiating blowdown and data is recorded.
6. Repeats steps 2-5 as needed to collect data.

Initially, 2-3 filling and exhaust cycles were completed to flush the chamber. A vacuum pump could also be used to clear the chamber before filling, but was found to be unnecessary once testing began.

5.3 Results and Discussion

Blowdown measurements were taken at 0.050" and 0.100" valve lifts for the original (GPTech1) and modified (GPTech1_mod1) exhaust ports using both compressed nitrogen and carbon dioxide. Five sets of data are compared for each lift, port, and compressed gas combination. Measurements were taken every 2 ms and consisted of a high and low voltage for the sample period. A total of 300 measurements were taken for each blowdown resulting in a 0.598 s testing period. The raw voltage measurements were converted to pressure using:

$$P_c = \left(V_{ave} - V_{off}\right) f_{vm} f_{sc} \tag{5.2}$$

where P_c is the calculated chamber pressure, V_{ave} is the average of the high and low voltage during the sample period, V_{off} is the offset voltage, f_{vm} is the voltage multiplier and f_{sc} is the scaling factor. The voltage multiplier, f_{vm}, for the pressure sensor was 30 lb/in^2/v. The voltage offset, V_{off}, was calculated as 0.18 v to zero the measurements at atmospheric pressure. And the scaling factor, f_{sc}, was calculated as 0.821 to correct the measurements to a starting pressure of 120 lb/in^2. The same multipliers and offset were used for all data processing and the raw data using nitrogen is included in Appendix D as example output.

To obtain smoothed curves from the pressure measurements to be used for the port analysis, the data was first fit using a natural smoothing spline composed of piecewise cubic polynomials with a high weighting factor. This was accomplished using

the *acspline* function within GNUPLOT with a weight factor of 1.0e7 to adequately capture the entire pressure versus time curve. The curves were then output as 500 data points. Examples of measured data and the smoothed spline fit and the variation of five consecutive datasets are shown in Figures 5.12 and 5.13 for the modified port (GPTech1_mod1) and both lift values.

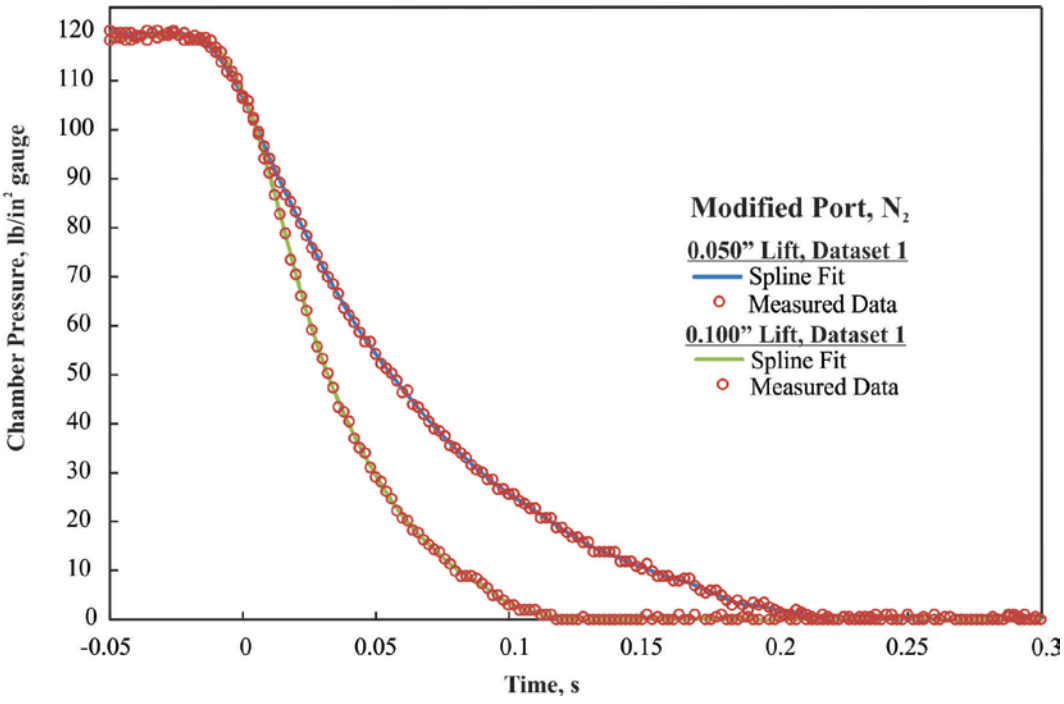

Figure 5.12. Example measured data and spline fits for blowdown testing (GPTech1_mod1).

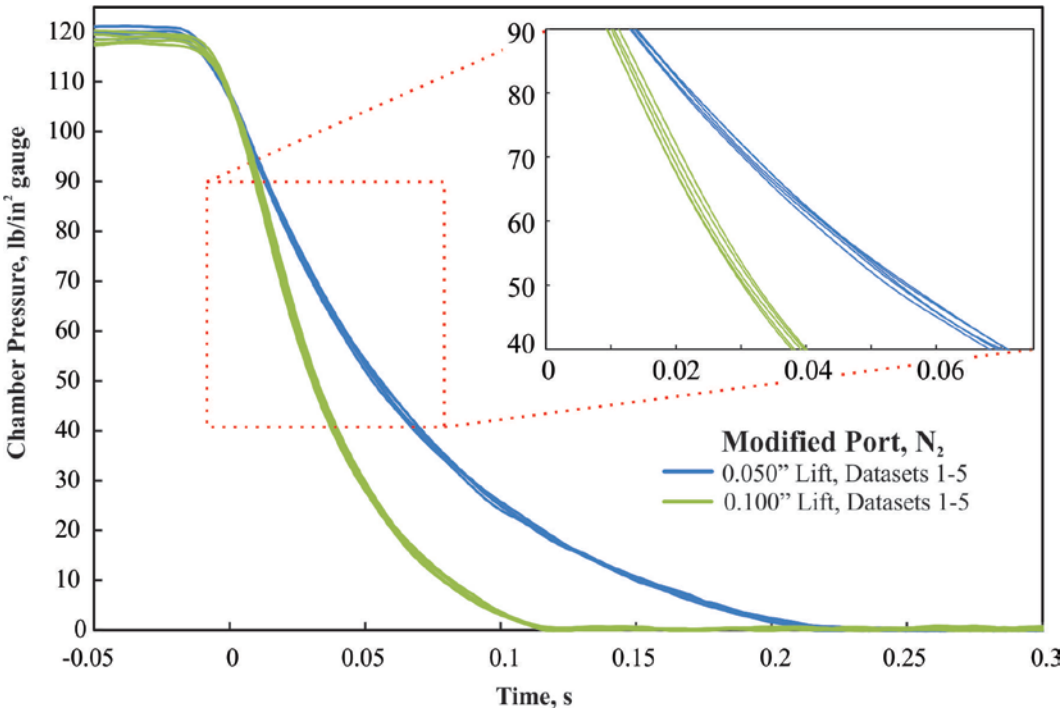

Figure 5.13. Example variations for splines fit to blowdown testing (GPTech1_mod1).

The temperatures of the gases within the chamber are estimated assuming adiabatic, isentropic expansion:

$$T_2 = T_1\left(\frac{P_2}{P_1}\right)^{\frac{\gamma-1}{\gamma}} \tag{5.3}$$

where T_2 and T_1 are the temperatures at times 2 and 1 of the expansion process, P_2 and P_1 are the pressures at times 2 and 1 of the expansions process and γ is the specific heat ratio of the gas. The mass of gas within the chamber at each time step is then calculated using the ideal gas law:

$$m = \frac{P_c V_c}{R T_g} \tag{5.4}$$

where P_c is the chamber pressure, V_c is the chamber volume (133.46 in^3), R is the specific gas constant (1775 ft-lb/slug-°R for nitrogen and 1130 ft-lb/slug-°R for carbon

dioxide) and T_g is the estimated gas temperature. The mass flow rate between each set of points on the spline is calculated using:

$$\dot{m} = \frac{m_2 - m_1}{t_2 - t_1} \tag{5.5}$$

where m_2 and m_1 are the masses of the gas within the chamber at times t_1 and t_2. An effective flow coefficient, C_{ef}, is then calculated using:

$$C_{ef} = \frac{\dot{m}}{\dot{m}_{theoretical}} \tag{5.6}$$

$$\dot{m}_{theoretical} = A_f \frac{P_c}{\sqrt{RT_c}} \sqrt{\gamma} \left(\frac{2}{\gamma + 1} \right)^{\left(\frac{\gamma+1}{2(\gamma-1)} \right)} \tag{5.7}$$

where A_f is the flow area (valve curtain area) and T_c is the gas temperature within the chamber. The ratios of specific heats were taken as constant values below 40°F due to the lower limit of curve fit data and the apparent leveling off of values below this temperature. The estimated effective flow coefficient is very sensitive to slight variations in pressure and the fluctuations present within the natural spline fit to the entire pressure versus time curve artificially introduced oscillations in the calculated values (Figure 5.14 and 5.15). To avoid this, pressure versus time data was refit with a 3rd order polynomial within the range of pressures between full valve opening and the beginning of the transition from theoretical choked flow (Figure 5.16). The data was fit by minimizing the sum of the absolute error between the measured and estimated pressure versus time curves using the GRG solver within Excel and a standard 3rd order polynomial:

$$P_c = a_1 t^3 + a_2 t^2 + a_3 t + a_4 \tag{5.8}$$

Where a_1, a_2, a_3, and a_4 are fit coefficients and t is time. This provided a smoothed curve to be used for the analysis of blowdown test results. The 0.100" lift data was fit

between 15 and 75 lb/in^2 with an intended focus range of 20 to 70 lb/in^2. The 0.050" lift data was fit between 25 and 95 lb/in^2 with an intended focus range of 20 to 90 lb/in^2. These ranges are based on analyzing the mass flow rates throughout the blowdown process and determining when the valve was fully opened. It was assumed that the valve had fully opened when the mass flow rate changed proportionally to chamber pressure as predicted using Equation 5.7 (Figure 5.4). The minimum error producing coefficients for the polynomial fits are listed in Table 5.3. The natural spline fit was used for estimates outside these pressure ranges.

Interpolating between the pressures calculated using the polynomial fits, the effective flow coefficients were calculated and compared for each of the port, lift, and compressible gas combinations and averaged for the 5 datasets. Figures 5.17 to 5.20 compare the effective flow coefficient, C_{ef}, between the original and modified ports for both lift values and both gases using the individual datasets and the average. Figure 5.21 presents the percentage gained or lost in average flow coefficient for the port modification as a function of chamber pressure.

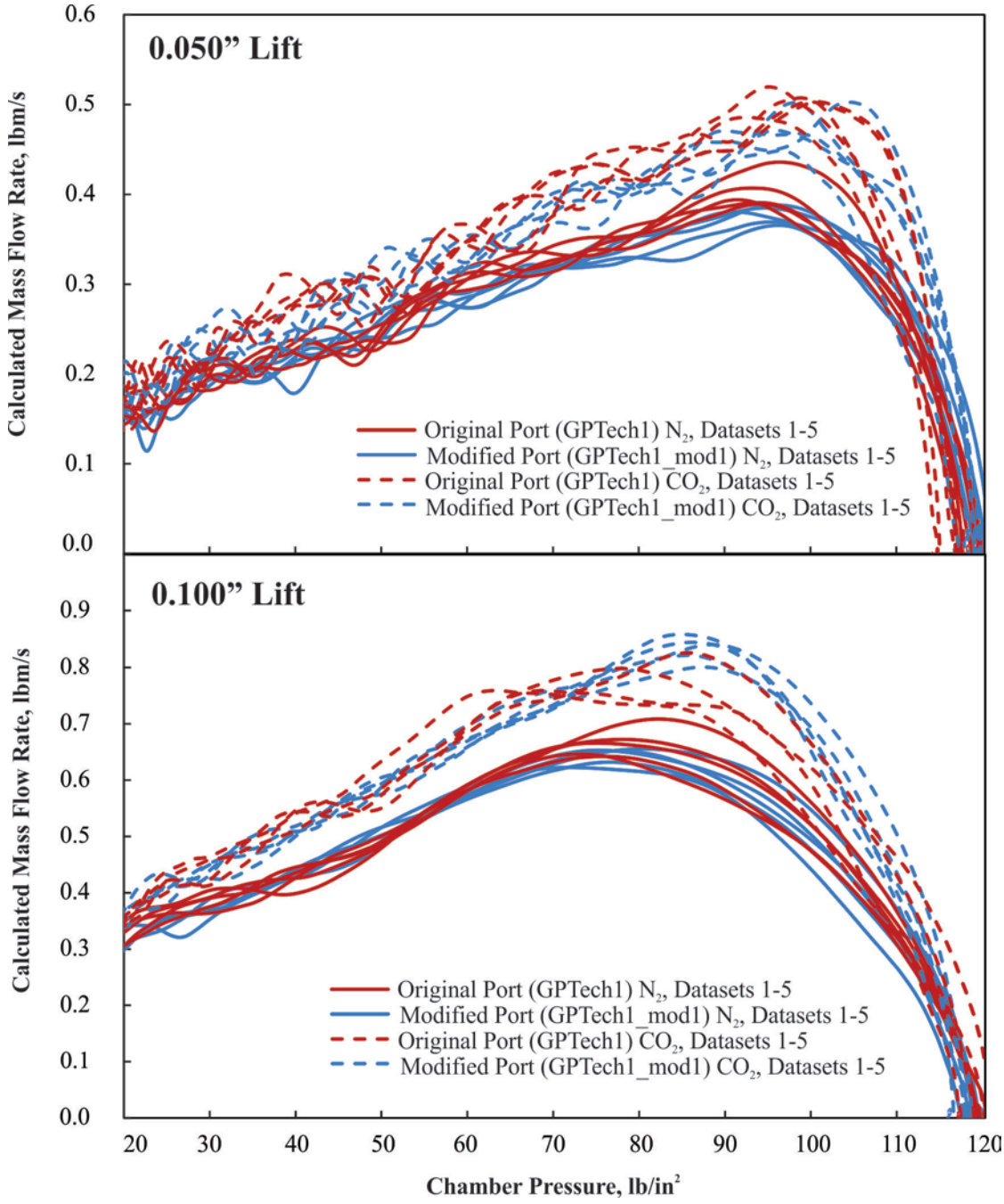

Figure 5.14. Calculated mass flow rates for spline fits for 0.050” and 0.100”

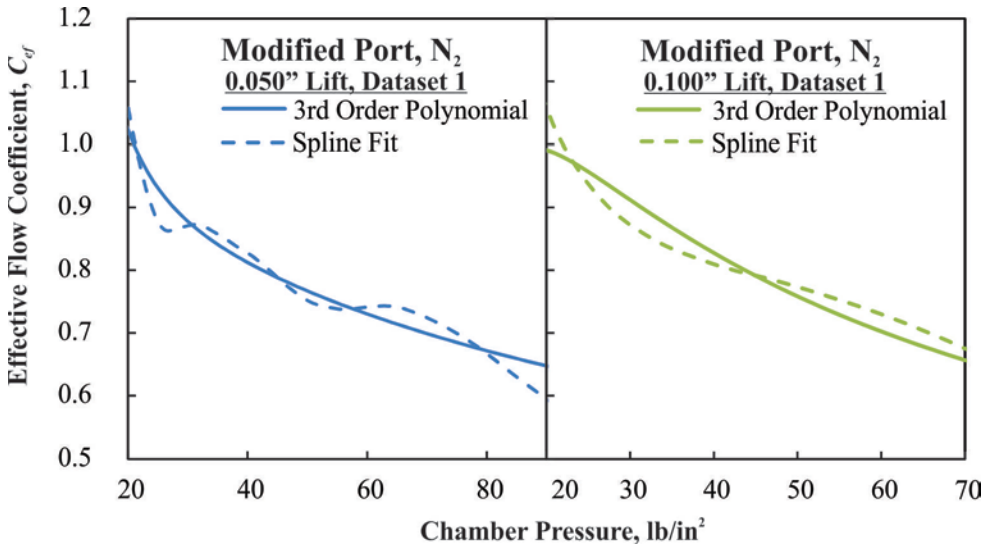

Figure 5.15. Example flow coefficients calculated for spline and polynomial fits for 0.050" and 0.100" lifts using N_2.

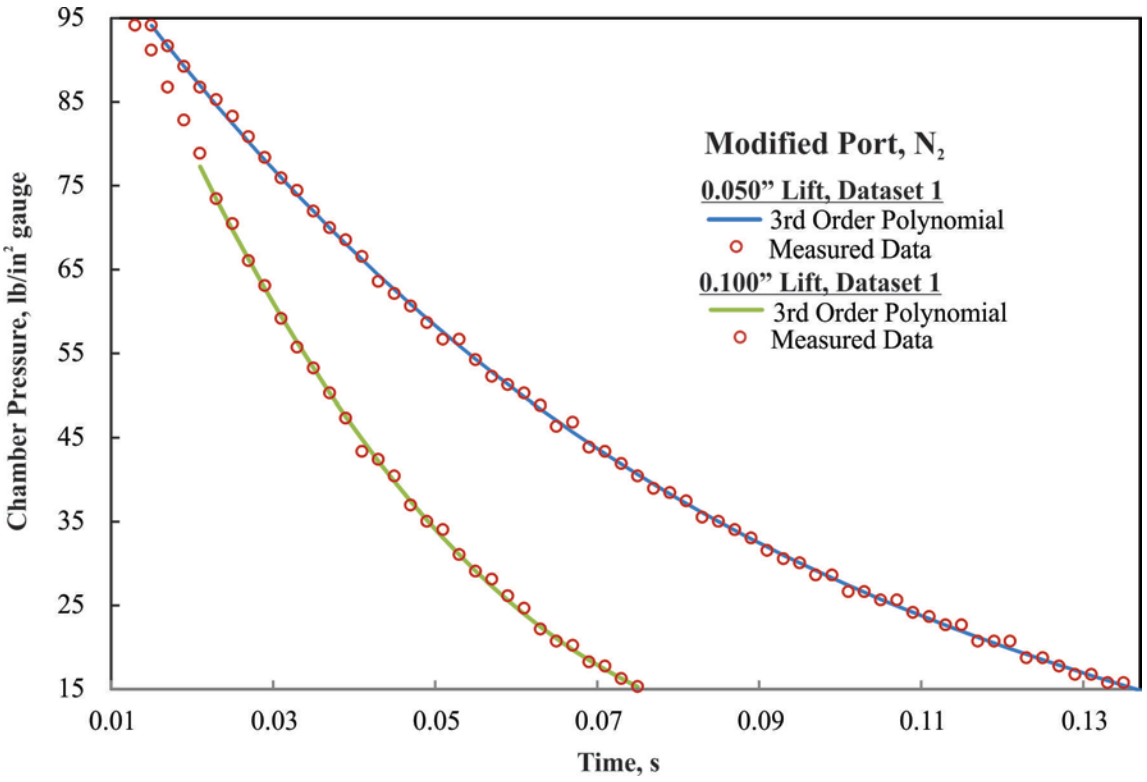

Figure 5.16. Example polynomial fits for 0.050" and 0.100" lifts using N_2.

0.050" Lift, N_2

Modified Port (GPTECH1_mod1)

	a_1	a_2	a_3	a_4
Dataset 1	-15430.31	7173.78	-1377.71	107.19
Dataset 2	-15033.43	7296.70	-1410.85	108.45
Dataset 3	-17896.19	8056.05	-1457.23	107.41
Dataset 4	-20341.63	8401.27	-1461.37	107.83
Dataset 5	-18091.29	8041.93	-1456.74	108.49

Original Port (GPTECH1)

	a_1	a_2	a_3	a_4
Dataset 1	-21999.88	8754.45	-1496.73	109.38
Dataset 2	-21350.73	8936.63	-1529.02	109.02
Dataset 3	-19341.53	8520.77	-1507.30	108.67
Dataset 4	-24782.81	9497.61	-1546.69	108.17
Dataset 5	-22317.49	8928.99	-1513.35	109.00

0.100" Lift, N_2

Modified Port (GPTECH1_mod1)

	a_1	a_2	a_3	a_4
Dataset 1	-41451.03	19075.18	-2527.83	112.98
Dataset 2	-118671.86	30670.92	-3079.18	121.73
Dataset 3	-35882.80	18791.24	-2502.33	110.33
Dataset 4	-120855.92	29285.20	-2904.58	115.95
Dataset 5	-94232.08	25854.27	-2764.55	112.95

Original Port (GPTECH1)

	a_1	a_2	a_3	a_4
Dataset 1	-196296.89	38798.39	-3292.01	120.96
Dataset 2	-121842.75	28512.80	-2774.32	108.92
Dataset 3	-83333.81	24202.24	-2645.47	108.97
Dataset 4	-124406.29	28095.29	-2753.27	110.72
Dataset 5	-96280.65	26673.50	-2865.22	117.67

0.050" Lift, CO_2

Modified Port (GPTECH1_mod1)

	a_1	a_2	a_3	a_4
Dataset 1	-7965.54	4446.36	-1072.32	110.69
Dataset 2	-8560.26	4640.23	-1087.34	108.98
Dataset 3	-6192.40	3858.36	-1017.43	108.15
Dataset 4	-7250.11	4226.91	-1052.43	108.14
Dataset 5	-7458.10	4216.24	-1040.42	108.44

Original Port (GPTECH1)

	a_1	a_2	a_3	a_4
Dataset 1	-8400.46	4636.43	-1091.39	107.60
Dataset 2	-9915.75	4976.07	-1106.99	108.18
Dataset 3	-7024.69	4154.78	-1043.07	106.92
Dataset 4	-7450.28	4353.49	-1074.60	108.17
Dataset 5	-6595.51	4151.97	-1061.49	107.82

0.100" Lift, CO_2

Modified Port (GPTECH1_mod1)

	a_1	a_2	a_3	a_4
Dataset 1	-30883.35	12492.22	-1932.48	111.68
Dataset 2	-39511.18	14136.15	-2036.11	113.81
Dataset 3	-39471.20	14767.10	-2096.71	113.81
Dataset 4	-24877.84	11715.92	-1914.44	111.62
Dataset 5	-29900.20	12657.64	-1984.22	114.71

Original Port (GPTECH1)

	a_1	a_2	a_3	a_4
Dataset 1	-50898.39	17107.52	-2305.37	123.31
Dataset 2	-64890.51	18495.87	-2234.68	114.82
Dataset 3	-47235.36	15777.45	-2146.74	116.51
Dataset 4	-38418.50	14265.27	-2069.63	115.35
Dataset 5	-69240.38	19677.03	-2376.59	121.56

Table 5.3. Polynomial fit coefficients (Equation 5.8) for pressure versus time blowdown test measurements.

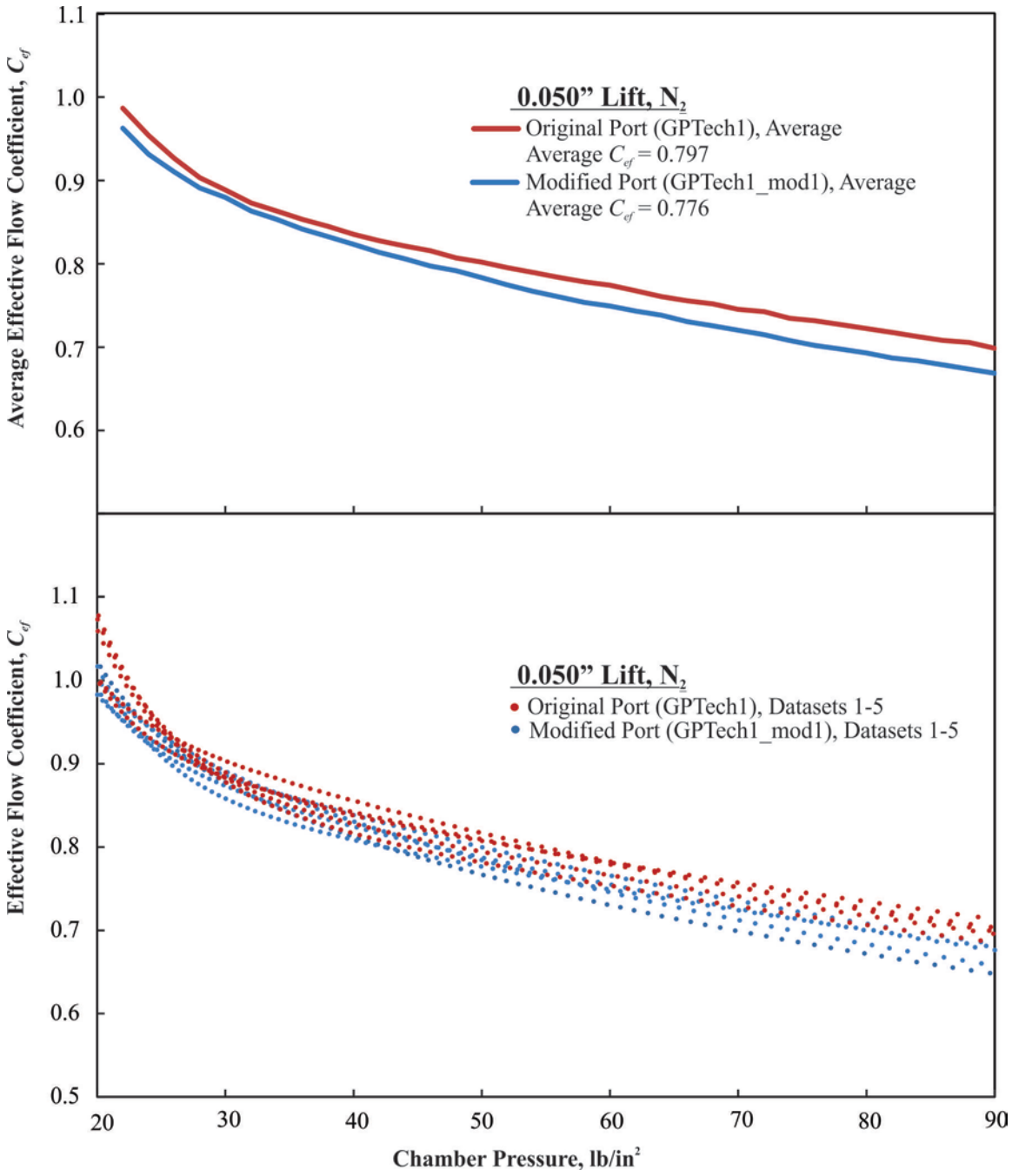

Figure 5.17. Individual dataset and average flow coefficients for 0.050" lift using N_2.

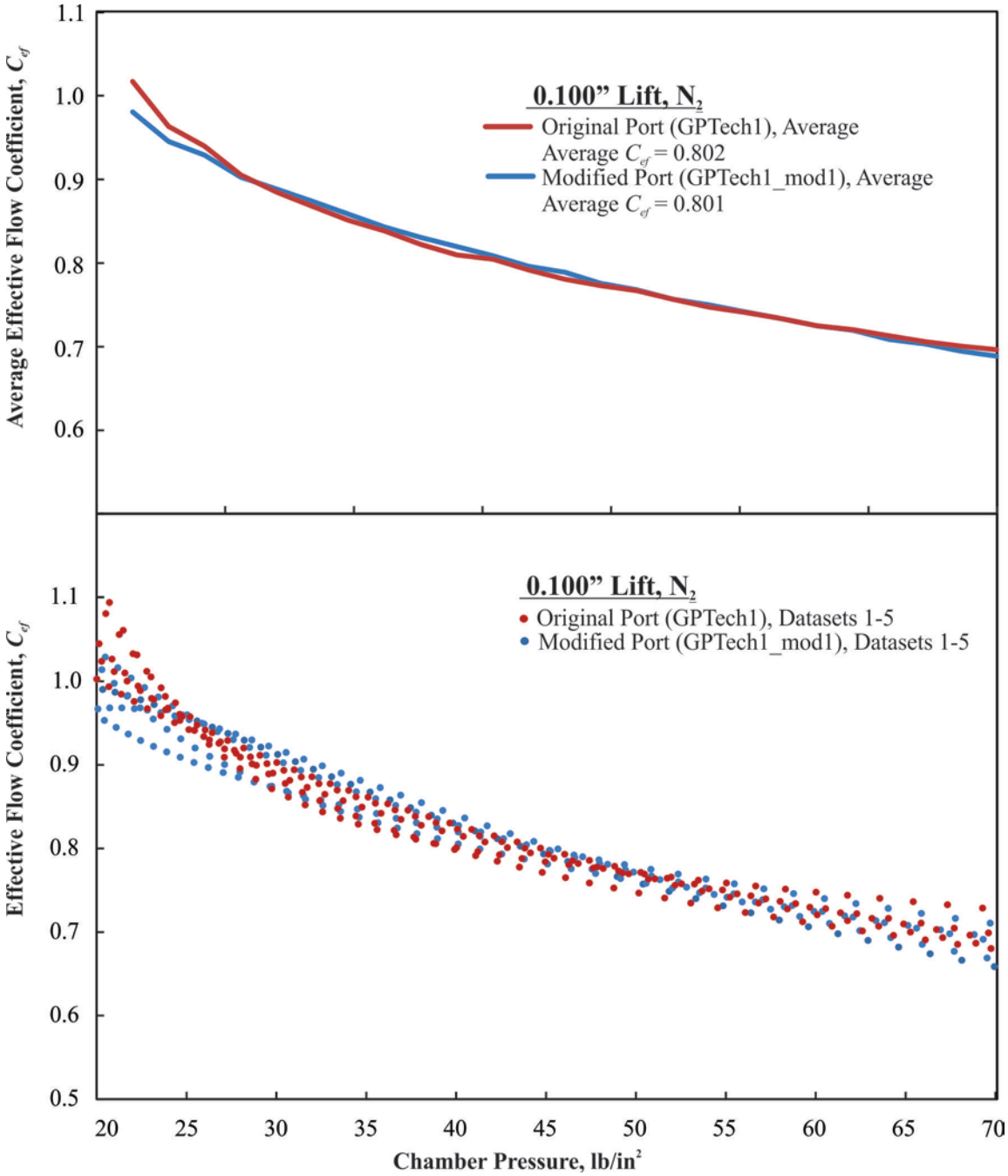

Figure 5.18. Individual dataset and average flow coefficients for 0.100" lift using N_2.

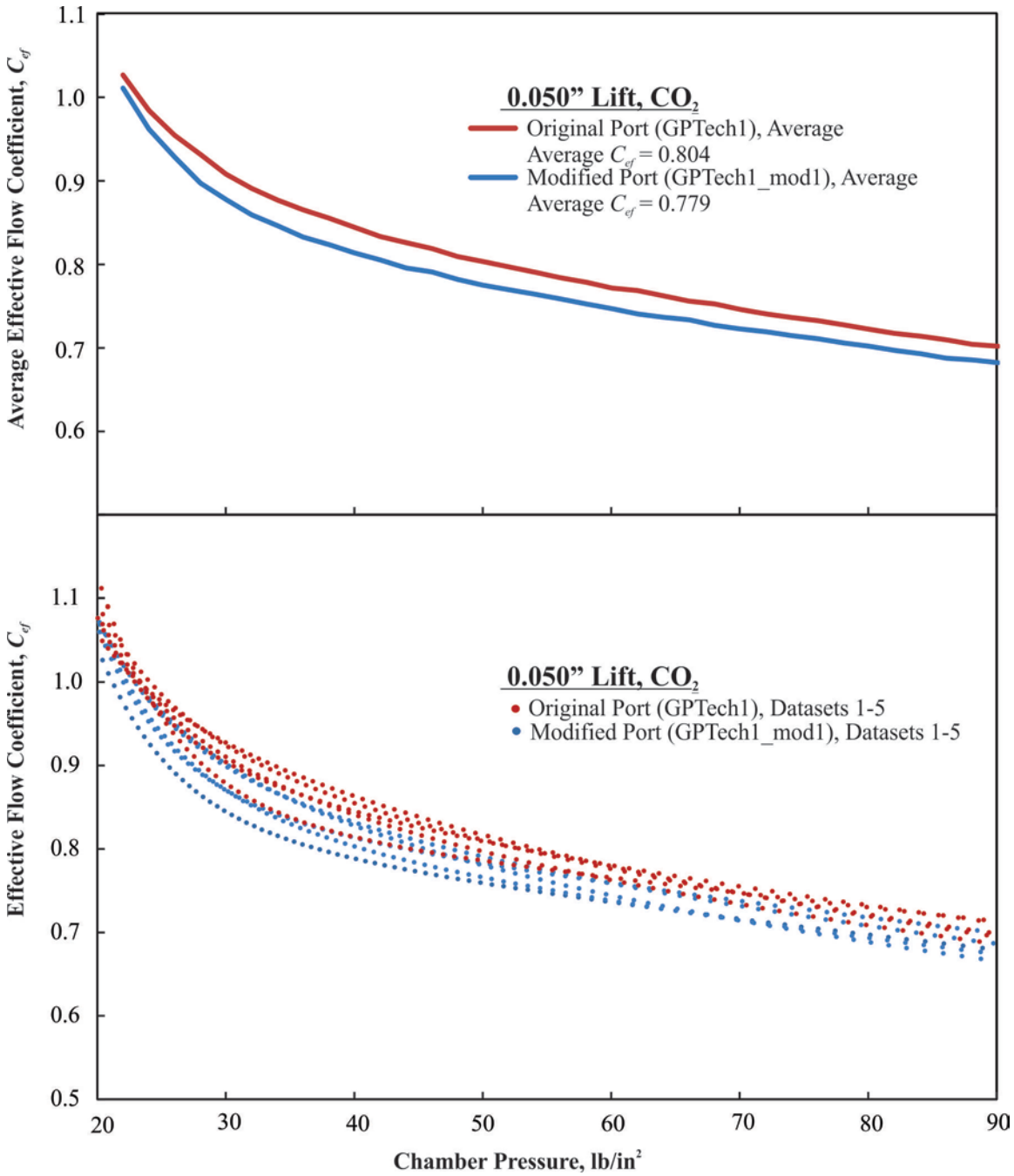

Figure 5.19. Individual dataset and average flow coefficients for 0.050" lift using CO_2.

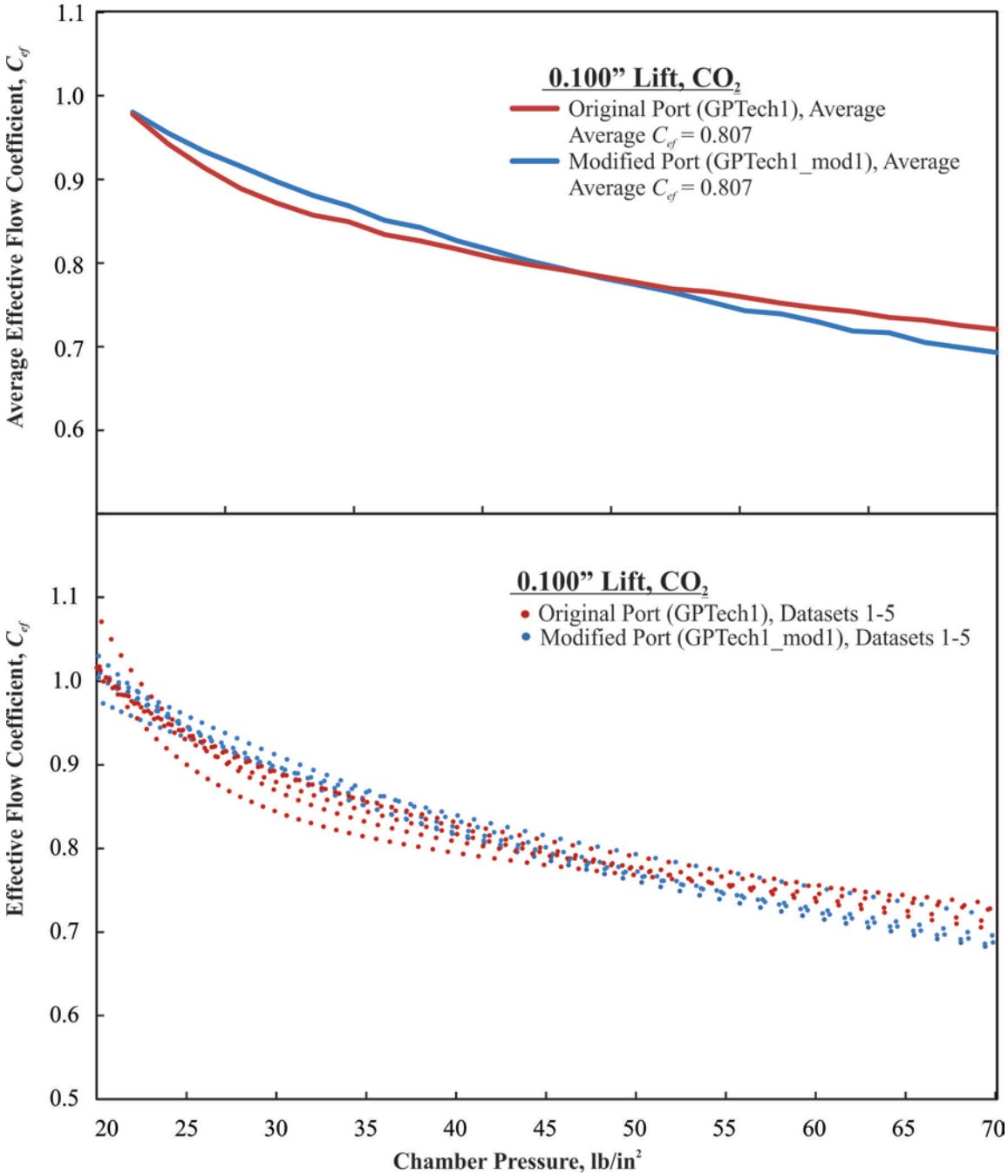

Figure 5.20. Individual dataset and average flow coefficients for 0.100" lift using CO_2.

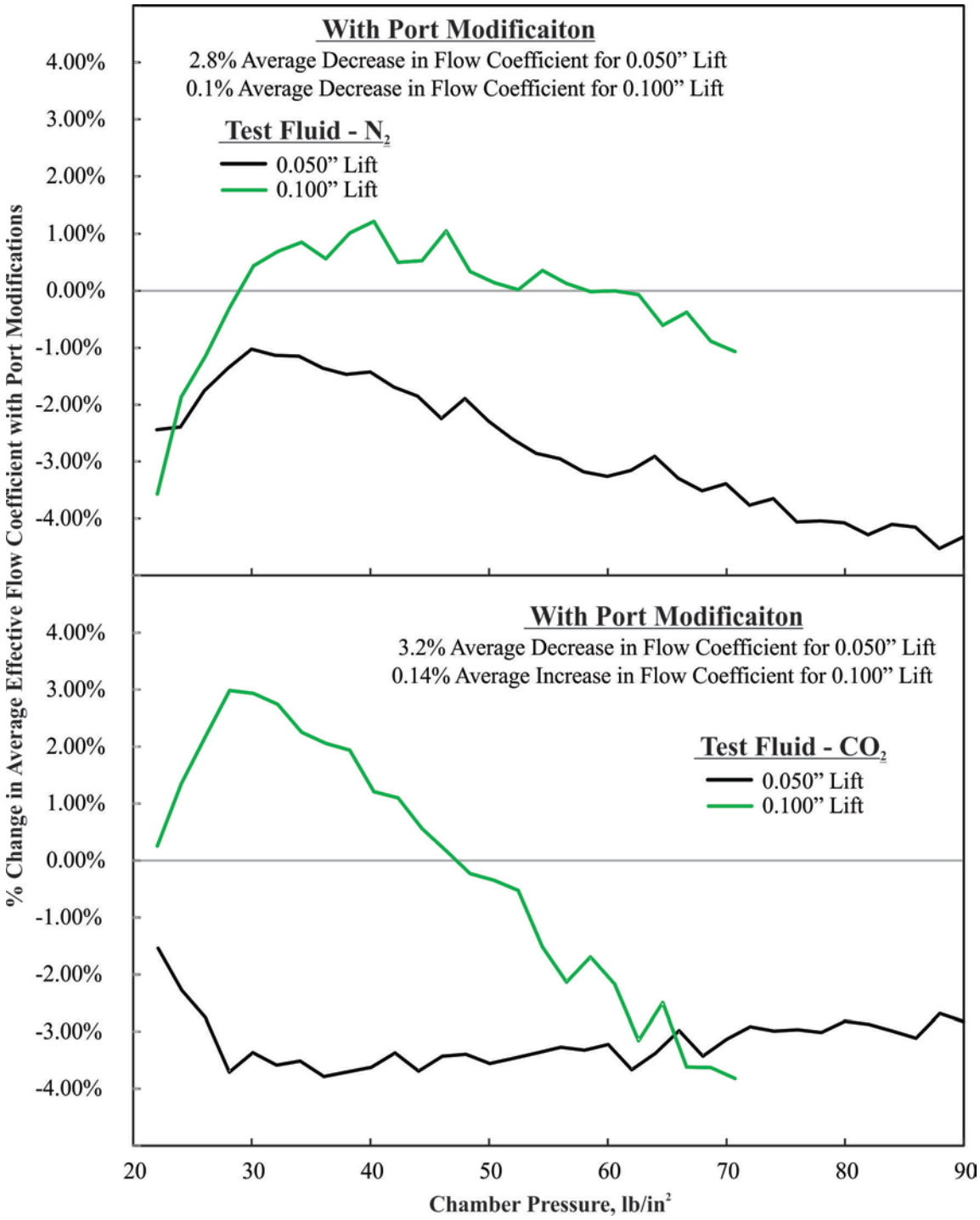

Figure 5.21. Percentage gained or lost in average flow coefficient, C_{ef}, due to port modifications.

The blowdown test results (Figures 5.17 to 5.20) show that, when using nitrogen as the test gas, the measured flow coefficient (C_{ef}) averaged over the range of chamber pressures analyzed was decreased 2.8% at 0.050" lift and was decreased 0.1% at 0.100"

lift by the port modifications. The average effective flow coefficients over the range of pressures analyzed for 0.050" lift were 0.797 and 0.776 for the original and modified port, respectively. The average effective flow coefficients over the range of pressures analyzed for 0.100" lift were 0.802 and 0.801 for the original and modified port, respectively. When using carbon dioxide as the test gas, the average flow coefficient was decreased 3.2% at 0.050" lift and decreased 0.14% at 0.100" lift by the port modifications. The average effective flow coefficients over the range of pressures analyzed for 0.050" lift were 0.804 and 0.779 for the original and modified port, respectively. The average effective flow coefficients over the range of pressures analyzed for 0.100" lift were 0.807 and 0.807 for the original and modified port, respectively. The general trend is for the original port (GPTech1) to outperform the modified port (GPTech1_mod1) with larger differences at higher pressures.

For the lower lift value of 0.050", the differences in measured performance were greater than for lift values of 0.100". For higher pressures, the original port consistently outperformed the modified port. For 0.050" lift values, this held true for all pressures within the focal range with decreases in the magnitude of differences at lower pressures. For 0.100" lift values, the original port outperforms the modified at high pressures, then at pressures below approximately 45 to 50 lb/in^2, the modified port appears to be more efficient. This indicates that the potential effects of local pressure rises around the valve during critical flow may be dependent upon upstream pressure and increased flow rates.

An additional, simplistic measure of port efficiency was used to compare the modified and original port geometries. The elapsed time between several pressure drop

ranges was calculated by interpolating between the pressures calculated using the polynomial fit data:

$$\Delta t = t_2 - t_1 \tag{5.9}$$

where t_2 and t_1 are the interpolated testing times when P_2 and P_1 are achieved within the chamber, respectively. The percent change in time for each pressure drop and port geometry was calculated for the different lifts and gases and the results for the five datasets were averaged for each combination (Tables 5.4 to 5.7).

0.050" Lift, N_2

P_1 (lb/in^2)	P_2 (lb/in^2)	t_2-t_1, Δt (s)		% Change
		Modified Port	Original Port	w/ Mod.
90.0	85.0	0.004155	0.003972	4.60%
85.0	80.0	0.004367	0.004182	4.41%
80.0	75.0	0.004607	0.004420	4.23%
75.0	70.0	0.004879	0.004695	3.93%
70.0	65.0	0.005194	0.005008	3.72%
65.0	60.0	0.005558	0.005376	3.40%
60.0	55.0	0.005987	0.005809	3.06%
55.0	50.0	0.006500	0.006329	2.71%
50.0	45.0	0.007123	0.006961	2.32%
45.0	40.0	0.007893	0.007747	1.89%
40.0	35.0	0.008866	0.008732	1.54%
35.0	30.0	0.010122	0.009987	1.34%
30.0	25.0	0.011759	0.011573	1.61%
25.0	20.0	0.013873	0.013461	3.07%
			Average % Change =	3.0%

Table 5.4. Elapsed time analysis of blowdown testing for 0.050" lift using nitrogen.

0.100" Lift, N_2

P_1 (lb/in^2)	P_2 (lb/in^2)	t_2-t_1, Δt (s) Modified Port	t_2-t_1, Δt (s) Original Port	% Change w/ Mod.
70.0	65.0	0.002721	0.002684	1.37%
65.0	60.0	0.002893	0.002888	0.19%
60.0	55.0	0.003101	0.003083	0.60%
55.0	50.0	0.003330	0.003328	0.07%
50.0	45.0	0.003615	0.003659	-1.20%
45.0	40.0	0.003952	0.004028	-1.88%
40.0	35.0	0.004419	0.004460	-0.91%
35.0	30.0	0.004980	0.005061	-1.60%
30.0	25.0	0.005763	0.005754	0.16%
25.0	20.0	0.006900	0.006645	3.83%
			Average % Change =	0.1%

Table 5.5. Elapsed time analysis of blowdown testing for 0.100" lift using nitrogen.

0.050" Lift, CO_2

P_1 (lb/in^2)	P_2 (lb/in^2)	t_2-t_1, Δt (s) Modified Port	t_2-t_1, Δt (s) Original Port	% Change w/ Mod.
90.0	85.0	0.005718	0.005542	3.18%
85.0	80.0	0.006014	0.005824	3.27%
80.0	75.0	0.006356	0.006150	3.36%
75.0	70.0	0.006737	0.006515	3.41%
70.0	65.0	0.007180	0.006938	3.49%
65.0	60.0	0.007692	0.007424	3.62%
60.0	55.0	0.008291	0.007997	3.68%
55.0	50.0	0.009008	0.008677	3.82%
50.0	45.0	0.009862	0.009492	3.89%
45.0	40.0	0.010904	0.010488	3.96%
40.0	35.0	0.012186	0.011717	4.01%
35.0	30.0	0.013761	0.013242	3.92%
30.0	25.0	0.015657	0.015110	3.62%
25.0	20.0	0.017781	0.017302	2.77%
			Average % Change =	3.6%

Table 5.6. Elapsed time analysis of blowdown testing for 0. 050" lift using carbon dioxide.

0.100" Lift, CO_2

P_1 (lb/in^2)	P_2 (lb/in^2)	t_2-t_1, Δt (s)		% Change
		Modified Port	Original Port	w/ Mod.
70.0	65.0	0.003726	0.003606	3.33%
65.0	60.0	0.003957	0.003859	2.55%
60.0	55.0	0.004226	0.004155	1.71%
55.0	50.0	0.004542	0.004506	0.81%
50.0	45.0	0.004923	0.004929	-0.12%
45.0	40.0	0.005386	0.005446	-1.10%
40.0	35.0	0.005966	0.006090	-2.04%
35.0	30.0	0.006714	0.006898	-2.66%
30.0	25.0	0.007712	0.007908	-2.47%
25.0	20.0	0.009112	0.009128	-0.18%
			Average % Change =	0.0%

Table 5.7. Elapsed time analysis of blowdown testing for 0. 100" lift using carbon dioxide.

The elapsed time analysis of the blowdown test results (Tables 5.4 to 5.7) show that, when using nitrogen as the test gas, the averaged elapsed time between 90 and 20 lb/in^2 was increased 3.0% at 0.050" lift and the averaged elapsed time between 70 and 20 lb/in^2 was increased 0.1% at 0.100" lift by the port modifications. When using carbon dioxide as the test gas the averaged elapsed time between 90 and 20 lb/in^2 was increased 3.6% at 0.050" lift and the averaged elapsed time between 70 and 20 lb/in^2 remained the same for 0.100" lift. The general trend is for the original port (GPTech1) to outperform the modified port (GPTech1_mod1). The differences were again greater for the 0.050" lift values than the 0.100" lift values. For 0.100" lift the trend of the original port outperforming the modified port at the higher pressures, then reversing is observed. These findings are in agreement with the averaged effective flow coefficients analysis.

5.4 Conclusions of Task 2

An experimental testing apparatus was designed and constructed to test the blowdown performance of an original (GPTech1) and a modified (GPTech1_mod1)

Chevrolet SB2.2 cylinder head port using compressed gas. Two lift values, 0.050" and 0.100", were tested as well as two gas types, carbon dioxide and nitrogen. For 0.050" lift the port modifications reduced the average effective flow coefficient by 2.8% and 3.2% for nitrogen and carbon dioxide respectively. For 0.100" lifts, the results due to the port modifications were less conclusive with a measured 0.1% decrease in average effective flow coefficient using nitrogen and a 0.14% decrease when using carbon dioxide. There was a notable difference in flow rate and estimated flow coefficients when using nitrogen versus carbon dioxide; however, testing results were in agreement. Therefore, testing with either gas could be expected to produce similar delineations between test ports.

The more simplistic approach to evaluating port efficiency of analyzing the elapsed time between calculated pressure range drops resulted in very similar results. On average, the elapsed time between 90 to 20 lb/in^2 was increased 3.0% and 3.6% for 0.050" lift using nitrogen and carbon dioxide, respectively. The average elapsed time between 70 and 20 lb/in^2 was increased 0.1% for 0.100" lift using nitrogen and remained the same using carbon dioxide. These results indicate that simply evaluating the pressure versus time curve fits may be sufficient in port evaluation.

Both analysis methods indicated the ports' efficiency was dependent upon pressure. At higher pressures, the results of the 0.050" lift tests displayed higher differences than at lower pressures, but the original port was consistently the most efficient. The efficiency of the modified port surpassed that of the original port at 0.100" lift under lower pressures. At higher pressures, the original port was the most efficient. These results indicate a dependence on pressure and lift in determining the most efficient port during blowdown.

CHAPTER 6 - TASK 3: STEADY FLOW TESTING OF HIGH PERFORMANCE EXHAUST PORT

A steady flow, low pressure test rig was constructed to measure exhaust port performance under traditionally used testing conditions. These test results are used for comparison with the critical flow tests.

6.1 Experimental Apparatus and Setup

To maintain consistent conditions near the valve and port, the steady flow air rig used the fixed volume combustion chamber from Task 1 as its base. Additional flow piping, a plenum, and pump were used to provide a 28" H_2O pressure difference across the valve opening.

6.1.1 Flow Piping and Plenum

Two sections were made from 3" Schedule 40 PVC pipe to connect the chamber to the plenum. Section 1 was epoxied to a machined PVC flange (Figure 6.1C) and a Lasco 3" PVC socket flange (Figure 6.2). The irregular pentagonal bolt pattern in the PVC flange was used to bolt the section to the combustion chamber. The thru hole has a diameter of 3.068" to match the inner diameter of the 3" pipe. Pipe section 2 was epoxied to a machined PVC flange (Figure 6.1A) and a Lasco 3' PVC socket flange. A hexagonal 1/4" bolt pattern was used to bolt the section to the plate (Figure 6.1B) attached to the top of the plenum. The thru holes in these pieces have a diameter of 3.5" to match the outer diameter of the pipe. This pipe was passed through the flange and plate and epoxied in place extending halfway into the plenum.

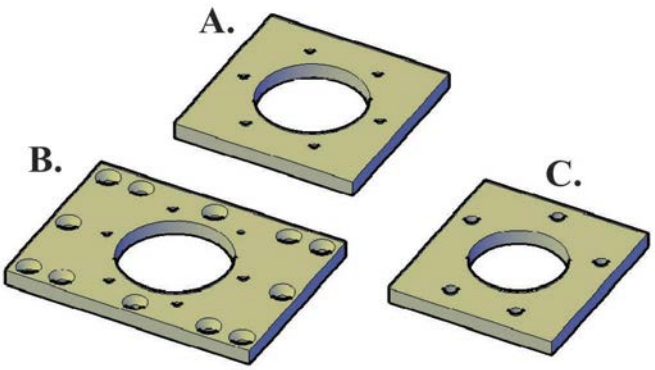

Figure 6.1. Steady Flow Setup Adapter Plates: A. PVC Section 1 to Plenum, B. Plenum Adapter, C. PVC Section 1 to Combustion Chamber.

The plenum is a high density polyethylene 30 gallon barrel. A 3.625" hole is cut into the top and an aluminum plate (Figure 6.1B) is attached to the top using 3/8" bolts and silicone sealant. To assemble the piping system, pipe section 1 is bolted to the chamber bottom, pipe section 2 is inserted and bolted to the plenum, a flow orifice and two rubber gaskets are placed between the two PVC socket flanges and the two flanges are held together using four 5/8" bolts. Additionally, a 1.5" PVC pipe is attached to the barrel and used to pump air into the plenum (Figure 6.3). The system was capped with the top plate used for the combustion testing and pressurized to ensure the system was adequately sealed (Figure 6.6).

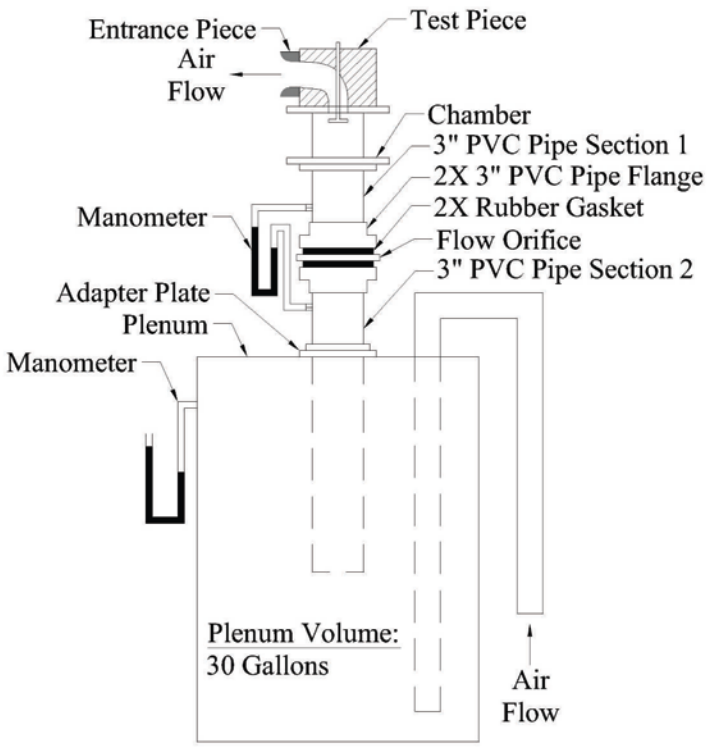

Figure 6.3. Steady Flow Test Arrangement.

6.1.2 Flow Measurement Setup

The square-edged flow orifice used for the steady flow testing was designed according to the Flow Meter Engineering Handbook [3]. The required maximum flow rate was determined to be 100 ft^3/min using Weld Tech's flow information for the exhaust port (Figure 5.3). The maximum pressure measurement of the inclined manometer used for testing is 8", which is well within the maximum recommended pressure difference across the orifice of 13.25" for a 1.01 lb/in^2 operating pressure and this flow rate. Using these values and the methodology found for gas flow orifice design within the reference text, the appropriate orifice bore diameter was calculated to be 1.598". The full calculations and required constants and conditions are listed in

Appendix B. The plate was machined from 0.100" aluminum and held in place by the 3" pipe flanges (Figure 6.3).

For the pipe size, flange taps for pressure measurements were recommended and used. Ideally, pressure taps would be placed 1.00" upstream and downstream of the orifice plate; however the pressure taps were placed approximately 1.25" upstream and downstream due to the pipe flange configuration. Therefore, a calibration of the flow measurements was required.

Pressure within the plenum was measured using a Dwyer vertical manometer with a maximum pressure of 36" of H_2O. For increased precision, the pressure drop across the orifice plate was measured using a Meriam Instrument (Model # 40HE35WM) 8"/50" inclined manometer with a maximum pressure of 8" H_2O (Figure 6.4).

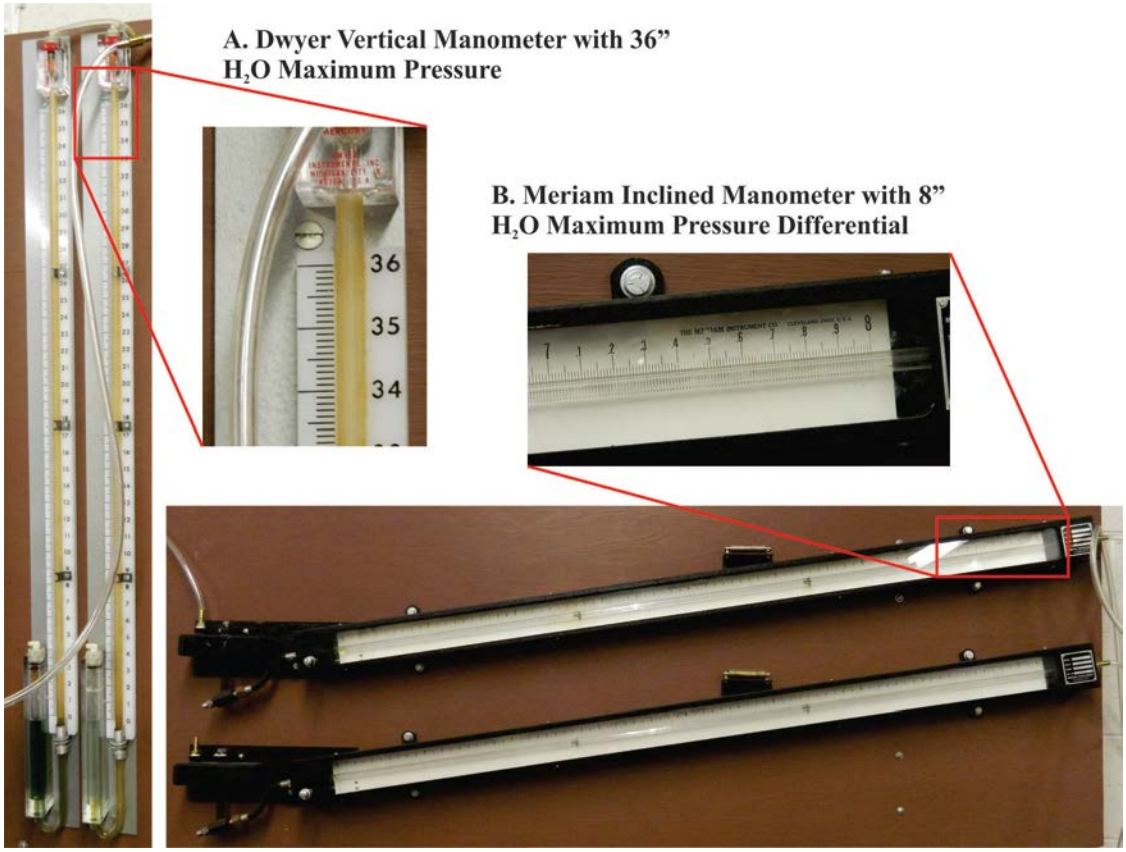

Figure 6.4. Manometers used for steady flow testing of exhaust port.

6.1.3 Valve and Exhaust Port Test Piece

The same cylinder head and extension piece used for simulated blowdown testing in Task 2 was used for the steady flow testing so results could be compared. The original port designed and machined by Weld Tech (GPTech1) was tested alongside an adjacent port (GPTech1_mod) that had been modified to increase flow on a traditional flow bench setup and decrease the volume of the port near the valve seat (Figures 5.4 to 5.6). The valve was held open at the desired lift using a custom holder and a modified depth micrometer (Figure 6.5).

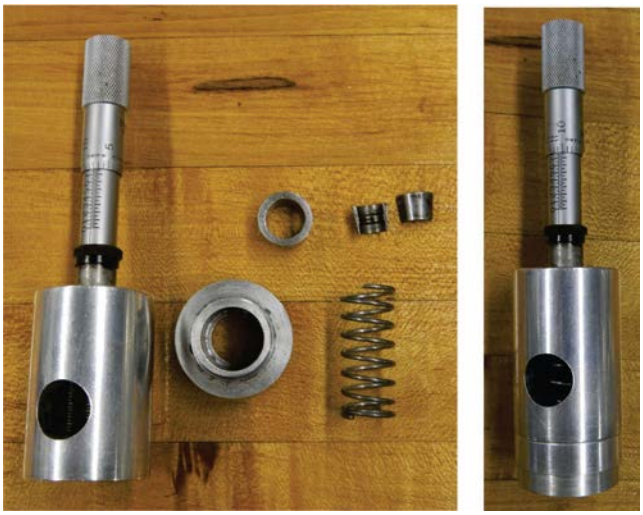

Figure 6.5. Custom valve holder used for steady flow testing.

6.1.4 Finished Experimental Setup

Figures 6.6 and 6.7 are photographs taken of the finished experimental setup for the steady flow testing of exhaust ports.

Figure 6.6. Finished steady flow test rig with chamber top in place for pressure testing.

Figure 6.7. Finished steady flow test rig with cylinder head attached.

6.2 Experimental Procedure

The experimental steady flow testing was completed as follows (references Figure 6.3 unless noted):

1. The exhaust valve is opened at the desired lift
2. The air pump is turned on.
3. The air flow is adjusted using a ball valve in line with the air pump on the 1.5" PVC pipe leading into the plenum until the manometer indicates a pressure within the plenum of 28" H_2O.
4. The pressure drop across the flow orifice is recorded and a corresponding flow rate is calculated.
5. The air pump is turned off.
6. Steps 1-5 are repeated for the desired range of lifts.

6.3 Results and Discussion

The flow rates for the original (GPTech1) and modified (GPTech1_mod1) exhaust port geometries were measured for lift values of 0.050", 0.100", and 0.125" using the steady flow air rig described. The flow coefficient, *C*, for the sharp-edged flow orifice was calculated as 0.685 using the traditional flow bench performance of the modified port at 0.100" lift (Table 5.3) and the standard orifice equation:

$$Q_f = CA\sqrt{\frac{2\Delta p}{\rho}} \text{ or } C = \frac{Q_f}{A\sqrt{\frac{2\Delta p}{\rho}}} \tag{6.1}$$

where Q_f is the flow rate through the orifice (57.7 ft^3/min or 0.962 ft^3/s), A is the cross sectional area of the orifice (2.01 in^2 or 0.0139 ft^2), Δp is the pressure drop across the orifice (2.41" H2O or 12.53 lb/ft^2), and ρ is the density of air at operating pressure

(0.00247 slugs/ft^3 @ 28" H_2O). The orifice flow coefficient was used to calculate a flow rate for each lift value using the measured pressure drop across the orifice. Equation 6.1 was then used to calculate a flow coefficient for the valve for each lift value. These valve flow coefficients were used to calculate corrected flow values for pressure drops across the valve other than 28" H_2O using equation 6.1. Table 6.1 and Figure 6.8 show the results for the steady flow testing of the original and modified GPTech1 exhaust ports.

		GPTech1 (Original Port)			**GPTech1_mod1 (Modified Port)**		
	Flow Area	Δp, Orifice	Δp, Valve	Flow Coef	Δp, Orifice	Δp, Valve	Flow Coef
Lift (in.)	A (ft^2)	(in. H_2O)	(in. H_2O)	C	(in. H_2O)	(in. H_2O)	C
0.050	0.00177	0.54	28.0	0.747	0.62	28.0	0.801
0.100	0.00355	2.14	28.0	0.744	2.41	28.0	0.789
0.125	0.00443	3.35	26.8	0.761	3.48	27.3	0.769

Table 6.1. Steady flow testing results for GPTech1 and GPTech1_mod1 exhaust ports.

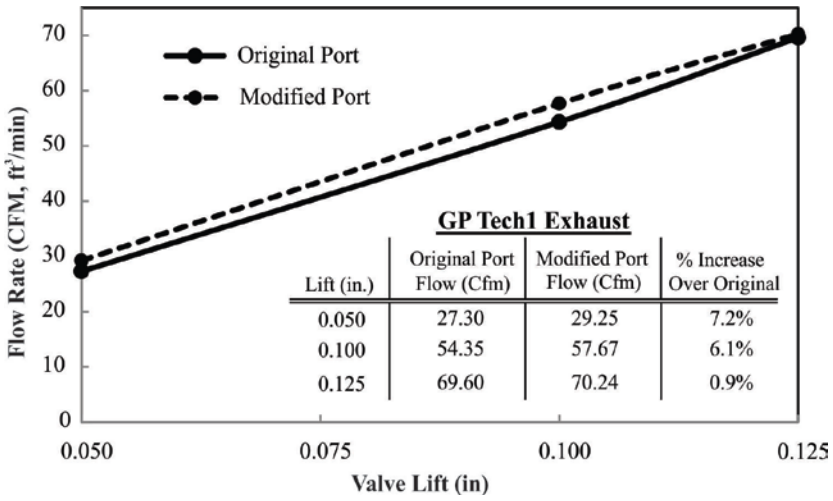

Figure 6.8. Corrected flow rates for original and modified GPTech1 exhaust ports.

As shown the modifications to the port geometry increased flow rates at the lower lifts by as much as 7.2%. As lift values increase to 0.125", the effects of adding material in the port near the valve seat resulting in pressure recovery dissipated to 0.9%. These results are consistent with typical intake port improvement techniques.

6.4 Conclusions of Task 3

A steady flow air rig was designed and constructed to measure the flow rate of two exhaust port geometries. Using the same stainless steel chamber as its base, the rig allows testing of exhaust ports in near identical geometric conditions as used for the blowdown testing in Task 2. The flow orifice was designed for low lifts and flow rates up to 100 cfm. The modified exhaust port (GPTech1_mod1) was found to have low lift flow rates 7.2% higher at 0.050" lift than the original port (GPTech1). The improvements fade to 6.1% at 0.100" lift and then to 0.9% at 0.125" lift. These results are as anticipated using the same techniques to achieve pressure recovery downstream of the valve that are successful in producing performance increases for intake ports under steady flow, low pressure testing.

CHAPTER 7 - COMPARISON OF TESTING METHODS

The testing methods used for comparing the performance of the modified (GPTech1_mod1) and original (GPTech1) exhaust ports (Figures 5.4 and 5.5, Table 5.2) include a traditional flow bench, a custom designed steady flow, low pressure air rig (Figure 6.6 and 6.7), and an experimental blowdown testing apparatus which utilizes compressed gas (Figure 5.10). The feasibility of the use of lean hydrogen combustion products was also investigated, but the repeatability of consistent testing conditions was compromised due to high heat losses to the chamber causing rapid cooling of the gases.

Measurements taken using the custom, steady flow air rig show increases in calculated flow coefficients (Figure 6.8) for the lift values tested (0.050" to 0.125") for the modified port (GPTech1_mod1) over the original (GPTech1). The increases were 7.2% at 0.050" lift, 6.1% at 0.100" lift, and 0.9% at 0.125" lift. These results are in agreement with the traditional flow bench results which showed an increase in flow coefficient of 6.6% for the modified port at 0.100" lift. The results using the traditional flow bench at lower lifts were inconclusive due to poor readability at these lower pressure measurements.

Test results obtained using the blowdown testing apparatus show decreases in the calculated flow coefficient for the modified port (GPTech1_mod1). Using compressed nitrogen, the port modifications resulted in a decrease in average effective flow coefficient of 2.8% and 0.1% for 0.050" lift and 0.100" lift, respectively. Using compressed carbon dioxide, the modified port showed decreased average effective flow coefficients of 3.2% at 0.050" lift and 0.14% at 0.100". Analyzing the elapsed time between ranges of pressure drops resulted in similar results with 3.0% and 3.6% increases

in elapsed time for 0.050” lift using nitrogen and carbon dioxide, respectively. The results at 0.100” were less conclusive with an increase of 0.1% using nitrogen and no calculated difference using carbon dioxide. These results and results from the other testing methods are summarized in Table 7.1.

Traditional Flow Bench

Measured Flow Rate in (ft^3/min)

Lift	Original Port (GPTech1)	Modified Port (GPTech1_Mod1)	% Change w/ Mod.
0.05*	29.4	29.4	0.0%
0.1"	54.2	57.7	6.6%

*Measurements at 0.050" lift are inaccurate with 400 CFM orifice plate

Steady-Flow Air Rig

Measured Flow Rate in (ft^3/min)

Lift	Original Port (GPTech1)	Modified Port (GPTech1_Mod1)	% Change w/ Mod.
0.05"	27.3	29.3	7.2%
0.1"	54.4	57.7	6.1%

Compressed Gas Blowdown (N_2)

Measured Average Effective Flow Coefficient, C_{ef}

Lift	Original Port (GPTech1)	Modified Port (GPTech1_Mod1)	% Change w/ Mod.
0.05"	0.797	0.776	-2.8%
0.1"	0.802	0.801	-0.1%

Elapsed Time Between High and Low Pressures

Lift	Original Port (GPTech1)	Modified Port (GPTech1_Mod1)	% Change w/ Mod.
0.05"	0.09825	0.10088	3.0%
0.1"	0.04167	0.04159	0.1%

Compressed Gas Blowdown (CO_2)

Measured Average Effective Flow Coefficient, C_{ef}

Lift	Original Port (GPTech1)	Modified Port (GPTech1_Mod1)	% Change w/ Mod.
0.05"	0.804	0.779	-3.2%
0.1"	0.807	0.807	-0.1%

Elapsed Time Between High and Low Pressures

Lift	Original Port (GPTech1)	Modified Port (GPTech1_Mod1)	% Change w/ Mod.
0.05"	0.13715	0.13242	3.6%
0.1"	0.05627	0.05652	0.0%

Table 7.1. Steady flow testing results for GPTech1 and GPTech1_mod1 exhaust ports.

The testing also indicated the effective flow coefficient's dependence on upstream pressure. At higher pressures the original port was consistently more efficient; however as pressure decreased the measured differences began to decrease. In the case of 0.100" lift, the modified port had a higher flow coefficient for the lower range of chamber pressures. This would indicate that at higher pressures, the increase in flow rates results in less efficient port performance possibly due to higher localized pressures downstream of the curtain area.

The results in Table 7.1 show that the decreased port volume and flow area of the modified port produces a general trend of decreased performance during low lift blowdown, while indicating an increased performance during low pressure, steady flow. These decreases could translate into increased cylinder pressures during the exhaust stroke resulting in increased pumping work losses [15]. The decreased blowdown ability of the port may explain, at least partially, the discrepancies between steady flow testing results and actual engine performance.

Additional benefits of an increased area and volume within the exhaust flow path were investigated using Performance Trend's Engine Analyzer v3.4 software. The performance of a stock and modified 1998 NASCAR Cup engine were predicted. The modified version increased the exhaust flow path's diameter 2.6% from 1.90" to 1.95", which increased the flow area by 5.3%. The predicted engine power decreased at engine speeds below 5,000 RPM and increased power for engine speeds above 7,500 RPM. Over the typical operating range of 7,000 to 10,000 RPM the average power increased 3.9 horsepower. This is likely the result of decreased back pressure at higher engine speeds which decreases pumping losses and increases scavenging. Therefore, a portion

of the increased engine performance seen by Weld Tech with the larger exhaust port could be attributable to this phenomenon as well. The results and engine specifications used for these predictions are included in Appendix C.

CHAPTER 8 - CONCLUSIONS

The performances of two automotive exhaust ports were measured using a traditional flow bench, a custom steady flow air rig, and an experimental blowdown testing apparatus. One port was modified using traditional techniques to improve low lift flows of automotive intake ports. The particular head and port was chosen based on communications with designers indicating modifications had been done to the final geometry that decreased its performance using traditional testing methods, while improving its actual performance. Material was added near the valve seat to aid in pressure recovery and decrease losses associated with flow separation. These modifications were completed using information about the original port from the designers. Overall the port volume was decreased from 116.5 cm^3 to 111.0 cm^3 (4.7%).

As anticipated, the performance using steady flow testing improved 7.2% at 0.050" lift and 6.1% at 0.100" lift. Tests conducted using the experimental blowdown testing apparatus showed decreases in average effective flow coefficients of 2.8% and 3.2% at 0.050" lift using nitrogen and carbon dioxide, respectively. Tests conducted at 0.100" lift were less conclusive with a 0.1% decrease in flow coefficient using nitrogen and a 0.14% decrease using carbon dioxide. Tests at 0.100" lift also indicated a higher dependence on upstream pressure on flow coefficients.

The general trend of decreased performance of low lift blowdown resulting from traditionally guided port modification techniques may explain, at least partially, the discrepancies between steady flow testing and engine performance. Additional benefits to the larger port volume and increased flow area were investigated using engine performance predictions for a stock and modified 1998 NASCAR cup engine using

Engine Analyzer v3.4. A 5.3% increase in flow path diameter resulted in power losses at lower engine speeds, but an average increase of 3.9 horsepower over the operating range of 7,000 to 10,000 RPM. This is likely the result of reduced back pressure at high engine speeds and decreases in pumping losses.

Nitrogen and carbon dioxide were both used for the blowdown testing. The results were in agreement with one another, indicating that both gases have similar abilities in deciphering port differences during blowdown. Elapsed time analysis was also used to determine port efficiency and produced similar results to analyzing effective flow coefficients. This simplistic approach may be more appealing if these techniques were adopted into industry. Lastly, the use of lean-hydrogen combustion as a source for increased pressure and fluid property modifications was deemed infeasible for the current testing setup. Heat losses to the chamber cause rapid decreases in temperature and pressure following combustion resulting in inconsistent testing conditions.

REFERENCES

1. Cheers, F., *Elements of Compressible Flow*, John Wiley & Sons LTD., New York, NY, USA, 1963

2. Cunningham, R. G., "Orifice Meters with Supercritical Compressible Flow", Transactions of ASME, July 1951

3. Cusick, C. F., *Flow Meter Engineering Handbook*, 3rd Edition, Minneapolis-Honeywell Regulator Company, Philidelphia, PA, USA, 1961

4. Drell, I. and Belles, F., "Survey of Hydrogen Combustion Properties", T.N. No. 1383, NACA 1957

5. Driskell, L.R., *Control Valve Selection and Sizing*, Instrument Society of America, 1982

6. Eppes, J., Livengood, J. and Taylor, C., "The Effect of Changing the Ratio of Exhaust-Valve Flow Capacity to Inlet-Valve Flow Capacity on Volumetric Efficiency and Output of a Single-Cylinder Engine", T.N. No. 1365, NACA, 1947

7. Fukutani I. and Watanabe E., "Air Flow through Poppet Inlet Valves – Analysis of Static and Dynamic Flow Coefficients", SAE Paper No. 820154, presented at SAE Congress, Detroit, February 1982

8. Heywood, John, *Internal Combustion Engine Fundamentals*, McGraw Hill, New York, NY, USA, 1988

9. Keenan, J., Chao, J., and Kaye, J., *Gas Tables: Thermodynamic Properties of Air, Products of Combustion, and Component Gases; Compressible Flow Functions*, 2nd Edition, John Wiley and Sons, New York, NY, USA, 1980

10. Leydorf, G., Minty, R., and Fingeroot, M., "Design Refinement of Induction and Exhaust Systems Using Steady-State Flow Bench Techniques", SAE paper No. 720214, Automotive Engineering Congress, Detroit, MI, January, 1972

11. Livengood, J. and Eppes, J., "Effect of Changing Manifold Pressure, Exhaust Pressure, and Valve Timing on the Air Capacity and Output of a Four-Stroke Engine Operated with Inlet Valves of Various Diameters and Lifts", T.N. No. 1366, NACA 1947

12. Perry, Jr. J.A., "Critical Flow Through Sharp-Edged Orifices", Transactions of ASME, 1949, 71:737

13. Saad, M., *Compressible Fluid Flow*, 2nd Edition, Prentice Hall, Englewood Cliffs, NJ, USA, 1993

14. Stanitz, J., Lucia, R. and Masselle, F., "Steady- and Intermittent-Flow Coefficients of Poppet Intake Valves", T.N. No.1035, NACA 1946

15. Stone, Richard, *Introduction to Internal Combustion Engines*, 3rd Edition, SAE, Warrendale, PA, USA, 1999

16. Swain, M.R., Filoso, P. and Swain, M.N., "Ignition of Lean Hydrogen-Air Mixtures", Int. J. Hydrogen Energy, 2005, Vol. 30, pg 1447-1455

17. Taylor, Charles, *The Internal Combustion Engine in Theory and Practice*, Volume 1, 2nd Edition, The M.I.T. Press, Cambridge, MA, USA, 1985

18. Taylor, Charles, *The Internal Combustion Engine in Theory and Practice*, Volume 2, Revised Edition, The M.I.T. Press, Cambridge, MA, USA, 1985

19. Turns, Stephen, *An Introduction to Combustion*, 2nd Edition, McGraw Hill, New York, NY, USA, 2000

20. Waldron, C. D., "Intermittent-Flow Coefficients of a Poppet Valve", T.N. No. 701, NACA, 1939

21. Ward-Smith, A.J., "Critical Flowmetering: The Characteristics of Cylindrical Nozzles with Sharp Upstream Edges", Int. J. Heat & Fluid Flow, 1979, Vol 1, No 3

22. Weld Tech CNC Ported Heads, " WELD TECH: GP Tech GM SB2.2 - GP Tech 1", D. Weld, Inc., Accessed on Feb. 2013 at *http://www.weldtech.com/products/GPTech1.html*

23. White, Frank, *Fluid Mechanics*, 5th Edition, McGraw Hill, New York, NY, USA, 2003

APPENDIX A: PREDICTION OF COMBUSTION PRESSURE AND TEMPERATURE

A.1 Simplified Combustion Prediction Approach

1. For Lean Combustion ($\phi \leq 1$) Assuming Complete Combustion:

$$\phi H_2 + \frac{1}{2}\left(O_2 + 3.76N_2\right) \rightarrow \phi H_2O + 1.88N_2 + \left(\frac{1-\phi}{2}\right)O_2 \tag{A1}$$

ϕ = Equivalence Ratio

2. Molar Rate of Combustion:

$$MRC = \frac{\left(\#moles\right)_{\text{Pr}oducts}}{\left(\#moles\right)_{\text{Re}ac\,\text{tan}ts}} = \frac{\phi + 4.76}{2\left(\phi + 2.38\right)} \tag{A2}$$

3. Number of moles of reactants, n_R (Ideal gas law):

$$PV = n_R RT \Rightarrow n_R = \left(\frac{PV}{RT}\right)_{\text{Re}ac\,\text{tan}ts} \tag{A3}$$

P = Pressure of mixture

V = Volume of mixture

T = Temperature of mixture

R = gas constant

4. Number moles of products, n_P:

$$n_p = \left(MRC\right)n_R = \left(\frac{\phi + 4.76}{2\left(\phi + 2.38\right)}\right)n_R \tag{A4}$$

5. Energy addition to system (assume instantaneous, complete combustion):

$$q = LHV\left(LB_{Fuel}\right) \tag{A5}$$

q = Energy addition due to combustion

LHV = Lower Heating Value of fuel

$$LB_{Fuel} = \text{Mass of fuel}$$

6. Temperature change due to combustion:

$$q = \Delta T C_v n_p \Rightarrow \Delta T = \frac{q}{C_v n_p} \tag{A6}$$

$\Delta T =$ Change in temperature due to combustion

$C_v =$ Specific heat of gas mixture

7. Resulting temperature, T_f:

$$T_f = T_0 + \Delta T \tag{A7}$$

T_0 = Initial temperature of mixture

8. Resulting Pressure, P_f, (Using ideal gas law):

$$P_f = \left(\frac{V}{n_p R T_f} \right)_{\text{Products}} \tag{A8}$$

A.2 Improved "Segmented" Combustion Predictions

This method uses the balanced chemical reaction, MRC equation, total moles of reactants and products, and total energy addition given above in the simplified method. In addition, it uses the following equations:

1. Air Fuel Ratio, *AFR*:

$$AFR = \left(\frac{1 - VR}{VR} \right) \left(\frac{MW_{air}}{MW_{H_2}} \right) \tag{A9}$$

VR = volume ratio as previously described

MW = molecular weight of substance (air or hydrogen)

2. Equivalence Ratio, φ:

$$\phi = \frac{AFR_{Stoichiometric}}{AFR_{Actual}} \tag{A10}$$

3. Energy addition from each slice of combustion, q_n:

$$q_n = \frac{q}{n} \tag{A11}$$

n = number of slices for combustion

q = total energy released as defined in simplified method

4. Number of moles of reactants and products in each slice, n_{rn} and n_{pn}:

$$n_{rn} = \frac{n_r}{n},\ n_{pn} = \frac{n_p}{n} \tag{A12}$$

5. Ideal number of moles of each compound before combustion (from chemical balance):

Hydrogen: $inr_{H_2} = \phi$

Oxygen: $inr_{O_2} = 0.5$

Nitrogen: $inr_{N_2} = 1.88$

Total: $inrtot = inr_{H_2} + inr_{O_2} + inr_{N_2}$ (A13)

6. Ideal number of moles of each compound after combustion (from chemical balance):

Water Vapor: $inp_{H_2O} = \phi$

Oxygen: $inp_{O_2} = \left(\frac{1-\phi}{2}\right)$ (A14)

Nitrogen: $inp_{N_2} = 1.88$

Total: $inptot = inp_{H_2O} + inp_{O_2} + inp_{N_2}$ (A15)

7. Equations for constant pressure specific heat, c_p, based on temperature for each compound in reactants and products, Temperature in Kelvin:

$$\frac{c_p}{R_u} = a_1 + a_2 T + a_3 T^2 + a_4 T^3 + a_5 T^4 \tag{A16}$$

Specific Heat Calculation Constants (T < 1000 K)					
	a_1	a_2	a_3	a_4	a_5
H_2	3.298E+00	8.249E-04	-8.143E-07	-9.475E-11	4.135E-13
H_2O	3.387E+00	3.475E-03	-6.355E-06	6.969E-09	-8.431E-13
N_2	3.299E+00	1.408E-03	-3.963E-06	5.642E-09	-2.445E-12
O_2	3.213E+00	1.127E-03	-5.756E-07	1.314E-09	-8.769E-13
Specific Heat Calculation Constants (T ≥1000 K)					
	a_1	a_2	a_3	a_4	a_5
H_2	2.991E+00	7.001E-04	-5.634E-08	-9.232E-12	1.583E-15
H_2O	2.672E+00	3.056E-03	-8.730E-07	1.201E-10	-6.392E-15
N_2	2.927E+00	1.488E-03	-5.685E-07	1.010E-10	-6.753E-15
O_2	3.698E+00	6.135E-04	-1.259E-07	1.775E-11	-1.136E-15

Table A1. Curve Fit Constants for Specific Heat, C_p.

8. The constant volume specific heat, c_v, is calculated using:

$$R_u = c_p - c_v \tag{A17}$$

R_u = universal gas constant

9. The average c_v and γ of the mixture can be found using:

$$c_{v(ave)} = (c_v)_{H_2}\left(\frac{n_{H_2}}{n_{Total}}\right) + (c_v)_{H_2O}\left(\frac{n_{H_2O}}{n_{Total}}\right) + (c_v)_{N_2}\left(\frac{n_{N_2}}{n_{Total}}\right) + (c_v)_{O_2}\left(\frac{n_{O_2}}{n_{Total}}\right) \tag{A18}$$

$$\gamma_{ave} = \frac{c_{v(ave)} + R_u}{c_{v(ave)}} \tag{A19}$$

n_{H_2} = number of moles of hydrogen

n_{H_2O} = number of moles of water vapor

n_{N_2} = number of moles of nitrogen

n_{O_2} = number of moles of oxygen

n_{total} = total number of moles in mixture

10. The temperature change due to combustion of one of the slices before expansion, represents a high pressure, high temperature segment within the gas:

$$\Delta T_{BE} = \frac{q_n}{C_{vn} n_{pn}} \tag{A20}$$

ΔT_{BE} = Change in temperature due to combustion before expansion

C_{vn} = Specific heat of gas mixture within the combusted segment

11. The pressure within this slice can be found by rearranging the ideal gas law given above in the simplified approach.

12. The volume of the high and low pressure gases after isentropic expansion is given by:

$$VLPAE = \left(\frac{V_{Total}}{1 + \left(\frac{PHPBE}{PLPBE} \right)^{\frac{1}{\gamma_{ave}}} \left(\frac{VHPBE}{VLPBE} \right)} \right) \tag{A21}$$

$$VHPAE = V_{Total} - VLPAE \tag{A22}$$

VLPAE = Volume of the low pressure gases after expansion

VHPAE = Volume of the high pressure gases after expansion

VLPBE = Volume of the low pressure gases before expansion

VHPBE = Volume of the high pressure gases before expansion

PLPBE = Pressure of the low pressure gases before expansion

PHPBE = Pressure of the high pressure gases before expansion

V_{Total} = Total volume of gases in mixture

13. The new temperatures of each slice can be found again by applying the ideal gas law.

14. Using these temperatures and the curve fit equations given above for the specific heats of each of the component gases to obtain the new value of specific heat for each slice and an average for the mix.

Convergence criteria in the form of percent change between iterations and number of segments is set within the input file to ensure convergence. A maximum number of iterations is specified in the input file and after each iteration the percent change from the previous iteration is calculated for pressure and temperature:

$$\Delta\%_{pressure} = \frac{abs(P^i - P^{i-1})}{P^i} \times 100 \tag{A23}$$

$$\Delta\%_{tempurature} = \max\left[\frac{abs(T_k^i - T_k^{i-1})}{T_k^i} \right]_{k=1}^{n} \times 100 \tag{A24}$$

P^i = Calculated pressure for iteration *i*

P^{i-1} = Calculated pressure for iteration *i-1*

T_n^i = Calculated temperature for iteration *i*, segment *n*

T_n^{i-1} = Calculated temperature for iteration *i-1*, segment *n*

If the calculated Δ% for both pressure and temperature is less than the input criteria or the maximum number of iterations is reached, the iteration loop is exited. Similarly, a maximum number of segments is set within the input file and after all segments undergo "combustion", the change in final pressure and temperature from is calculated and compared to the previous number of segments' results:

$$\Delta\%_{pressure} = \frac{abs(P_f^n - P_f^{n-1})}{P_f^n} \times 100 \tag{A25}$$

$$\Delta\%_{tempurature} = \frac{abs(T_f^n - T_f^{n-1})}{T_f^n} \times 100 \tag{A26}$$

P_f^n = Calculated final pressure using *n* segments

P_f^{n-1} = Calculated final pressure using *n-1* segments

T_f^n = Calculated final temperature using *n* segments

T_f^{n-1} = Calculated final temperature using *n-1* segments

A.3 Fortran Program Code for Combustion Prediction

Sample Input File (combustion.inp):

```
Mx. No. of segments  Mx. No. Iterations  Temp Conv. Crit. %   Press. Conv. Crit. %
               1000               1000                0.05                  0.05
Comb. Efficiency  Starting Temp  Starting Pressure
            1.00            75               14.7
hydrogen Vol. Ratio  Total Volume
               0.08         44.75
```

Within the input file the appropriate units are units are in^3, lb_f/in^3, and ºF.

Sample Output File Using Sample Input (combustion.out):

```
Hydrogen Volume Ratio=  8.000000000000000E-002 vol H2/vol Air
 Total volume=   44.7500000000000      in^3
 Starting Pressure=   14.7000000000000      psi
 Starting Temperature=   534.670013427734      deg. R
 Air to Fuel Ratio=   165.141370743605
 Equivelance Ratio=  0.207700826768079
 Total Heat Addition=   22865.7278920406      BTUs
 Number of segments =           5
 Temperature History (deg. R)
    534.670   1689.311   1851.562   1972.194   2057.829   2113.034
    534.670    613.288   1731.606   1844.423   1924.510   1976.139
    534.670    613.288    672.191   1769.676   1846.517   1896.054
    534.670    613.288    672.191    715.986   1798.960   1847.221
    534.670    613.288    672.191    715.986    747.075   1818.770
 Pressure History (psi)
  14.700  22.405  30.001  37.359  44.368  50.940
 Iteration per Segment
       5       5       5       5       5
 Max. Iterations =           5
 Avg. Iterations =   5.00000000000000
 *****************************************
 Final Ave Temperature =   1930.24365883144     deg. R
 Final Pressure =   50.9395395685964     psi
 Final (Cp/Cv)ave=   1.32417430370010
 *****************************************
```

Fortran Code:

```
C     Hydrogen_Combustion.for
C     Progam estimates final temperature and pressure of segmented hydrogen
C      combustion within a closed chamber.
C     Author: Jeremy D. Decker
      integer::n,num_it,i,j,k,imax,nmax,ns
      doubleprecision::CE,T0,P0,T0R,VR,Vtot,AFR,ER,MRC,Qtot,P_old
```

```
      doubleprecision::Qn,nrtot,nr,np,CvAve,nz,kave,ki,Tf,Tf_old,Pf_old
      doubleprecision::temp_crit,pres_crit,Tdiff,Pdiff,iave
      doubleprecision::inrH2,inrO2,inrN2,inrtot
      doubleprecision::inpH2O,inpN2,inpO2,inptot
      doubleprecision::deltaT,THPBE,VHPBE,PHPBE,VLPBE,PLPBE,VLPAE,VHPAE
      doubleprecision::THPAE,PHPAE,CR,Tave
      doubleprecision::MWair,MWh2,AFRstoich,LHV
      doubleprecision,dimension(:),allocatable::P,V,Cvmix,Vtemp
      doubleprecision,dimension(:,:),allocatable::T,Cv
      doubleprecision,dimension(:),allocatable::Ttemp,Ttemp_old
      integer,dimension(:),allocatable::it
c     Input Files
        open(unit=10,file='Combustion.inp')
c     Output Files
      open(unit=15,file='Combustion.out') !output file
c     Read in combustion input file
      read(10,*) !title line
      read(10,*)nmax,num_it,temp_crit,pres_crit
      read(10,*) !title line
      read(10,*)CE,T0,P0
      read(10,*) !title line
      read(10,*)VR,Vtot

      temp_crit=temp_crit/100. !convert from %
      pres_crit=pres_crit/100. !convert from %
c     Allocate and initialize arrays
      allocate (T(nmax+1,nmax))
      allocate (P(nmax+1))
      allocate (V(nmax))
      allocate (Cv(nmax,4))
      allocate (Cvmix(nmax))
      allocate (Vtemp(nmax))
      allocate (Ttemp(nmax))
      allocate (Ttemp_old(nmax))
      allocate (it(nmax))

      T0R=T0+459.67
c     Setup Constants
      MWair=28.95  !molecular weight of air
      MWh2=2.016   !molecular weight of H2
      AFRstoich=34.3
      LHV=54608  !lower heating value of H2
      Ru=1545.349*12. !Universal Gas constant in in-lbf/R lbmol
c     Calculate Air-to-Fuel ratio (mass air/mass fuel)
      AFR=(1/(VR/(1-VR)))*(MWair/MWh2)
c     Calculate Fuel-Air equivelance ratio (AFRstoich/AFR or FAR/FARstoich)
      ER=AFRstoich/AFR
c     Calculate Molar Rate of Combustion
      MRC=(ER+4.76)/(2*(ER+2.38))
c     Calculate heat addition from combustion
      Qtot=CE*ER*MWh2*LHV
c     Molar calculations
      nrtot=P0*Vtot/(Ru*T0R) !total number of moles reactants
      inrH2=ER
      inrO2=0.5
      inrN2=1.88
      inrtot=ER+0.5+1.88
      inptot=inrtot*MRC
      inpH2O=ER
      inpN2=1.88
      inpO2=(1-ER)/2

      write(15,*)'Hydrogen Volume Ratio=',VR,'vol H2/vol Air'
      write(15,*)'Total volume=',Vtot,'in^3'
      write(15,*)'Starting Pressure=',P0,'psi'
      write(15,*)'Starting Temperature=',T0R,'deg. R'
      write(15,*)'Air to Fuel Ratio=',AFR
      write(15,*)'Equivelance Ratio=',ER
      write(15,*)'Total Heat Addition=',Qtot,'BTUs'

      do n=2,nmax
```

```
      T=T0+459.67
      P_old=0.
      Cv=0.
      Cvmix=0.
      Ttemp=T0+459.67
      Ttemp_old=Ttemp
      it=0
      P=P0
      nz=dble(n)
      V=Vtot/nz
      Vtemp=Vtot/nz
      Qn=Qtot/nz !per slice
      nr=nrtot/nz !moles of reactants per segment
      np=nr*MRC !moles of products per segment
      do i=1,n !loop to go through "combustion" for each segment
      do i2=1,num_it
        do k=1,n !calculate Cv of each component gas for each segment
          if(i2.eq.1)then
            Tave=T(i,k)
          else !calculate an avg temp from starting and ending values
            if(k.eq.i)then
              Tave=(T(i,k)+THPBE)/2.
            else
              Tave=(T(i,k)+Ttemp(k))/2.
            endif
          endif
          call Cv_approx(Tave,Cv(k,1),Cv(k,2),Cv(k,3),Cv(k,4))
        enddo

        do k=1,i !calculate Cv for each segment that has combusted
          Cvmix(k)=Cv(k,2)*inpH2O/inptot+Cv(k,3)*inpN2/inptot+
            Cv(k,4)*inpO2/inptot
        enddo

        do k=i+1,n
          Cvmix(k)=Cv(k,1)*inrH2/inrtot+Cv(k,4)*inrO2/inrtot+
            Cv(k,3)*inrN2/inrtot
        enddo
        CvAve=0. !reset average
        do k=1,n
          CvAve=CvAve+Cvmix(k)
        enddo
        CvAve=CvAve/nz !average Cv of all segments
        kave=(CvAve+1.987)/Cvave
        if(i2.eq.1)then !k for high pressure segment
          ki=kave
        else
          ki=(Cvmix(i)+1.987)/Cvmix(i)
        endif

c       calculate deltaT and resulting temperature for slice undergoing combustion
        deltaT=Qtot/(Cvmix(i)*inptot)
c       calculate before expansion components
        THPBE=deltaT+T(i,i)
        VHPBE=V(i)
        PHPBE=(np*Ru*THPBE)/VHPBE
        VLPBE=Vtot-VHPBE
        PLPBE=P(i)
c       calculate after expansion components
        VLPAE=Vtot/(1+((PHPBE/PLPBE)**(1/kave)*(VHPBE/VLPBE)))
        VHPAE=Vtot-VLPAE
        THPAE=THPBE*(VHPBE/VHPAE)**(ki-1)
        PHPAE=PHPBE*(VHPBE/VHPAE)**(ki)
        P(i+1)=PHPAE
c       calculate compression ratio of low pressure gases
        CR=VLPAE/VLPBE
c       calculate new values of volume for each slice
        do k=1,n
          if(k.eq.i)then
            Vtemp(k)=VHPAE
          else
```

```
            Vtemp(k)=V(k)*CR
          endif
        enddo
c       calculate new values of temperature for each slice
        do k=1,n
          if(k.eq.i)then
            Ttemp(k)=THPAE
          elseif(k.lt.i)then
            Ttemp(k)=Vtemp(k)*PHPAE/(np*Ru)
          elseif(k.gt.i)then
            Ttemp(k)=Vtemp(k)*PHPAE/(nr*Ru)
          endif
        enddo


c       check for convergence
        Tdiff=0.
        Pdiff=0.
        if(i2.gt.1)then
          do k=1,n
            Tdiff=max(abs(Ttemp(k)-Ttemp_old(k))/Ttemp(k),Tdiff)
          enddo
          Pdiff=abs(P(n+1)-P_old)/P(n+1)
          if(Tdiff.le.temp_crit.and.Pdiff.le.pres_crit)then
            it(i)=i2
            go to 10
          endif
        endif
c       transfer new values of temp and pressure to old values for
c        convergence check
        do k=1,n
          Ttemp_old(k)=Ttemp(k)
        enddo
        P_old=P(n+1)
      enddo !i2=1,num_it
10    continue !continue here if convergence criteria met
C     move temperature and volume values from temps to final
      do k=1,n
        T(i+1,k)=Ttemp(k)
        V(k)=Vtemp(k)
      enddo
      enddo !i=1,n

c     Test for #segment convergence
      Tf=0.
      do k=1,n
        Tf=Tf+T(n+1,k)
      enddo
      Tf=Tf/nz
      Tdiff=0.
      Pdiff=0.
      if(n.gt.2)then
        Tdiff=abs(Tf-Tf_old)/Tf
        Pdiff=abs(P(n+1)-Pf_old)/P(n+1)
        if(Tdiff.le.temp_crit.and.Pdiff.le.pres_crit)then
          ns=n
          go to 20
        endif
      endif

      Tf_old=Tf
      Pf_old=P(n+1)
      enddo !n=1,nmax
20    continue
c     write out temperature and pressure arrays
      write(15,*)"Number of segments =",ns
      write(15,*)"Temperature History (deg. R)"
      Tf=0.
      iave=0
      imax=0
      do k=1,n
```

```
        write(15,100)(T(i,k),i=1,n+1)
        Tf=Tf+T(n+1,k)
        iave=iave+dble(it(k))
        imax=max(it(k),imax)
      enddo
      Tf=Tf/nz
      iave=iave/nz
      write(15,*)"Pressure History (psi)"
      write(15,200)(P(i),i=1,n+1)
      write(15,*)"Iteration per Segment"
      write(15,300)(it(i),i=1,n)
      write(15,*)"Max. Iterations =",imax
      write(15,*)"Avg. Iterations =",iave
      write(15,*)"*****************************************"
      write(15,*)"Final Ave Temperature =",Tf,"deg. R"
      write(15,*)"Final Pressure =",P(n+1),"psi"
      write(15,*)"Final (Cp/Cv)ave=",(Cvave+1.987)/Cvave
      write(15,*)"*****************************************"

100   format(10000f11.3)
200   format(10000f8.3)
300   format(10000i8)
      end
c*****Specific Heat approx. Subroutine************************
      subroutine Cv_approx(T,CvH2,CvH2O,CvN2,CvO2)
c     Calculates Specific heat of H2, H20, N2 and O2
c      using curve fit parameters and a given temperature
c     local variables
      doubleprecision::CvH2,CvH2O,CvN2,CvO2,T,Ru,Tk
      doubleprecision::CpH2_R,CpH2O_R,CpN2_R,CpO2_R
      doubleprecision,dimension(:,:),allocatable::a1,a2

      allocate(a1(5,4)) !coefficients below 1000k
      allocate(a2(5,4)) !coefficients above 1000k

c     set a1 coefficients
      a1(1,1)=3.298 !a1 H2
      a1(2,1)=0.0008249 !a2 H2
      a1(3,1)=-0.0000008143 !a3 H2
      a1(4,1)=-0.00000000009475 !a4 H2
      a1(5,1)=0.0000000000004135 !a5 H2

      a1(1,2)=3.387 !a1 H2O
      a1(2,2)=0.003475 !a2 H2O
      a1(3,2)=-0.000006355 !a3 H2O
      a1(4,2)=0.000000006969 !a4 H2O
      a1(5,2)=-0.0000000000008431 !a5 H2O

      a1(1,3)=3.299 !a1 N2
      a1(2,3)=0.001408 !a2 N2
      a1(3,3)=-0.000003963 !a3 N2
      a1(4,3)=0.000000005642 !a4 N2
      a1(5,3)=-0.000000000002445 !a5 N2

      a1(1,4)=3.213 !a1 02
      a1(2,4)=0.001127 !a2 02
      a1(3,4)=-0.0000005756 !a3 02
      a1(4,4)=0.000000001314 !a4 02
      a1(5,4)=-0.0000000000008769 !a5 02

c     set a2 coefficients
      a2(1,1)=2.991 !a1 H2
      a2(2,1)=0.0007001 !a2 H2
      a2(3,1)=-0.00000005634 !a3 H2
      a2(4,1)=-0.000000000009232 !a4 H2
      a2(5,1)=0.000000000000001583 !a5 H2

      a2(1,2)=2.672 !a1 H2O
      a2(2,2)=0.003056 !a2 H2O
      a2(3,2)=-0.0000008730 !a3 H2O
      a2(4,2)=0.0000000001201 !a4 H2O
```

```
      a2(5,2)=-0.000000000000006392 !a5 H2O

      a2(1,3)=2.927 !a1 N2
      a2(2,3)=0.001488 !a2 N2
      a2(3,3)=-0.0000005685 !a3 N2
      a2(4,3)=0.0000000001010 !a4 N2
      a2(5,3)=-0.000000000000006753 !a5 N2

      a2(1,4)=3.698 !a1 02
      a2(2,4)=0.0006135 !a2 02
      a2(3,4)=-0.0000001259 !a3 02
      a2(4,4)=0.00000000001775 !a4 02
      a2(5,4)=-0.000000000000001136 !a5 02

c     convert T from rankine to K for curve fit
      Tk=T*0.5556

      if(T.le.1000)then
        CpH2_R=a1(1,1)+a1(2,1)*Tk+a1(3,1)*Tk**2+a1(4,1)*Tk**3+
         a1(5,1)*Tk**4
        CpH2O_R=a1(1,2)+a1(2,2)*Tk+a1(3,2)*Tk**2+a1(4,2)*Tk**3+
         a1(5,2)*Tk**4
        CpN2_R=a1(1,3)+a1(2,3)*Tk+a1(3,3)*Tk**2+a1(4,3)*Tk**3+
         a1(5,3)*Tk**4
        CpO2_R=a1(1,4)+a1(2,4)*Tk+a1(3,4)*Tk**2+a1(4,4)*Tk**3+
         a1(5,4)*Tk**4
      else
        CpH2_R=a2(1,1)+a2(2,1)*Tk+a2(3,1)*Tk**2+a2(4,1)*Tk**3+
         a2(5,1)*Tk**4
        CpH2O_R=a2(1,2)+a2(2,2)*Tk+a2(3,2)*Tk**2+a2(4,2)*Tk**3+
         a2(5,2)*Tk**4
        CpN2_R=a2(1,3)+a2(2,3)*Tk+a2(3,3)*Tk**2+a2(4,3)*Tk**3+
         a2(5,3)*Tk**4
        CpO2_R=a2(1,4)+a2(2,4)*Tk+a2(3,4)*Tk**2+a2(4,4)*Tk**3+
         a2(5,4)*Tk**4
      endif
C     convert Cp/R into Cv using Cp-Cv=Ru
      Ru=1.987
      CvH2=Ru*(CpH2_R-1)
      CvH2O=Ru*(CpH2O_R-1)
      CvN2=Ru*(CpN2_R-1)
      CvO2=Ru*(CpO2_R-1)

      end subroutine CV_approx
```

APPENDIX B: ORIFICE PLATE DESIGN CALCULATIONS

The sharp edge orifice used for steady flow measurements was designed according to *Flow Meter Engineering Handbook* [3]. The required maximum flow rate, Q_h, was determined to be 100 ft^3/min or 6,000 ft^3/hr for lift values of approximately 0.00-0.150". First an approximate orifice bore check was completed and then a more precise orifice bore calculation was completed using this information.

Approximate orifice bore check:

1. The maximum differential pressure, Δp, for the inclined manometer used for testing is 8" H_2O which is within the range of recommended for a static operating pressure of 28" H_2O, which is 13.25" (interpolation from Table 2 within the text).

2. The differential range correction factor, F_d, was calculated using:

$$F_d = 0.2146\sqrt{\Delta p} \tag{B1}$$

Δp = differential pressure in inches H_2O

3. The operating conditions correction factor, F_{oc}, was calculated using:

$$F_{oc} = 0.2011\left(\sqrt{p_o}\right)\left(\sqrt{\frac{1.00}{SG}}\right)\left(22.80\sqrt{\frac{1}{460 + t_o}}\right) \tag{B2}$$

p_o = absolute operating pressure in lb/in^2

SG = specific gravity under operating conditions

t_o = operating temperature in ºF

The SG under operating conditions was found to be 1.0687 using the ideal gas law for a p_o of 15.71 lb/in^2 and a t_o of 75ºF. Using these values and a Δp of 8.00" H_2O, F_d and F_{oc} was found to be 0.607 and 0.760 respectivly.

4. The corrected maximum flow, Q', was then found to be 13006 ft^3/hr using:

$$Q' = \frac{Q_h}{F_d F_{oc}} \tag{B3}$$

5. Using Table 20 from the text and interpolating for a 3" Std. pipe size, the orifice diameter to pipe inside diameter ratio, d/D, was calculated as 0.528. This results in an orifice diameter, d, of 1.620" for a pipe inside diameter of 3.068".

Precise orifice bore calculation:

6. The orifice factor, S_o, must be calculated to find a more precise orifice bore diameter. Equations B4-B12 and the values listed in Table B1 were used to calculate a S_o of 0.1719.

$$S_o = \frac{Q_h}{218.44 F_a D^2 F_{hm} F_{pb} F_{tb} F_{pf} F_{tf} F_g Y} \tag{B4}$$

$$F_{hm} = \sqrt{\Delta p} \tag{B5}$$

$$Y = 1 - \left[0.41 + 0.35 \left(\frac{d}{D} \right)^4 \right] \frac{x}{\gamma} \tag{B6}$$

$$x = \frac{\Delta p}{p_o} \tag{B7}$$

$$F_{pb} = \frac{1}{p_b} \tag{B8}$$

$$F_{tb} = t_b + 460 \tag{B9}$$

$$F_{pf} = \sqrt{p_o} \tag{B10}$$

$$F_{tf} = \sqrt{\frac{1}{t_o + 460}} \tag{B11}$$

$$F_g = \sqrt{\frac{1}{SG}} \tag{B12}$$

F_a = area correction factor, determined from Curve 4 in text.

γ = ratio of specific heats for air, 1.40

p_b = absolute base pressure in lb/in^2

t_b = base temperature ºF

Values Used for Calculation of So		
Q_h =	4500	ft^3/hr
D^2 =	9.4126	in^2
Δp =	0.4783	lb/in^2
p_o =	15.71	lb/in^2
t_o =	75	ºF
p_b =	14.7	lb/in^2
t_b =	75	ºF
x =	0.0011	
Fa =	1.00	
Fhm =	2.8284	
Fpb =	0.0680	
Ftb =	535	
Fpf =	3.967	
Ftf =	0.0432	
Fg =	0.9673	
Y =	0.9943	

Table B1. Values Used for Calculations of Orifice Factor, S_o.

7. The Reynolds number, R_D, was calculated as 43,869 using:

$$R_D = \frac{0.48239 Q_{ha} SG}{D\mu} \tag{B13}$$

$$Q_{ha} = 0.80 Q_h \quad \text{(B14)}$$

μ = absolute viscosity in centipoises

8. Interpolating from Table 47 from the text for 3" Std. Pipe and using a R_D and S_o of 43,869 and 0.1719 respectively, the ratio of orifice bore and pipe internal dimensions was calculated as 0.5210. This results in a 1.598" diameter orifice bore.

APPENDIX C: Performance Simulations Using Engine Analyzer

Performance Trend's Engine Analyzer v3.4 was used to predict the power output for a 1998 NASCAR Cup Engine. Two versions of the engine were simulated with differences in primary exhaust header diameter. The stock version had a 1.90" diameter exhaust header diameter and the modified version had a 1.95" primary exhaust header diameter. This represents a 2.6% change in diameter and a 5.3% change in flow area.

The results are included as Figures C1 to C5 and predict decreases in horsepower for engines speeds below 5,000 RPM and increases in horsepower for engines speeds above 7,500 RPM. The increase in exhaust diameter decrease predicted power by 6.0 HP at 4,000 RPM and 3 HP at 4,500 RPM. Power increased by 1 to 9 HP for engine speeds of 7,500 to 10,000 RPM. The typical operating range during race conditions for such an engine is 7,000 to 10,000 RPM. Since the operating range for the engine is above those engine speed values which see a decrease in power, the average predicted power over the operating range increases by 3.9 HP with the increased diameter of the exhaust flow path (Table C1). The increased area and volume decreases exhaust system back pressure at the higher engine speeds, which reduces pumping losses and increases exhaust scavenging.

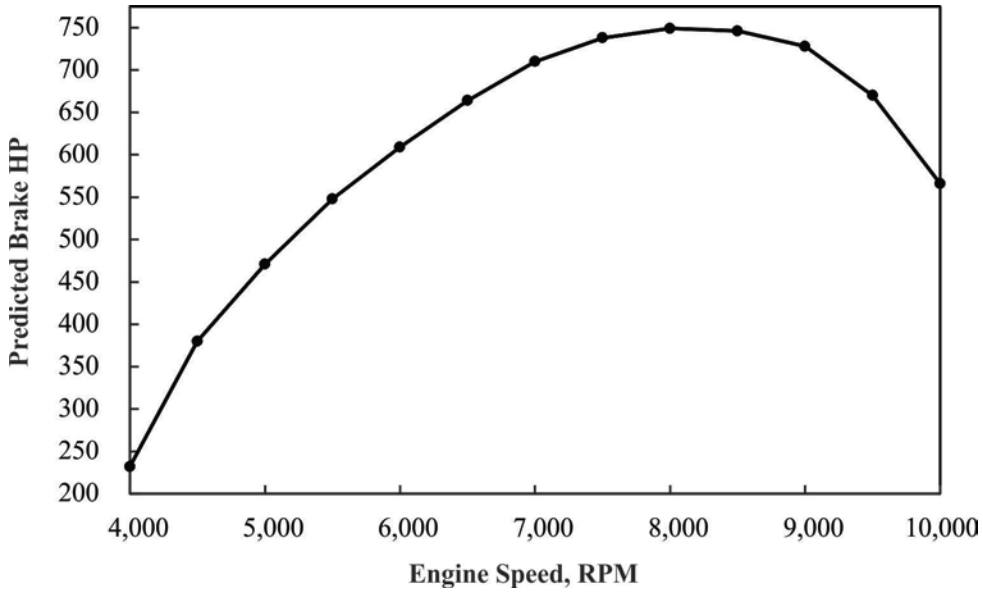

Figure C1. Predicted horsepower versus engine speed for stock 1998 NASCAR Engine

Predicted HP Using Engine Analyzer v3.4
Stock Vs. Modified 1998 NASCAR Cup Engine

RPM	Stock HP	Modified HP	ΔHP
4000	238	232	-6.0
4500	383	380	-3.0
5000	471	471	0.0
5500	547	548	1.0
6000	609	609	0.0
6500	664	664	0.0
7000	710	710	0.0
7500	737	738	1.0
8000	747	749	2.0
8500	743	746	3.0
9000	724	728	4.0
9500	662	670	8.0
10000	557	566	9.0

RPM	Stock Average HP	Modified Average HP	ΔHP
7,000 - 10,000	697.1	701.0	3.9

Table C1. Predicted engine power for stock and modified 1998 NASCAR Engine.

Engine Analyzer v3.4 0 This Report Printed:
Eng: stock Chevy Winston Cup Race 0 2:46:51 pm 06-16-13
Calculated Test Results Performance Trends (C) 2009 Page: 1

Projected Performance

RPM	4000	4500	5000	5500	6000	6500	7000	7500	8000	8500	9000	9500	10000
Brake Tq	313	447	495	523	533	536	532	516	490	459	422	366	293
Brake HP	238	383	471	547	609	664	710	737	747	743	724	662	557
Exh Pres	.0	.0	.0	.0	.0	.0	.0	.0	.0	.0	.0	.0	.0
Int Vacuum	.2	.4	.6	.8	1.0	1.3	1.5	1.7	1.8	2.0	2.1	2.1	1.9
Vol Eff %	72.8	91.8	100.8	107.2	112.7	116.1	117.8	116.3	114.1	112.2	109.6	104.1	96.3
Actual CFM	323	475	585	679	774	860	941	989	1028	1072	1105	1099	1068
Fuel Flow	118	174	214	248	283	314	344	361	376	392	404	402	390
A/F Mix Qal	96.9	100.0	100.0	100.0	100.0	100.0	100.0	100.0	100.0	100.0	100.0	100.0	100.0
BSFC	.496	.454	.454	.463	.465	.474	.485	.490	.503	.527	.558	.607	.701
BSAC	6.217	5.689	5.689	5.688	5.828	5.943	6.078	6.148	6.310	6.616	7.002	7.613	8.787
Friction HP	43	54	66	82	99	117	144	181	222	268	319	373	433
Mach #	.180	.203	.225	.248	.270	.293	.315	.338	.360	.383	.405	.428	.450
Piston Spd	2220	2498	2775	3053	3330	3608	3885	4163	4440	4718	4995	5273	5550
Piston Gs	967	1224	1511	1828	2175	2553	2961	3399	3867	4366	4894	5453	6042
Overlap %VE	-4.8	6.0	6.8	6.4	6.1	5.8	5.9	5.3	4.6	4.5	4.3	2.3	-1.9
Int AvgVel	152	171	190	209	228	247	266	285	304	323	342	361	380
In InertiaPrs	1.7	2.6	3.7	4.7	5.5	6.1	6.2	6.0	5.6	5.2	4.6	4.0	3.3
In ResTunPrs	0.0	0.0	0.0	0.0	0.0	0.0	.3	0.0	-.2	.1	.4	.1	-.1
Ex AvgVel	174	196	218	240	262	283	305	327	349	371	392	414	436
ExTun Prs	.2	-.9	-1.7	-1.8	-2.0	-2.1	-2.3	-2.2	-2.0	-1.7	-1.4	-1.1	-.8
Valve Toss	None	None	None	None	None	None	None	None	None	None	None	None	None
Spark Adv	34	35	36	36	36	37	37	38	38	38	39	39	40

	Pk Tq	536	Avg Tq	456	Pk HP	747	Avg HP	599

```
------ Valve Flow & Cam Calculations ---------------------  --Int--  --Exh--
Overlap Area, sq in*deg    52.0      Total Avg Flow Coef     .438     .526
Total Exh/Int %            68.9      Lobe Area, inch*deg    32.06    32.15
Lobe Separation, deg      106.0      Vlv Area, deg*sq in    521.5    359.5
                                     Lobe Centerlins, deg   104.0    108.0

------ General Engine Calculations ----------------------------------------
Displacement, cc          5835.1     Displacement, cu in          356.02
Dynamic Comp. Ratio          7.08    Compression Ratio             12.00
Theo. Crank Comprssn, PSI    173     Clearance Volume, ccs         66.3
                                     Est Idle Vac, ''Hg            3.0
```

Figure C2. Engine Analyzer output for stock NASCAR engine.

Engine Analyzer v3.4 0 This Report Printed:
Eng: stock Chevy Winston Cup Race 0 2:46:51 pm 06-16-13
Calculated Test Results Performance Trends (C) 2009 Page: 2

Short Block

Engine Specs		**Losses**	
Example:	: 98 Winston Cup SB Chevy	Accs:	Small water pump only (or underdrive pulley)
Bore, in	4.125	Sump:	Dry Sump
Stroke, in	3.33	Pstn/brngs:	Race-Very small skirts and bearings
# of Cylinders	8		
Rod Length, in	6		

Head(s)

General Specs		**Intake**	
Example:	Head: 98 WnstnCup CNC Ported SB2	Layout:	1 valve & 1 port
Chamber:	Compact Wedge	Valve Diameter, in	2.15
Compression Ratio	12	Avg Port Diameter, in	2.01
		Port Volume, ccs	286
		Port Length, in	5.5
		Flow Efficiency, %	63
		Exhaust	
		Layout:	1 valve & 1 port
		Valve Diameter, in	1.62
		Flow Efficiency, %	65

Intake System

Manifold Specs

Example:	Mnfld: Large Runner SB2 Intake	**Carburetor Specs**	
Design:	Single Plane-carb(s)	Type:	Use Specs Below
Runner Diameter, in	2.06	CFM Rating	950
Runner Length, in	5.5	Vac Secondaries:	No
Flow Efficiency, %	100		
Intake Heat:	No Heat		

Exhaust Specs

Header Specs		**Exhaust System**	
Example:	2" Dia x 34" Len Primary	Type:	Open Exhaust (no mufflers)
Design:	Tube Headers	Exh System CFM Rating	na
Primary Diameter, in	1.9		
Primary Length, in	34		
Flow Efficiency, %	90		
Collector Length, in	10		

Cam/Valve Train

General Specs		**General Specs, cont**	
Example:	Cam: 98 Wnstn Cup Flat Tappet	Total Cam Advance	2.0 Advance
Rating Lift:	.050 inches	Profile:	Aggr Solid Flat
		Vlv/Trn:	Pushrod w RockrArm (race)
Intake		Exhaust	
Centerline, deg ATDC	104	Centerline, deg BTDC	108
Duration @ .050"	268	Duration @ .050"	272
Opening @ .050", BTDC	30	Opening @ .050", BBDC	64
Closing @ .050", ABDC	58	Closing @ .050", ATDC	28
Max Lobe Lift, in	.37	Max Lobe Lift, in	.37
Lash at Valve, in	.016	Lash at Valve, in	.02
Rocker Arm Ratio	1.8	Rocker Arm Ratio	1.8

Calculate Performance Conditions

Test Conditions

Type:	Std Dyno (60 deg, 29.92")	**Fuel Specs**	
Coolant Temp, deg F	185	Fuel Type:	Gasoline
Nitrous Oxide Specs		Fuel Octane (R+M)/2	120
System:	No Nitrous Injection		

Figure C3. Engine Analyzer specifications for stock NASCAR engine.

Engine Analyzer v3.4 0 This Report Printed:
Eng: Chevy Winston Cup mod exh 0 2:48:13 pm 06-16-13
Calculated Test Results Performance Trends (C) 2009 Page: 1

Projected Performance

RPM	4000	4500	5000	5500	6000	6500	7000	7500	8000	8500	9000	9500	10000
Brake Tq	304	443	494	523	533	536	533	517	492	461	425	370	297
Brake HP	232	380	471	548	609	664	710	738	749	746	728	670	566
Exh Pres	.0	.0	.0	.0	.0	.0	.0	.0	.0	.0	.0	.0	.0
Int Vacuum	.2	.4	.6	.8	1.0	1.3	1.5	1.7	1.8	2.0	2.1	2.1	2.0
Vol Eff %	71.6	91.4	100.7	107.2	112.7	116.0	117.8	116.4	114.2	112.4	109.8	104.5	96.8
Actual CFM	317	471	583	679	774	860	940	989	1029	1074	1109	1105	1073
Fuel Flow	116	172	213	248	283	314	344	362	376	393	405	404	392
A/F Mix Qal	96.8	100.0	100.0	100.0	100.0	100.0	100.0	100.0	100.0	100.0	100.0	100.0	100.0
BSFC	.501	.453	.453	.453	.464	.473	.484	.490	.502	.526	.556	.603	.692
BSAC	6.284	5.685	5.681	5.680	5.823	5.934	6.071	6.144	6.296	6.599	6.979	7.562	8.686
Friction HP	43	54	66	81	98	116	143	180	220	267	317	371	430
Mach #	.180	.203	.225	.248	.270	.293	.315	.338	.360	.383	.405	.428	.450
Piston Spd	2220	2498	2775	3053	3330	3608	3885	4163	4440	4718	4995	5273	5550
Piston Gs	967	1224	1511	1828	2175	2553	2961	3399	3867	4366	4894	5453	6042
Overlap %VE	-5.9	5.6	6.7	6.4	6.1	5.8	5.9	5.3	4.7	4.6	4.4	2.7	-1.4
Int AvgVel	152	171	190	209	228	247	266	285	304	323	342	361	380
In InertiaPrs	1.7	2.6	3.7	4.7	5.5	6.1	6.2	6.0	5.6	5.2	4.6	4.0	3.3
In ResTunPrs	0.0	0.0	0.0	0.0	0.0	0.0	.3	0.0	-.2	.1	.4	.1	-.1
Ex AvgVel	166	186	207	228	248	269	290	310	331	352	373	393	414
ExTun Prs	.3	-.7	-1.6	-1.8	-1.9	-2.1	-2.3	-2.2	-2.1	-1.8	-1.5	-1.2	-.9
Valve Toss	None	None	None	None	None	None	None	None	None	None	None	None	None
Spark Adv	34	35	36	36	36	37	37	38	38	38	39	39	40

	Pk Tq	536	Avg Tq	456	Pk HP	749	Avg HP	601

----- Valve Flow & Cam Calculations

			--Int--	--Exh--
Overlap Area, sq in*deg	52.0	Total Avg Flow Coef	.438	.527
Total Exh/Int %	69.1	Lobe Area, inch*deg	32.06	32.15
Lobe Separation, deg	106.0	Vlv Area, deg*sq in	521.5	360.2
		Lobe Centerlins, deg	104.0	108.0

----- General Engine Calculations

Displacement, cc	5835.1	Displacement, cu in	356.02
Dynamic Comp. Ratio	7.08	Compression Ratio	12.00
Theo. Crank Comprssn,PSI	173	Clearance Volume, ccs	66.3
		Est Idle Vac, ''Hg	3.0

Figure C4. Engine Analyzer output for modified NASCAR engine.

Engine Analyzer v3.4 0 This Report Printed:
Eng: Chevy Winston Cup mod exh 0 2:48:13 pm 06-16-13
Calculated Test Results Performance Trends (C) 2009 Page: 2

Short Block

Engine Specs		**Losses**	
Example:	: 98 Winston Cup SB Chevy	Accs:	Small water pump only (or underdrive pulley)
Bore, in	4.125	Sump:	Dry Sump
Stroke, in	3.33	Pstn/brngs:	Race-Very small skirts and bearings
# of Cylinders	8		
Rod Length, in	6		

Head(s)

General Specs		**Intake**	
Example:	Head: 98 WnstnCup CNC Ported SB2	Layout:	1 valve & 1 port
Chamber:	Compact Wedge	Valve Diameter, in	2.15
Compression Ratio	12	Avg Port Diameter, in	2.01
		Port Volume, ccs	286
		Port Length, in	5.5
		Flow Efficiency, %	63
		Exhaust	
		Layout:	1 valve & 1 port
		Valve Diameter, in	1.62
		Flow Efficiency, %	65

Intake System

Manifold Specs		**Carburetor Specs**	
Example:	Mnfld: Large Runner SB2 Intake	Type:	Use Specs Below
Design:	Single Plane-carb(s)	CFM Rating	950
Runner Diameter, in	2.06	Vac Secondaries:	No
Runner Length, in	5.5		
Flow Efficiency, %	100		
Intake Heat:	No Heat		

Exhaust Specs

Header Specs		**Exhaust System**	
Type:	Use Specs Below	Type:	Open Exhaust (no mufflers)
Design:	Tube Headers	Exh System CFM Rating	na
Primary Diameter, in	1.95		
Primary Length, in	34		
Flow Efficiency, %	90		
Collector Length, in	10		

Cam/Valve Train

General Specs		**General Specs, cont**	
Example:	Cam: 98 Winstn Cup Flat Tappet	Total Cam Advance	2.0 Advance
Rating Lift:	.050 inches	Profile:	Aggr Solid Flat
		Vlv Trn:	Pushrod w RockrArm (race)
Intake		Exhaust	
Centerline, deg ATDC	104	Centerline, deg BTDC	108
Duration @ .050"	268	Duration @ .050"	272
Opening @ .050", BTDC	30	Opening @ .050", BBDC	64
Closing @ .050", ABDC	58	Closing @ .050", ATDC	28
Max Lobe Lift, in	.37	Max Lobe Lift, in	.37
Lash at Valve, in	.016	Lash at Valve, in	.02
Rocker Arm Ratio	1.8	Rocker Arm Ratio	1.8

Calculate Performance Conditions

Test Conditions		**Fuel Specs**	
Type:	Std Dyno (60 deg, 29.92")	Fuel Type:	Gasoline
Coolant Temp, deg F	185	Fuel Octane (R+M)/2	120
Nitrous Oxide Specs			
System:	No Nitrous Injection		

Figure C5. Engine Analyzer specifications for modified NASCAR engine.

APPENDIX D: Blowdown Testing Raw Data

Modified Port 0.050" lift N_2

		Run 1		Run 2		Run 3		Run 4		Run 5	
	Time	V_{high}	V_{low}	V_{high}	V_{low}	V_{high}	V_{low}	V_{high}	V_{low}	V_{high}	V_{low}
Point 1	-0.102	5.04	5.08	5.00	5.04	5.08	5.08	5.08	5.12	5.08	5.08
Point 2	-0.100	5.04	5.08	5.00	5.04	5.04	5.08	5.08	5.08	5.04	5.08
Point 3	-0.098	5.00	5.04	5.00	5.04	5.08	5.12	5.08	5.12	5.08	5.08
Point 4	-0.096	5.04	5.04	5.04	5.04	5.08	5.12	5.08	5.12	5.08	5.08
Point 5	-0.094	5.04	5.04	5.00	5.00	5.04	5.08	5.08	5.12	5.04	5.08
Point 6	-0.092	5.04	5.08	5.00	5.04	5.04	5.08	5.08	5.12	5.04	5.04
Point 7	-0.090	5.04	5.04	5.04	5.04	5.08	5.08	5.12	5.16	5.04	5.08
Point 8	-0.088	5.04	5.08	5.00	5.04	5.04	5.08	5.08	5.12	5.00	5.04
Point 9	-0.086	5.04	5.08	5.00	5.00	5.04	5.08	5.08	5.12	5.08	5.08
Point 10	-0.084	5.04	5.08	5.00	5.04	5.04	5.04	5.04	5.08	5.04	5.04
Point 11	-0.082	5.04	5.08	5.00	5.00	5.04	5.04	5.08	5.08	5.08	5.08
Point 12	-0.080	5.04	5.08	5.00	5.04	5.04	5.04	5.12	5.16	5.04	5.04
Point 13	-0.078	5.08	5.08	5.00	5.00	5.08	5.12	5.04	5.08	5.04	5.08
Point 14	-0.076	5.04	5.08	5.00	5.04	5.04	5.04	5.08	5.08	5.04	5.08
Point 15	-0.074	5.04	5.04	5.00	5.04	5.08	5.08	5.08	5.12	5.04	5.08
Point 16	-0.072	5.04	5.08	5.00	5.00	5.04	5.08	5.08	5.12	5.08	5.08
Point 17	-0.070	5.00	5.04	5.00	5.04	5.04	5.08	5.12	5.12	5.04	5.08
Point 18	-0.068	5.00	5.04	5.00	5.04	5.08	5.08	5.08	5.08	5.04	5.08
Point 19	-0.066	5.04	5.04	4.96	5.00	5.04	5.04	5.08	5.08	5.04	5.08
Point 20	-0.064	5.04	5.08	5.00	5.04	5.04	5.04	5.08	5.12	5.08	5.08
Point 21	-0.062	5.04	5.08	5.00	5.00	5.04	5.08	5.12	5.12	5.04	5.08
Point 22	-0.060	5.04	5.04	5.00	5.04	5.04	5.04	5.08	5.08	5.04	5.08
Point 23	-0.058	5.04	5.08	5.00	5.04	5.00	5.04	5.08	5.12	5.04	5.08
Point 24	-0.056	5.04	5.04	5.00	5.00	5.04	5.08	5.08	5.12	5.04	5.04
Point 25	-0.054	5.08	5.08	5.00	5.00	5.04	5.08	5.08	5.08	5.04	5.04
Point 26	-0.052	5.04	5.04	5.00	5.00	5.04	5.04	5.08	5.12	5.04	5.04
Point 27	-0.050	5.04	5.08	4.96	5.00	5.04	5.04	5.08	5.12	5.00	5.04
Point 28	-0.048	5.04	5.04	4.96	5.00	5.04	5.08	5.08	5.12	5.04	5.04
Point 29	-0.046	5.04	5.04	5.00	5.04	5.04	5.08	5.08	5.12	5.04	5.04
Point 30	-0.044	5.04	5.04	5.00	5.00	5.04	5.04	5.08	5.08	5.04	5.08
Point 31	-0.042	5.04	5.04	4.96	5.00	5.04	5.08	5.08	5.12	5.04	5.08
Point 32	-0.040	5.00	5.04	4.96	5.00	5.04	5.08	5.12	5.12	5.04	5.04
Point 33	-0.038	5.00	5.04	5.00	5.00	5.04	5.08	5.08	5.08	5.04	5.04
Point 34	-0.036	5.04	5.08	5.00	5.04	5.08	5.08	5.08	5.12	5.04	5.04
Point 35	-0.034	5.04	5.04	4.96	5.00	5.04	5.04	5.08	5.12	5.00	5.04
Point 36	-0.032	5.04	5.08	5.00	5.04	5.04	5.08	5.08	5.12	5.04	5.04
Point 37	-0.030	5.00	5.04	5.00	5.04	5.00	5.04	5.12	5.12	5.04	5.08
Point 38	-0.028	5.04	5.04	5.00	5.00	5.04	5.04	5.08	5.08	5.04	5.08
Point 39	-0.026	5.04	5.08	5.00	5.00	5.04	5.04	5.04	5.08	5.00	5.04
Point 40	-0.024	5.00	5.04	5.00	5.04	5.08	5.12	5.04	5.08	5.00	5.04
Point 41	-0.022	5.04	5.04	5.00	5.00	5.04	5.08	5.08	5.12	5.00	5.04
Point 42	-0.020	5.00	5.00	4.96	5.00	5.04	5.08	5.08	5.08	5.00	5.04
Point 43	-0.018	5.00	5.04	4.96	5.00	5.00	5.04	5.08	5.08	5.00	5.00
Point 44	-0.016	4.96	5.00	4.96	4.96	5.00	5.04	5.08	5.08	5.00	5.00
Point 45	-0.014	4.96	4.96	4.96	4.96	5.00	5.00	5.04	5.08	4.96	5.00
Point 46	-0.012	4.92	4.92	4.92	4.92	4.96	5.00	5.00	5.00	4.96	4.96
Point 47	-0.010	4.88	4.88	4.88	4.88	4.92	4.92	4.92	4.96	4.96	4.96
Point 48	-0.008	4.80	4.80	4.84	4.84	4.84	4.88	4.84	4.84	4.88	4.88
Point 49	-0.006	4.72	4.72	4.72	4.72	4.76	4.80	4.80	4.84	4.80	4.84

Modified Port 0.050" lift N_2 (cont.)

		Run 1		Run 2		Run 3		Run 4		Run 5	
	Time	V_{high}	V_{low}	V_{high}	V_{low}	V_{high}	V_{low}	V_{high}	V_{low}	V_{high}	V_{low}
Point 50	-0.004	4.68	4.68	4.68	4.72	4.72	4.72	4.72	4.76	4.72	4.76
Point 51	-0.002	4.60	4.60	4.56	4.60	4.60	4.64	4.60	4.64	4.64	4.68
Point 52	0.000	4.48	4.52	4.52	4.56	4.48	4.52	4.48	4.48	4.52	4.56
Point 53	0.002	4.40	4.44	4.44	4.48	4.44	4.44	4.36	4.44	4.44	4.52
Point 54	0.004	4.32	4.36	4.32	4.36	4.24	4.32	4.28	4.36	4.36	4.40
Point 55	0.006	4.20	4.24	4.24	4.32	4.20	4.24	4.20	4.24	4.24	4.28
Point 56	0.008	4.08	4.12	4.08	4.12	4.08	4.12	4.08	4.12	4.12	4.16
Point 57	0.010	4.00	4.00	4.00	4.08	3.96	4.00	4.00	4.04	4.04	4.04
Point 58	0.012	3.88	3.92	3.88	3.92	3.84	3.88	3.88	3.92	3.88	3.92
Point 59	0.014	3.76	3.84	3.80	3.88	3.76	3.80	3.76	3.80	3.80	3.84
Point 60	0.016	3.68	3.72	3.72	3.76	3.68	3.68	3.64	3.68	3.72	3.72
Point 61	0.018	3.64	3.64	3.60	3.64	3.52	3.60	3.60	3.60	3.64	3.64
Point 62	0.020	3.56	3.56	3.52	3.56	3.48	3.52	3.48	3.52	3.52	3.52
Point 63	0.022	3.44	3.48	3.44	3.48	3.40	3.40	3.36	3.40	3.44	3.48
Point 64	0.024	3.36	3.36	3.32	3.36	3.24	3.28	3.32	3.32	3.32	3.36
Point 65	0.026	3.24	3.28	3.28	3.32	3.16	3.20	3.24	3.24	3.24	3.24
Point 66	0.028	3.20	3.20	3.16	3.20	3.12	3.16	3.12	3.12	3.12	3.16
Point 67	0.030	3.08	3.12	3.12	3.12	3.04	3.04	3.08	3.08	3.08	3.08
Point 68	0.032	3.00	3.04	3.04	3.04	3.00	3.00	2.96	2.96	2.96	2.96
Point 69	0.034	2.96	2.96	2.92	2.96	2.84	2.84	2.88	2.92	2.92	2.96
Point 70	0.036	2.88	2.88	2.84	2.84	2.76	2.76	2.80	2.80	2.84	2.84
Point 71	0.038	2.76	2.76	2.80	2.80	2.72	2.76	2.72	2.72	2.76	2.76
Point 72	0.040	2.68	2.72	2.68	2.72	2.60	2.64	2.68	2.72	2.68	2.68
Point 73	0.042	2.64	2.64	2.64	2.68	2.60	2.60	2.60	2.60	2.64	2.64
Point 74	0.044	2.56	2.56	2.56	2.56	2.48	2.52	2.56	2.56	2.56	2.60
Point 75	0.046	2.48	2.48	2.48	2.48	2.44	2.44	2.48	2.52	2.48	2.48
Point 76	0.048	2.48	2.48	2.48	2.48	2.36	2.36	2.40	2.40	2.44	2.44
Point 77	0.050	2.36	2.40	2.36	2.36	2.28	2.28	2.32	2.32	2.36	2.36
Point 78	0.052	2.28	2.32	2.32	2.32	2.24	2.24	2.24	2.24	2.24	2.28
Point 79	0.054	2.24	2.28	2.20	2.20	2.16	2.16	2.20	2.24	2.24	2.24
Point 80	0.056	2.20	2.24	2.16	2.20	2.08	2.12	2.16	2.16	2.16	2.16
Point 81	0.058	2.16	2.16	2.16	2.16	2.04	2.04	2.12	2.12	2.08	2.12
Point 82	0.060	2.04	2.08	2.08	2.12	2.04	2.04	2.00	2.04	2.04	2.04
Point 83	0.062	2.08	2.08	2.04	2.04	1.96	2.00	1.96	1.96	2.00	2.00
Point 84	0.064	1.96	1.96	1.96	1.96	1.92	1.92	1.96	1.96	1.92	1.92
Point 85	0.066	1.92	1.96	1.92	1.92	1.84	1.84	1.88	1.88	1.84	1.88
Point 86	0.068	1.88	1.88	1.88	1.88	1.80	1.80	1.84	1.84	1.84	1.84
Point 87	0.070	1.80	1.84	1.84	1.84	1.76	1.76	1.80	1.80	1.80	1.80
Point 88	0.072	1.76	1.76	1.80	1.80	1.72	1.72	1.72	1.72	1.80	1.80
Point 89	0.074	1.72	1.76	1.72	1.72	1.64	1.68	1.68	1.72	1.72	1.76
Point 90	0.076	1.68	1.72	1.64	1.68	1.64	1.64	1.64	1.68	1.68	1.68
Point 91	0.078	1.60	1.64	1.60	1.64	1.56	1.60	1.60	1.64	1.60	1.64
Point 92	0.080	1.60	1.60	1.60	1.64	1.56	1.60	1.56	1.60	1.56	1.60
Point 93	0.082	1.56	1.56	1.52	1.56	1.48	1.52	1.56	1.56	1.56	1.56
Point 94	0.084	1.52	1.52	1.48	1.52	1.48	1.48	1.44	1.48	1.52	1.52
Point 95	0.086	1.44	1.48	1.44	1.48	1.40	1.44	1.48	1.48	1.48	1.48
Point 96	0.088	1.40	1.44	1.40	1.44	1.36	1.40	1.40	1.44	1.40	1.44
Point 97	0.090	1.40	1.40	1.36	1.40	1.32	1.32	1.36	1.40	1.36	1.36
Point 98	0.092	1.32	1.36	1.32	1.36	1.28	1.32	1.32	1.32	1.32	1.36
Point 99	0.094	1.32	1.36	1.28	1.32	1.24	1.28	1.32	1.32	1.24	1.28

Modified Port 0.050" lift N_2 (cont.)

		Run 1		Run 2		Run 3		Run 4		Run 5	
	Time	V_{high}	V_{low}	V_{high}	V_{low}	V_{high}	V_{low}	V_{high}	V_{low}	V_{high}	V_{low}
Point 100	0.096	1.24	1.28	1.28	1.32	1.20	1.24	1.24	1.28	1.28	1.28
Point 101	0.098	1.24	1.28	1.20	1.24	1.16	1.20	1.20	1.24	1.20	1.24
Point 102	0.100	1.20	1.24	1.16	1.20	1.12	1.16	1.16	1.20	1.20	1.20
Point 103	0.102	1.20	1.24	1.16	1.20	1.12	1.12	1.16	1.20	1.16	1.16
Point 104	0.104	1.16	1.16	1.12	1.20	1.08	1.12	1.08	1.12	1.16	1.16
Point 105	0.106	1.12	1.16	1.08	1.12	1.08	1.12	1.08	1.12	1.08	1.12
Point 106	0.108	1.08	1.12	1.04	1.08	1.08	1.12	1.08	1.12	1.04	1.04
Point 107	0.110	1.08	1.12	1.04	1.08	1.04	1.08	1.04	1.08	1.04	1.04
Point 108	0.112	1.00	1.04	1.04	1.08	0.96	1.00	1.00	1.04	1.04	1.08
Point 109	0.114	1.00	1.04	0.96	1.00	1.00	1.00	1.00	1.04	0.96	1.00
Point 110	0.116	1.00	1.04	0.96	1.00	0.92	0.96	0.92	0.96	0.96	1.00
Point 111	0.118	0.92	0.96	0.92	0.96	0.88	0.92	0.92	0.96	0.92	0.96
Point 112	0.120	0.92	0.96	0.92	0.96	0.88	0.88	0.88	0.92	0.88	0.92
Point 113	0.122	0.88	0.92	0.84	0.88	0.84	0.88	0.88	0.92	0.84	0.88
Point 114	0.124	0.84	0.88	0.84	0.88	0.84	0.88	0.88	0.92	0.84	0.88
Point 115	0.126	0.84	0.88	0.84	0.88	0.84	0.84	0.80	0.80	0.84	0.88
Point 116	0.128	0.80	0.84	0.80	0.88	0.84	0.84	0.80	0.84	0.84	0.84
Point 117	0.130	0.80	0.84	0.76	0.80	0.76	0.80	0.76	0.80	0.80	0.80
Point 118	0.132	0.72	0.76	0.76	0.80	0.72	0.80	0.76	0.80	0.80	0.84
Point 119	0.134	0.72	0.76	0.76	0.80	0.72	0.80	0.72	0.76	0.72	0.76
Point 120	0.136	0.72	0.76	0.72	0.76	0.72	0.76	0.76	0.80	0.76	0.76
Point 121	0.138	0.72	0.76	0.68	0.72	0.72	0.76	0.64	0.68	0.72	0.72
Point 122	0.140	0.72	0.76	0.68	0.72	0.68	0.72	0.68	0.72	0.72	0.76
Point 123	0.142	0.64	0.68	0.64	0.72	0.64	0.68	0.68	0.68	0.64	0.68
Point 124	0.144	0.64	0.68	0.64	0.68	0.64	0.68	0.60	0.68	0.60	0.64
Point 125	0.146	0.64	0.68	0.60	0.64	0.60	0.64	0.56	0.60	0.64	0.64
Point 126	0.148	0.60	0.64	0.60	0.64	0.56	0.64	0.60	0.60	0.60	0.64
Point 127	0.150	0.60	0.60	0.60	0.60	0.56	0.60	0.60	0.64	0.60	0.64
Point 128	0.152	0.60	0.68	0.60	0.60	0.52	0.56	0.56	0.60	0.60	0.60
Point 129	0.154	0.56	0.60	0.52	0.56	0.52	0.56	0.56	0.60	0.56	0.60
Point 130	0.156	0.52	0.56	0.56	0.56	0.52	0.56	0.52	0.56	0.56	0.60
Point 131	0.158	0.52	0.56	0.52	0.56	0.52	0.56	0.52	0.56	0.56	0.60
Point 132	0.160	0.52	0.56	0.52	0.56	0.52	0.56	0.52	0.56	0.48	0.52
Point 133	0.162	0.48	0.52	0.52	0.56	0.44	0.52	0.48	0.52	0.48	0.52
Point 134	0.164	0.48	0.52	0.48	0.52	0.44	0.48	0.44	0.48	0.48	0.52
Point 135	0.166	0.52	0.52	0.44	0.52	0.44	0.48	0.44	0.52	0.44	0.48
Point 136	0.168	0.52	0.52	0.44	0.48	0.40	0.44	0.44	0.48	0.44	0.44
Point 137	0.170	0.44	0.48	0.40	0.48	0.40	0.44	0.44	0.48	0.44	0.48
Point 138	0.172	0.40	0.44	0.40	0.44	0.40	0.44	0.40	0.44	0.40	0.48
Point 139	0.174	0.36	0.44	0.40	0.44	0.36	0.40	0.40	0.44	0.36	0.40
Point 140	0.176	0.40	0.44	0.40	0.44	0.36	0.40	0.40	0.44	0.40	0.44
Point 141	0.178	0.40	0.44	0.36	0.40	0.36	0.40	0.36	0.44	0.40	0.44
Point 142	0.180	0.36	0.40	0.36	0.40	0.32	0.40	0.36	0.36	0.36	0.40
Point 143	0.182	0.32	0.36	0.36	0.40	0.28	0.36	0.32	0.36	0.36	0.40
Point 144	0.184	0.28	0.32	0.32	0.36	0.32	0.36	0.32	0.36	0.36	0.40
Point 145	0.186	0.32	0.36	0.32	0.36	0.32	0.36	0.28	0.32	0.32	0.36
Point 146	0.188	0.28	0.32	0.32	0.36	0.28	0.32	0.32	0.36	0.32	0.36
Point 147	0.190	0.24	0.28	0.24	0.32	0.28	0.32	0.32	0.36	0.28	0.32
Point 148	0.192	0.28	0.36	0.28	0.32	0.24	0.32	0.28	0.32	0.28	0.32
Point 149	0.194	0.28	0.32	0.24	0.32	0.24	0.32	0.28	0.36	0.24	0.28

Modified Port 0.050" lift N_2 (cont.)

		Run 1		Run 2		Run 3		Run 4		Run 5	
	Time	V_{high}	V_{low}	V_{high}	V_{low}	V_{high}	V_{low}	V_{high}	V_{low}	V_{high}	V_{low}
Point 150	0.196	0.28	0.36	0.28	0.32	0.24	0.32	0.24	0.32	0.28	0.32
Point 151	0.198	0.28	0.28	0.24	0.28	0.20	0.24	0.28	0.32	0.28	0.32
Point 152	0.200	0.24	0.28	0.28	0.32	0.20	0.28	0.24	0.32	0.28	0.32
Point 153	0.202	0.24	0.24	0.28	0.32	0.24	0.24	0.20	0.28	0.24	0.28
Point 154	0.204	0.20	0.24	0.24	0.28	0.24	0.28	0.24	0.28	0.24	0.28
Point 155	0.206	0.20	0.24	0.20	0.24	0.20	0.24	0.20	0.28	0.20	0.24
Point 156	0.208	0.24	0.28	0.20	0.24	0.20	0.24	0.28	0.32	0.20	0.24
Point 157	0.210	0.24	0.24	0.16	0.20	0.20	0.20	0.20	0.24	0.28	0.28
Point 158	0.212	0.20	0.24	0.20	0.24	0.16	0.20	0.20	0.24	0.16	0.20
Point 159	0.214	0.20	0.20	0.20	0.24	0.16	0.20	0.20	0.24	0.20	0.20
Point 160	0.216	0.16	0.20	0.16	0.20	0.16	0.20	0.20	0.24	0.20	0.24
Point 161	0.218	0.20	0.24	0.16	0.20	0.16	0.20	0.16	0.20	0.20	0.24
Point 162	0.220	0.16	0.24	0.16	0.20	0.12	0.16	0.20	0.24	0.20	0.24
Point 163	0.222	0.16	0.20	0.20	0.24	0.16	0.20	0.20	0.24	0.16	0.20
Point 164	0.224	0.16	0.20	0.16	0.24	0.12	0.20	0.20	0.24	0.16	0.20
Point 165	0.226	0.16	0.24	0.16	0.20	0.16	0.20	0.20	0.24	0.20	0.20
Point 166	0.228	0.20	0.20	0.16	0.20	0.16	0.20	0.16	0.20	0.20	0.24
Point 167	0.230	0.16	0.20	0.16	0.24	0.20	0.24	0.16	0.20	0.16	0.20
Point 168	0.232	0.16	0.20	0.12	0.16	0.12	0.20	0.16	0.24	0.16	0.20
Point 169	0.234	0.16	0.20	0.16	0.20	0.16	0.20	0.16	0.20	0.16	0.20
Point 170	0.236	0.20	0.20	0.16	0.20	0.16	0.20	0.16	0.20	0.16	0.20
Point 171	0.238	0.20	0.24	0.16	0.20	0.16	0.20	0.16	0.16	0.16	0.20
Point 172	0.240	0.16	0.20	0.16	0.20	0.16	0.20	0.16	0.20	0.16	0.20
Point 173	0.242	0.20	0.24	0.12	0.16	0.12	0.16	0.12	0.16	0.16	0.20
Point 174	0.244	0.16	0.20	0.16	0.20	0.12	0.16	0.12	0.20	0.16	0.24
Point 175	0.246	0.16	0.20	0.12	0.16	0.16	0.20	0.16	0.20	0.16	0.20
Point 176	0.248	0.16	0.20	0.16	0.20	0.12	0.16	0.12	0.16	0.16	0.20
Point 177	0.250	0.20	0.24	0.16	0.20	0.20	0.24	0.12	0.20	0.16	0.20
Point 178	0.252	0.16	0.20	0.16	0.20	0.16	0.20	0.16	0.20	0.12	0.16
Point 179	0.254	0.16	0.20	0.12	0.20	0.16	0.20	0.16	0.20	0.12	0.20
Point 180	0.256	0.16	0.20	0.16	0.20	0.12	0.20	0.12	0.16	0.16	0.20
Point 181	0.258	0.12	0.16	0.16	0.20	0.20	0.24	0.12	0.20	0.16	0.20
Point 182	0.260	0.16	0.20	0.16	0.20	0.16	0.20	0.16	0.20	0.20	0.24
Point 183	0.262	0.16	0.20	0.16	0.20	0.16	0.20	0.12	0.20	0.16	0.20
Point 184	0.264	0.12	0.20	0.16	0.20	0.12	0.20	0.16	0.24	0.12	0.16
Point 185	0.266	0.16	0.24	0.16	0.20	0.12	0.16	0.16	0.20	0.12	0.16
Point 186	0.268	0.16	0.20	0.12	0.16	0.16	0.20	0.16	0.20	0.16	0.20
Point 187	0.270	0.16	0.20	0.16	0.20	0.16	0.20	0.12	0.20	0.16	0.16
Point 188	0.272	0.12	0.16	0.16	0.20	0.16	0.16	0.16	0.20	0.16	0.20
Point 189	0.274	0.16	0.20	0.16	0.20	0.16	0.20	0.16	0.20	0.16	0.20
Point 190	0.276	0.16	0.20	0.12	0.20	0.12	0.16	0.16	0.20	0.16	0.20
Point 191	0.278	0.16	0.20	0.20	0.20	0.16	0.20	0.20	0.20	0.12	0.20
Point 192	0.280	0.12	0.16	0.16	0.20	0.16	0.20	0.12	0.16	0.16	0.20
Point 193	0.282	0.16	0.20	0.16	0.20	0.20	0.24	0.16	0.20	0.12	0.16
Point 194	0.284	0.16	0.20	0.20	0.24	0.16	0.20	0.16	0.20	0.20	0.24
Point 195	0.286	0.16	0.16	0.16	0.20	0.16	0.20	0.20	0.24	0.16	0.20
Point 196	0.288	0.20	0.24	0.16	0.20	0.16	0.20	0.16	0.20	0.16	0.20
Point 197	0.290	0.20	0.20	0.16	0.20	0.16	0.20	0.16	0.20	0.12	0.16
Point 198	0.292	0.16	0.20	0.16	0.20	0.20	0.20	0.16	0.20	0.16	0.16
Point 199	0.294	0.20	0.24	0.12	0.16	0.20	0.20	0.16	0.20	0.16	0.20

Modified Port 0.050" lift N_2 (cont.)

		Run 1		Run 2		Run 3		Run 4		Run 5	
	Time	V_{high}	V_{low}	V_{high}	V_{low}	V_{high}	V_{low}	V_{high}	V_{low}	V_{high}	V_{low}
Point 200	0.296	0.16	0.20	0.16	0.20	0.16	0.20	0.16	0.16	0.16	0.20
Point 201	0.298	0.16	0.20	0.16	0.20	0.12	0.16	0.20	0.24	0.16	0.20
Point 202	0.300	0.16	0.20	0.12	0.16	0.16	0.20	0.16	0.20	0.16	0.20
Point 203	0.302	0.16	0.16	0.16	0.20	0.16	0.20	0.16	0.20	0.16	0.20
Point 204	0.304	0.16	0.20	0.16	0.20	0.16	0.20	0.16	0.20	0.16	0.20
Point 205	0.306	0.16	0.20	0.16	0.16	0.12	0.16	0.16	0.20	0.12	0.16
Point 206	0.308	0.16	0.20	0.16	0.24	0.12	0.20	0.16	0.20	0.16	0.20
Point 207	0.310	0.16	0.20	0.16	0.20	0.16	0.20	0.20	0.24	0.16	0.20
Point 208	0.312	0.16	0.20	0.16	0.20	0.12	0.20	0.16	0.20	0.12	0.20
Point 209	0.314	0.16	0.20	0.16	0.20	0.16	0.20	0.16	0.20	0.16	0.20
Point 210	0.316	0.16	0.20	0.16	0.20	0.16	0.20	0.20	0.24	0.16	0.20
Point 211	0.318	0.20	0.24	0.16	0.20	0.16	0.20	0.16	0.20	0.16	0.20
Point 212	0.320	0.12	0.16	0.16	0.20	0.12	0.16	0.16	0.20	0.20	0.24
Point 213	0.322	0.16	0.20	0.16	0.16	0.12	0.16	0.16	0.20	0.12	0.20
Point 214	0.324	0.16	0.20	0.20	0.20	0.12	0.16	0.12	0.20	0.16	0.20
Point 215	0.326	0.16	0.24	0.16	0.20	0.16	0.16	0.16	0.20	0.16	0.20
Point 216	0.328	0.16	0.20	0.16	0.20	0.16	0.20	0.12	0.16	0.16	0.20
Point 217	0.330	0.16	0.20	0.12	0.16	0.12	0.16	0.16	0.20	0.20	0.24
Point 218	0.332	0.12	0.16	0.20	0.20	0.16	0.20	0.12	0.16	0.16	0.20
Point 219	0.334	0.20	0.20	0.16	0.20	0.16	0.20	0.12	0.16	0.20	0.24
Point 220	0.336	0.16	0.20	0.16	0.20	0.16	0.24	0.16	0.20	0.20	0.24
Point 221	0.338	0.20	0.24	0.12	0.16	0.16	0.20	0.16	0.20	0.20	0.24
Point 222	0.340	0.16	0.20	0.20	0.24	0.16	0.20	0.16	0.16	0.16	0.20
Point 223	0.342	0.16	0.24	0.16	0.20	0.16	0.20	0.12	0.16	0.16	0.20
Point 224	0.344	0.20	0.20	0.12	0.16	0.16	0.16	0.12	0.16	0.16	0.24
Point 225	0.346	0.16	0.20	0.16	0.24	0.12	0.16	0.16	0.16	0.16	0.24
Point 226	0.348	0.16	0.20	0.12	0.20	0.16	0.20	0.12	0.16	0.16	0.20
Point 227	0.350	0.16	0.24	0.16	0.20	0.16	0.20	0.16	0.20	0.16	0.20
Point 228	0.352	0.20	0.24	0.16	0.20	0.12	0.20	0.16	0.20	0.16	0.20
Point 229	0.354	0.16	0.20	0.16	0.24	0.16	0.20	0.16	0.20	0.16	0.20
Point 230	0.356	0.12	0.16	0.12	0.20	0.16	0.20	0.16	0.20	0.16	0.20
Point 231	0.358	0.16	0.16	0.20	0.24	0.16	0.20	0.16	0.20	0.16	0.20
Point 232	0.360	0.20	0.24	0.16	0.20	0.12	0.16	0.16	0.20	0.12	0.20
Point 233	0.362	0.16	0.20	0.20	0.20	0.12	0.16	0.16	0.20	0.12	0.16
Point 234	0.364	0.12	0.20	0.16	0.16	0.16	0.20	0.12	0.16	0.16	0.20
Point 235	0.366	0.20	0.20	0.16	0.20	0.12	0.20	0.16	0.20	0.16	0.20
Point 236	0.368	0.16	0.20	0.16	0.20	0.12	0.16	0.16	0.20	0.12	0.16
Point 237	0.370	0.16	0.20	0.16	0.20	0.16	0.20	0.16	0.20	0.16	0.20
Point 238	0.372	0.20	0.20	0.12	0.16	0.16	0.20	0.20	0.20	0.20	0.24
Point 239	0.374	0.16	0.24	0.16	0.20	0.16	0.20	0.16	0.20	0.16	0.20
Point 240	0.376	0.20	0.24	0.12	0.16	0.16	0.20	0.16	0.20	0.16	0.24
Point 241	0.378	0.12	0.16	0.16	0.20	0.16	0.20	0.16	0.20	0.16	0.20
Point 242	0.380	0.12	0.16	0.16	0.20	0.16	0.20	0.16	0.20	0.16	0.20
Point 243	0.382	0.20	0.24	0.12	0.16	0.12	0.16	0.16	0.20	0.16	0.20
Point 244	0.384	0.16	0.20	0.12	0.16	0.20	0.24	0.16	0.20	0.16	0.20
Point 245	0.386	0.16	0.20	0.08	0.12	0.16	0.20	0.16	0.20	0.16	0.20
Point 246	0.388	0.16	0.16	0.16	0.20	0.16	0.20	0.16	0.20	0.16	0.20
Point 247	0.390	0.16	0.20	0.16	0.20	0.16	0.20	0.12	0.16	0.16	0.20
Point 248	0.392	0.16	0.20	0.16	0.20	0.16	0.16	0.20	0.24	0.16	0.24
Point 249	0.394	0.20	0.20	0.08	0.12	0.20	0.24	0.16	0.20	0.12	0.16

Modified Port 0.050" lift N_2 (cont.)

		Run 1		Run 2		Run 3		Run 4		Run 5	
	Time	V_{high}	V_{low}	V_{high}	V_{low}	V_{high}	V_{low}	V_{high}	V_{low}	V_{high}	V_{low}
Point 250	0.396	0.16	0.24	0.16	0.20	0.16	0.20	0.16	0.20	0.16	0.20
Point 251	0.398	0.16	0.20	0.16	0.20	0.16	0.16	0.12	0.16	0.20	0.24
Point 252	0.400	0.16	0.20	0.12	0.16	0.20	0.24	0.16	0.20	0.20	0.24
Point 253	0.402	0.16	0.24	0.12	0.20	0.16	0.20	0.16	0.20	0.16	0.20
Point 254	0.404	0.16	0.24	0.16	0.20	0.16	0.20	0.16	0.24	0.20	0.24
Point 255	0.406	0.16	0.20	0.16	0.20	0.12	0.20	0.20	0.24	0.16	0.20
Point 256	0.408	0.16	0.20	0.12	0.16	0.16	0.20	0.16	0.20	0.20	0.20
Point 257	0.410	0.20	0.20	0.12	0.20	0.16	0.20	0.16	0.20	0.20	0.20
Point 258	0.412	0.16	0.20	0.16	0.20	0.16	0.20	0.20	0.20	0.16	0.20
Point 259	0.414	0.16	0.20	0.16	0.20	0.16	0.20	0.20	0.24	0.16	0.20
Point 260	0.416	0.16	0.20	0.12	0.20	0.16	0.20	0.16	0.20	0.16	0.20
Point 261	0.418	0.16	0.20	0.16	0.20	0.16	0.20	0.16	0.20	0.16	0.20
Point 262	0.420	0.16	0.20	0.16	0.20	0.16	0.20	0.20	0.20	0.16	0.20
Point 263	0.422	0.16	0.20	0.12	0.20	0.16	0.20	0.16	0.20	0.20	0.20
Point 264	0.424	0.16	0.20	0.20	0.24	0.16	0.20	0.16	0.20	0.12	0.16
Point 265	0.426	0.20	0.20	0.16	0.20	0.16	0.20	0.16	0.20	0.20	0.24
Point 266	0.428	0.16	0.16	0.16	0.20	0.16	0.20	0.16	0.20	0.12	0.16
Point 267	0.430	0.16	0.20	0.16	0.20	0.16	0.20	0.16	0.20	0.16	0.20
Point 268	0.432	0.16	0.20	0.12	0.16	0.16	0.16	0.16	0.20	0.12	0.20
Point 269	0.434	0.16	0.20	0.16	0.16	0.16	0.20	0.16	0.20	0.16	0.20
Point 270	0.436	0.20	0.24	0.16	0.20	0.12	0.20	0.20	0.20	0.16	0.16
Point 271	0.438	0.16	0.20	0.16	0.20	0.12	0.20	0.16	0.16	0.12	0.16
Point 272	0.440	0.16	0.20	0.12	0.20	0.16	0.20	0.16	0.20	0.16	0.24
Point 273	0.442	0.16	0.20	0.16	0.24	0.16	0.20	0.16	0.20	0.16	0.20
Point 274	0.444	0.12	0.20	0.12	0.16	0.20	0.24	0.12	0.20	0.16	0.20
Point 275	0.446	0.16	0.20	0.12	0.16	0.16	0.20	0.16	0.20	0.16	0.16
Point 276	0.448	0.16	0.20	0.16	0.20	0.16	0.20	0.16	0.20	0.16	0.16
Point 277	0.450	0.12	0.16	0.16	0.20	0.16	0.20	0.16	0.24	0.16	0.20
Point 278	0.452	0.20	0.24	0.16	0.20	0.20	0.20	0.12	0.20	0.16	0.20
Point 279	0.454	0.16	0.20	0.20	0.20	0.16	0.20	0.16	0.20	0.12	0.16
Point 280	0.456	0.16	0.20	0.12	0.20	0.16	0.20	0.12	0.16	0.16	0.20
Point 281	0.458	0.20	0.24	0.16	0.20	0.16	0.20	0.12	0.16	0.16	0.20
Point 282	0.460	0.12	0.16	0.12	0.20	0.20	0.20	0.16	0.20	0.16	0.20
Point 283	0.462	0.16	0.20	0.20	0.24	0.20	0.24	0.16	0.20	0.12	0.16
Point 284	0.464	0.16	0.20	0.12	0.16	0.16	0.20	0.16	0.20	0.12	0.20
Point 285	0.466	0.12	0.20	0.16	0.20	0.16	0.20	0.16	0.20	0.16	0.20
Point 286	0.468	0.16	0.20	0.16	0.20	0.20	0.20	0.20	0.24	0.16	0.20
Point 287	0.470	0.12	0.16	0.12	0.20	0.12	0.16	0.16	0.20	0.16	0.16
Point 288	0.472	0.12	0.16	0.12	0.20	0.16	0.20	0.16	0.20	0.16	0.20
Point 289	0.474	0.16	0.24	0.16	0.20	0.16	0.20	0.20	0.24	0.16	0.20
Point 290	0.476	0.16	0.20	0.12	0.20	0.16	0.20	0.20	0.24	0.12	0.16
Point 291	0.478	0.16	0.20	0.12	0.16	0.12	0.20	0.16	0.20	0.12	0.16
Point 292	0.480	0.16	0.20	0.12	0.16	0.16	0.20	0.16	0.20	0.16	0.20
Point 293	0.482	0.20	0.24	0.16	0.16	0.16	0.20	0.20	0.20	0.16	0.20
Point 294	0.484	0.16	0.20	0.16	0.20	0.12	0.16	0.16	0.20	0.16	0.20
Point 295	0.486	0.16	0.20	0.16	0.20	0.20	0.24	0.16	0.20	0.12	0.16
Point 296	0.488	0.16	0.20	0.16	0.20	0.12	0.16	0.16	0.20	0.20	0.24
Point 297	0.490	0.20	0.24	0.16	0.20	0.16	0.20	0.16	0.20	0.16	0.20
Point 298	0.492	0.20	0.24	0.16	0.20	0.12	0.20	0.16	0.16	0.12	0.16
Point 299	0.494	0.16	0.20	0.16	0.24	0.16	0.20	0.16	0.20	0.12	0.20
Point 300	0.496	0.16	0.20	0.16	0.20	0.16	0.20	0.16	0.20	0.16	0.20

Modified Port 0.100" lift N_2

		Run 1		Run 2		Run 3		Run 4		Run 5	
	Time	V_{high}	V_{low}	V_{high}	V_{low}	V_{high}	V_{low}	V_{high}	V_{low}	V_{high}	V_{low}
Point 1	-0.102	5.00	5.04	4.92	4.96	5.04	5.08	5.00	5.04	4.96	4.96
Point 2	-0.100	5.00	5.00	4.96	4.96	5.00	5.04	5.04	5.04	4.96	5.00
Point 3	-0.098	5.00	5.04	4.96	4.96	5.04	5.08	5.00	5.04	4.92	4.96
Point 4	-0.096	4.96	5.00	4.92	4.96	5.04	5.08	5.00	5.00	4.96	4.96
Point 5	-0.094	4.96	4.96	4.92	4.96	5.04	5.04	5.00	5.04	4.96	5.00
Point 6	-0.092	5.00	5.04	4.88	4.92	5.04	5.04	5.00	5.00	4.96	5.00
Point 7	-0.090	5.00	5.00	4.92	4.92	5.04	5.08	5.00	5.04	4.96	4.96
Point 8	-0.088	5.00	5.00	4.92	4.92	5.00	5.00	5.00	5.04	4.96	4.96
Point 9	-0.086	5.00	5.00	4.92	4.96	5.04	5.04	5.00	5.00	4.96	5.00
Point 10	-0.084	4.96	5.00	4.92	4.96	5.00	5.04	5.04	5.04	4.96	5.00
Point 11	-0.082	5.00	5.00	4.92	4.92	5.00	5.04	4.96	5.00	4.96	5.00
Point 12	-0.080	5.00	5.00	4.96	5.00	5.04	5.08	5.00	5.04	4.96	4.96
Point 13	-0.078	5.00	5.00	4.96	5.00	5.04	5.04	5.04	5.04	4.92	4.96
Point 14	-0.076	4.96	5.00	4.92	4.96	5.04	5.04	5.00	5.04	5.00	5.00
Point 15	-0.074	4.96	5.00	4.92	4.96	5.04	5.04	5.00	5.04	4.96	4.96
Point 16	-0.072	4.96	5.00	4.92	4.96	5.00	5.00	5.04	5.04	4.96	4.96
Point 17	-0.070	4.96	4.96	4.92	4.96	5.00	5.04	5.00	5.04	4.96	5.00
Point 18	-0.068	4.96	5.00	4.92	4.96	5.04	5.08	4.96	5.00	4.96	5.00
Point 19	-0.066	4.96	5.00	4.96	4.96	5.04	5.08	5.04	5.04	4.92	4.96
Point 20	-0.064	5.00	5.00	4.96	4.96	5.04	5.04	5.00	5.00	5.00	5.00
Point 21	-0.062	5.00	5.00	4.92	4.96	5.08	5.08	5.04	5.04	4.96	4.96
Point 22	-0.060	5.00	5.04	4.92	4.96	5.00	5.04	5.00	5.00	4.96	5.00
Point 23	-0.058	4.96	5.00	4.92	4.92	5.00	5.04	5.00	5.04	5.00	5.00
Point 24	-0.056	4.96	5.00	4.96	5.00	5.04	5.08	5.00	5.04	4.96	4.96
Point 25	-0.054	5.00	5.00	4.92	4.96	5.08	5.08	5.04	5.08	4.96	5.00
Point 26	-0.052	4.96	5.00	4.92	4.92	5.04	5.08	5.04	5.04	4.92	4.96
Point 27	-0.050	4.96	5.00	4.92	4.96	5.04	5.08	5.00	5.04	4.92	4.96
Point 28	-0.048	5.00	5.00	4.92	4.96	5.08	5.08	5.00	5.04	4.96	4.96
Point 29	-0.046	5.00	5.00	4.96	4.96	5.04	5.04	5.04	5.04	4.96	5.00
Point 30	-0.044	4.96	5.00	4.96	4.96	5.08	5.08	5.04	5.04	4.92	4.96
Point 31	-0.042	4.96	5.00	4.96	5.00	5.04	5.04	5.00	5.00	4.96	4.96
Point 32	-0.040	5.00	5.00	4.92	4.96	5.04	5.04	5.00	5.04	4.96	5.00
Point 33	-0.038	5.00	5.04	4.96	4.96	5.08	5.08	5.04	5.04	4.96	5.00
Point 34	-0.036	4.96	5.00	4.96	5.00	5.00	5.04	4.96	5.00	4.96	5.00
Point 35	-0.034	5.04	5.04	4.96	5.00	5.00	5.04	5.00	5.00	5.00	5.00
Point 36	-0.032	5.00	5.00	4.92	4.96	5.04	5.08	5.00	5.04	4.96	5.00
Point 37	-0.030	5.00	5.04	4.96	4.96	5.08	5.08	5.00	5.04	4.96	5.00
Point 38	-0.028	5.00	5.04	4.96	4.96	5.04	5.04	5.00	5.04	4.96	5.00
Point 39	-0.026	5.04	5.04	4.92	4.96	5.04	5.04	5.00	5.04	4.92	4.96
Point 40	-0.024	5.00	5.04	4.92	4.96	5.00	5.00	5.04	5.04	4.96	4.96
Point 41	-0.022	4.96	5.00	4.92	4.96	5.00	5.04	4.96	5.00	5.00	5.04
Point 42	-0.020	4.96	5.00	4.92	4.96	5.00	5.04	5.00	5.04	4.96	5.00
Point 43	-0.018	4.96	5.00	4.92	4.92	5.00	5.00	5.00	5.04	4.96	5.00
Point 44	-0.016	5.00	5.00	4.92	4.96	5.04	5.08	4.96	5.00	4.96	4.96
Point 45	-0.014	5.00	5.00	4.92	4.96	5.00	5.04	5.00	5.00	4.92	4.96
Point 46	-0.012	4.96	5.00	4.84	4.88	4.96	4.96	4.96	4.96	4.92	4.92
Point 47	-0.010	4.92	4.92	4.88	4.92	4.96	4.96	4.92	4.92	4.88	4.88
Point 48	-0.008	4.88	4.88	4.84	4.84	4.96	4.96	4.92	4.92	4.84	4.88
Point 49	-0.006	4.80	4.80	4.80	4.80	4.88	4.88	4.80	4.80	4.80	4.80

Modified Port 0.100" lift N_2 (cont.)

		Run 1		Run 2		Run 3		Run 4		Run 5	
	Time	V_{high}	V_{low}	V_{high}	V_{low}	V_{high}	V_{low}	V_{high}	V_{low}	V_{high}	V_{low}
Point 50	-0.004	4.72	4.72	4.68	4.72	4.76	4.80	4.72	4.76	4.76	4.76
Point 51	-0.002	4.64	4.68	4.60	4.64	4.64	4.72	4.64	4.68	4.60	4.64
Point 52	0.000	4.52	4.52	4.52	4.56	4.52	4.60	4.52	4.60	4.48	4.52
Point 53	0.002	4.44	4.52	4.44	4.48	4.44	4.48	4.44	4.48	4.36	4.44
Point 54	0.004	4.28	4.36	4.32	4.40	4.28	4.36	4.28	4.36	4.20	4.28
Point 55	0.006	4.16	4.24	4.20	4.24	4.08	4.20	4.16	4.24	4.04	4.16
Point 56	0.008	3.96	4.04	4.08	4.12	3.88	4.00	3.92	4.04	3.92	4.00
Point 57	0.010	3.84	3.92	3.92	4.00	3.72	3.80	3.76	3.88	3.72	3.84
Point 58	0.012	3.64	3.76	3.72	3.80	3.56	3.68	3.60	3.72	3.56	3.68
Point 59	0.014	3.48	3.60	3.52	3.60	3.36	3.48	3.44	3.56	3.36	3.48
Point 60	0.016	3.32	3.44	3.36	3.48	3.20	3.28	3.28	3.40	3.20	3.28
Point 61	0.018	3.12	3.20	3.24	3.32	3.04	3.12	3.08	3.16	3.00	3.12
Point 62	0.020	3.00	3.08	3.08	3.16	2.88	2.96	2.96	3.00	2.92	2.96
Point 63	0.022	2.84	2.88	2.88	2.96	2.76	2.80	2.76	2.84	2.68	2.76
Point 64	0.024	2.72	2.76	2.76	2.84	2.60	2.64	2.60	2.72	2.60	2.68
Point 65	0.026	2.56	2.60	2.60	2.64	2.44	2.52	2.52	2.56	2.44	2.48
Point 66	0.028	2.40	2.48	2.44	2.52	2.36	2.36	2.36	2.40	2.36	2.40
Point 67	0.030	2.32	2.36	2.36	2.40	2.24	2.28	2.24	2.28	2.20	2.28
Point 68	0.032	2.20	2.24	2.20	2.24	2.12	2.16	2.16	2.16	2.08	2.12
Point 69	0.034	2.08	2.12	2.08	2.12	2.00	2.04	2.04	2.08	1.96	2.00
Point 70	0.036	1.92	1.96	2.00	2.00	1.92	1.92	1.96	2.00	1.88	1.92
Point 71	0.038	1.88	1.92	1.92	1.92	1.80	1.80	1.84	1.88	1.76	1.80
Point 72	0.040	1.80	1.84	1.80	1.84	1.72	1.72	1.76	1.76	1.72	1.72
Point 73	0.042	1.68	1.68	1.68	1.72	1.64	1.64	1.68	1.68	1.60	1.64
Point 74	0.044	1.60	1.60	1.64	1.64	1.52	1.52	1.60	1.60	1.52	1.52
Point 75	0.046	1.56	1.56	1.52	1.52	1.48	1.48	1.52	1.52	1.44	1.48
Point 76	0.048	1.44	1.44	1.48	1.48	1.40	1.44	1.40	1.40	1.36	1.36
Point 77	0.050	1.36	1.36	1.40	1.40	1.32	1.32	1.32	1.32	1.28	1.28
Point 78	0.052	1.32	1.32	1.32	1.32	1.24	1.28	1.28	1.28	1.28	1.28
Point 79	0.054	1.24	1.24	1.24	1.24	1.16	1.20	1.20	1.20	1.24	1.24
Point 80	0.056	1.16	1.20	1.20	1.20	1.08	1.12	1.16	1.16	1.08	1.12
Point 81	0.058	1.08	1.08	1.12	1.12	1.04	1.08	1.08	1.12	1.08	1.08
Point 82	0.060	1.00	1.04	1.04	1.04	1.00	1.00	1.00	1.00	0.96	0.96
Point 83	0.062	1.00	1.00	0.96	0.96	0.92	0.92	0.96	0.96	0.96	0.96
Point 84	0.064	0.92	0.92	0.96	0.96	0.88	0.92	0.92	0.92	0.88	0.88
Point 85	0.066	0.88	0.92	0.88	0.88	0.88	0.88	0.88	0.92	0.80	0.84
Point 86	0.068	0.84	0.84	0.88	0.88	0.80	0.80	0.80	0.80	0.76	0.76
Point 87	0.070	0.80	0.80	0.80	0.84	0.76	0.80	0.76	0.80	0.72	0.76
Point 88	0.072	0.76	0.76	0.76	0.76	0.72	0.76	0.72	0.76	0.72	0.72
Point 89	0.074	0.72	0.76	0.72	0.76	0.64	0.68	0.68	0.72	0.64	0.68
Point 90	0.076	0.68	0.68	0.68	0.72	0.64	0.64	0.68	0.68	0.60	0.64
Point 91	0.078	0.64	0.64	0.64	0.64	0.60	0.64	0.64	0.68	0.60	0.60
Point 92	0.080	0.56	0.60	0.60	0.60	0.56	0.56	0.60	0.60	0.56	0.56
Point 93	0.082	0.52	0.56	0.60	0.60	0.52	0.56	0.56	0.60	0.52	0.56
Point 94	0.084	0.52	0.56	0.56	0.56	0.48	0.52	0.52	0.52	0.48	0.52
Point 95	0.086	0.52	0.56	0.52	0.52	0.44	0.48	0.48	0.52	0.44	0.48
Point 96	0.088	0.52	0.52	0.48	0.48	0.44	0.44	0.40	0.44	0.44	0.44
Point 97	0.090	0.48	0.48	0.48	0.52	0.44	0.48	0.44	0.48	0.40	0.44
Point 98	0.092	0.44	0.44	0.44	0.48	0.40	0.44	0.44	0.44	0.36	0.36
Point 99	0.094	0.36	0.40	0.36	0.40	0.32	0.36	0.36	0.40	0.32	0.40

Modified Port 0.100" lift N_2 (cont.)

		Run 1		Run 2		Run 3		Run 4		Run 5	
	Time	V_{high}	V_{low}	V_{high}	V_{low}	V_{high}	V_{low}	V_{high}	V_{low}	V_{high}	V_{low}
Point 100	0.096	0.36	0.40	0.36	0.36	0.32	0.36	0.32	0.36	0.32	0.36
Point 101	0.098	0.32	0.36	0.32	0.36	0.32	0.36	0.32	0.36	0.32	0.36
Point 102	0.100	0.28	0.32	0.32	0.36	0.32	0.32	0.28	0.32	0.28	0.32
Point 103	0.102	0.28	0.32	0.28	0.32	0.28	0.32	0.28	0.32	0.28	0.28
Point 104	0.104	0.24	0.28	0.28	0.28	0.24	0.28	0.24	0.32	0.24	0.28
Point 105	0.106	0.24	0.28	0.28	0.32	0.24	0.28	0.24	0.28	0.24	0.28
Point 106	0.108	0.24	0.28	0.24	0.28	0.20	0.24	0.24	0.28	0.24	0.28
Point 107	0.110	0.24	0.28	0.20	0.24	0.20	0.28	0.20	0.24	0.20	0.24
Point 108	0.112	0.20	0.24	0.20	0.24	0.16	0.24	0.20	0.24	0.20	0.24
Point 109	0.114	0.20	0.24	0.16	0.20	0.24	0.28	0.20	0.24	0.16	0.20
Point 110	0.116	0.20	0.24	0.16	0.20	0.16	0.20	0.20	0.24	0.16	0.20
Point 111	0.118	0.16	0.20	0.16	0.20	0.16	0.20	0.16	0.20	0.12	0.16
Point 112	0.120	0.16	0.20	0.16	0.20	0.16	0.20	0.16	0.20	0.16	0.20
Point 113	0.122	0.16	0.20	0.16	0.20	0.16	0.20	0.20	0.24	0.16	0.20
Point 114	0.124	0.16	0.20	0.12	0.16	0.20	0.24	0.20	0.24	0.12	0.16
Point 115	0.126	0.16	0.20	0.16	0.20	0.16	0.20	0.16	0.20	0.20	0.20
Point 116	0.128	0.20	0.20	0.16	0.20	0.16	0.20	0.16	0.20	0.16	0.16
Point 117	0.130	0.16	0.20	0.20	0.24	0.24	0.24	0.20	0.24	0.16	0.20
Point 118	0.132	0.16	0.20	0.20	0.20	0.16	0.20	0.16	0.20	0.20	0.24
Point 119	0.134	0.16	0.20	0.20	0.24	0.16	0.20	0.24	0.24	0.20	0.24
Point 120	0.136	0.16	0.20	0.16	0.20	0.16	0.20	0.20	0.24	0.20	0.24
Point 121	0.138	0.16	0.20	0.20	0.24	0.16	0.24	0.20	0.24	0.16	0.20
Point 122	0.140	0.16	0.20	0.16	0.24	0.20	0.24	0.20	0.24	0.16	0.20
Point 123	0.142	0.16	0.20	0.16	0.24	0.20	0.24	0.16	0.20	0.20	0.24
Point 124	0.144	0.16	0.20	0.16	0.20	0.20	0.24	0.16	0.20	0.16	0.20
Point 125	0.146	0.16	0.20	0.20	0.24	0.20	0.20	0.20	0.24	0.16	0.20
Point 126	0.148	0.16	0.20	0.20	0.20	0.20	0.24	0.16	0.20	0.20	0.20
Point 127	0.150	0.16	0.20	0.16	0.20	0.20	0.24	0.20	0.24	0.16	0.20
Point 128	0.152	0.20	0.24	0.16	0.20	0.16	0.20	0.20	0.24	0.16	0.20
Point 129	0.154	0.16	0.20	0.20	0.20	0.16	0.20	0.20	0.24	0.12	0.16
Point 130	0.156	0.20	0.20	0.20	0.20	0.16	0.20	0.20	0.20	0.16	0.24
Point 131	0.158	0.16	0.20	0.16	0.20	0.20	0.24	0.16	0.20	0.20	0.20
Point 132	0.160	0.16	0.20	0.16	0.20	0.16	0.20	0.16	0.20	0.16	0.20
Point 133	0.162	0.16	0.20	0.16	0.20	0.16	0.20	0.16	0.20	0.16	0.20
Point 134	0.164	0.20	0.24	0.20	0.20	0.16	0.20	0.12	0.16	0.16	0.24
Point 135	0.166	0.16	0.20	0.16	0.20	0.16	0.20	0.16	0.20	0.20	0.20
Point 136	0.168	0.16	0.20	0.16	0.20	0.16	0.20	0.16	0.20	0.16	0.20
Point 137	0.170	0.20	0.24	0.16	0.20	0.16	0.20	0.16	0.24	0.12	0.16
Point 138	0.172	0.12	0.20	0.12	0.20	0.16	0.20	0.16	0.20	0.16	0.24
Point 139	0.174	0.16	0.20	0.16	0.20	0.16	0.20	0.16	0.20	0.20	0.24
Point 140	0.176	0.16	0.20	0.16	0.20	0.16	0.20	0.16	0.20	0.16	0.20
Point 141	0.178	0.20	0.20	0.16	0.20	0.16	0.20	0.20	0.24	0.16	0.20
Point 142	0.180	0.20	0.24	0.16	0.20	0.16	0.16	0.16	0.20	0.16	0.20
Point 143	0.182	0.16	0.20	0.20	0.24	0.16	0.24	0.16	0.20	0.20	0.24
Point 144	0.184	0.16	0.20	0.16	0.20	0.16	0.20	0.16	0.20	0.16	0.20
Point 145	0.186	0.16	0.20	0.16	0.24	0.16	0.20	0.20	0.24	0.20	0.24
Point 146	0.188	0.16	0.24	0.16	0.20	0.20	0.24	0.16	0.20	0.16	0.20
Point 147	0.190	0.20	0.20	0.20	0.24	0.20	0.24	0.16	0.20	0.20	0.24
Point 148	0.192	0.16	0.20	0.16	0.20	0.16	0.20	0.16	0.20	0.16	0.20
Point 149	0.194	0.16	0.20	0.16	0.24	0.16	0.20	0.20	0.24	0.16	0.20

Modified Port 0.100" lift N_2 (cont.)

		Run 1		Run 2		Run 3		Run 4		Run 5	
	Time	V_{high}	V_{low}	V_{high}	V_{low}	V_{high}	V_{low}	V_{high}	V_{low}	V_{high}	V_{low}
Point 150	0.196	0.12	0.16	0.16	0.24	0.20	0.24	0.20	0.24	0.16	0.20
Point 151	0.198	0.16	0.20	0.16	0.20	0.16	0.24	0.20	0.20	0.20	0.24
Point 152	0.200	0.16	0.20	0.16	0.20	0.16	0.20	0.20	0.24	0.16	0.20
Point 153	0.202	0.20	0.20	0.20	0.20	0.16	0.20	0.16	0.20	0.16	0.20
Point 154	0.204	0.16	0.16	0.20	0.24	0.20	0.24	0.20	0.20	0.16	0.20
Point 155	0.206	0.16	0.20	0.20	0.24	0.20	0.20	0.16	0.24	0.20	0.24
Point 156	0.208	0.16	0.20	0.16	0.20	0.20	0.28	0.20	0.24	0.16	0.20
Point 157	0.210	0.20	0.24	0.16	0.24	0.16	0.20	0.20	0.24	0.16	0.20
Point 158	0.212	0.16	0.20	0.20	0.24	0.20	0.24	0.16	0.20	0.16	0.20
Point 159	0.214	0.16	0.20	0.16	0.20	0.16	0.24	0.20	0.24	0.16	0.20
Point 160	0.216	0.16	0.20	0.16	0.20	0.16	0.20	0.16	0.20	0.16	0.20
Point 161	0.218	0.16	0.20	0.16	0.20	0.20	0.24	0.20	0.20	0.16	0.20
Point 162	0.220	0.16	0.20	0.20	0.20	0.20	0.24	0.20	0.24	0.12	0.16
Point 163	0.222	0.16	0.20	0.16	0.20	0.12	0.16	0.16	0.20	0.20	0.24
Point 164	0.224	0.16	0.20	0.16	0.20	0.12	0.16	0.16	0.20	0.20	0.24
Point 165	0.226	0.16	0.24	0.16	0.20	0.16	0.20	0.16	0.24	0.16	0.20
Point 166	0.228	0.16	0.20	0.16	0.20	0.20	0.24	0.16	0.20	0.20	0.24
Point 167	0.230	0.16	0.20	0.16	0.20	0.20	0.24	0.16	0.20	0.20	0.24
Point 168	0.232	0.20	0.20	0.16	0.20	0.16	0.20	0.20	0.24	0.16	0.20
Point 169	0.234	0.20	0.20	0.16	0.16	0.16	0.20	0.20	0.24	0.16	0.20
Point 170	0.236	0.16	0.20	0.16	0.20	0.16	0.20	0.20	0.24	0.20	0.20
Point 171	0.238	0.16	0.20	0.16	0.20	0.12	0.16	0.16	0.20	0.20	0.24
Point 172	0.240	0.16	0.20	0.16	0.20	0.16	0.20	0.16	0.20	0.16	0.24
Point 173	0.242	0.20	0.24	0.16	0.20	0.16	0.20	0.16	0.20	0.16	0.20
Point 174	0.244	0.20	0.24	0.20	0.24	0.16	0.24	0.16	0.20	0.16	0.20
Point 175	0.246	0.16	0.20	0.16	0.20	0.16	0.20	0.16	0.20	0.12	0.20
Point 176	0.248	0.16	0.20	0.16	0.20	0.16	0.20	0.16	0.20	0.16	0.20
Point 177	0.250	0.20	0.24	0.20	0.20	0.20	0.24	0.20	0.20	0.16	0.20
Point 178	0.252	0.16	0.20	0.20	0.24	0.16	0.20	0.16	0.20	0.16	0.20
Point 179	0.254	0.16	0.20	0.16	0.20	0.16	0.20	0.20	0.24	0.16	0.24
Point 180	0.256	0.16	0.24	0.20	0.24	0.16	0.20	0.16	0.20	0.16	0.20
Point 181	0.258	0.12	0.20	0.16	0.20	0.20	0.24	0.24	0.24	0.16	0.20
Point 182	0.260	0.20	0.24	0.16	0.20	0.16	0.24	0.20	0.24	0.16	0.20
Point 183	0.262	0.16	0.20	0.16	0.20	0.20	0.24	0.20	0.24	0.16	0.20
Point 184	0.264	0.16	0.24	0.16	0.24	0.20	0.24	0.20	0.24	0.16	0.24
Point 185	0.266	0.12	0.16	0.16	0.20	0.16	0.20	0.16	0.20	0.16	0.20
Point 186	0.268	0.16	0.20	0.20	0.24	0.20	0.20	0.20	0.24	0.16	0.20
Point 187	0.270	0.16	0.20	0.20	0.24	0.20	0.20	0.20	0.24	0.16	0.20
Point 188	0.272	0.16	0.20	0.16	0.20	0.20	0.24	0.20	0.24	0.12	0.16
Point 189	0.274	0.16	0.20	0.16	0.20	0.20	0.24	0.20	0.20	0.12	0.16
Point 190	0.276	0.16	0.20	0.16	0.20	0.20	0.24	0.16	0.16	0.16	0.20
Point 191	0.278	0.16	0.20	0.16	0.24	0.20	0.24	0.16	0.20	0.20	0.20
Point 192	0.280	0.16	0.20	0.12	0.16	0.20	0.24	0.20	0.20	0.16	0.20
Point 193	0.282	0.16	0.24	0.16	0.20	0.20	0.20	0.20	0.20	0.16	0.20
Point 194	0.284	0.16	0.20	0.16	0.20	0.16	0.20	0.20	0.20	0.12	0.20
Point 195	0.286	0.16	0.20	0.20	0.20	0.16	0.16	0.20	0.24	0.20	0.20
Point 196	0.288	0.20	0.20	0.12	0.16	0.20	0.24	0.20	0.20	0.16	0.20
Point 197	0.290	0.20	0.24	0.20	0.24	0.16	0.20	0.16	0.20	0.16	0.20
Point 198	0.292	0.16	0.24	0.12	0.16	0.16	0.24	0.20	0.24	0.16	0.20
Point 199	0.294	0.16	0.20	0.16	0.16	0.20	0.24	0.16	0.20	0.16	0.20

Modified Port 0.100" lift N_2 (cont.)

		Run 1		Run 2		Run 3		Run 4		Run 5	
	Time	V_{high}	V_{low}	V_{high}	V_{low}	V_{high}	V_{low}	V_{high}	V_{low}	V_{high}	V_{low}
Point 200	0.296	0.16	0.20	0.16	0.20	0.20	0.24	0.12	0.16	0.20	0.20
Point 201	0.298	0.16	0.24	0.20	0.24	0.16	0.20	0.12	0.20	0.16	0.20
Point 202	0.300	0.12	0.16	0.16	0.20	0.20	0.24	0.20	0.24	0.20	0.24
Point 203	0.302	0.16	0.20	0.20	0.24	0.20	0.24	0.16	0.20	0.16	0.24
Point 204	0.304	0.16	0.20	0.16	0.20	0.20	0.24	0.16	0.20	0.16	0.20
Point 205	0.306	0.20	0.24	0.16	0.20	0.20	0.20	0.16	0.24	0.20	0.24
Point 206	0.308	0.12	0.16	0.16	0.20	0.16	0.20	0.20	0.24	0.20	0.24
Point 207	0.310	0.16	0.20	0.16	0.20	0.20	0.24	0.16	0.20	0.16	0.20
Point 208	0.312	0.16	0.20	0.20	0.20	0.16	0.20	0.16	0.20	0.16	0.20
Point 209	0.314	0.12	0.20	0.16	0.20	0.16	0.20	0.16	0.20	0.16	0.20
Point 210	0.316	0.16	0.24	0.20	0.24	0.20	0.24	0.16	0.20	0.20	0.24
Point 211	0.318	0.12	0.16	0.20	0.24	0.16	0.20	0.16	0.20	0.20	0.24
Point 212	0.320	0.16	0.20	0.16	0.20	0.16	0.20	0.20	0.20	0.12	0.16
Point 213	0.322	0.16	0.20	0.20	0.24	0.16	0.24	0.16	0.24	0.16	0.20
Point 214	0.324	0.12	0.16	0.20	0.24	0.16	0.20	0.20	0.24	0.12	0.16
Point 215	0.326	0.16	0.20	0.16	0.24	0.16	0.20	0.20	0.24	0.12	0.16
Point 216	0.328	0.16	0.20	0.20	0.24	0.20	0.24	0.16	0.20	0.16	0.20
Point 217	0.330	0.16	0.24	0.20	0.24	0.20	0.20	0.20	0.20	0.20	0.20
Point 218	0.332	0.16	0.16	0.20	0.24	0.20	0.20	0.20	0.24	0.12	0.16
Point 219	0.334	0.16	0.20	0.16	0.24	0.20	0.24	0.20	0.24	0.16	0.20
Point 220	0.336	0.16	0.20	0.16	0.24	0.20	0.24	0.20	0.20	0.16	0.20
Point 221	0.338	0.16	0.24	0.16	0.20	0.16	0.24	0.20	0.24	0.16	0.20
Point 222	0.340	0.16	0.20	0.20	0.24	0.20	0.20	0.16	0.20	0.16	0.20
Point 223	0.342	0.16	0.20	0.16	0.20	0.20	0.24	0.16	0.20	0.16	0.20
Point 224	0.344	0.16	0.20	0.16	0.20	0.16	0.20	0.16	0.24	0.16	0.20
Point 225	0.346	0.20	0.24	0.16	0.20	0.16	0.20	0.16	0.20	0.20	0.24
Point 226	0.348	0.16	0.20	0.16	0.24	0.16	0.20	0.16	0.20	0.20	0.24
Point 227	0.350	0.16	0.20	0.16	0.24	0.16	0.20	0.16	0.20	0.16	0.20
Point 228	0.352	0.16	0.20	0.16	0.20	0.16	0.20	0.20	0.24	0.16	0.20
Point 229	0.354	0.16	0.24	0.20	0.24	0.12	0.16	0.16	0.20	0.16	0.20
Point 230	0.356	0.16	0.20	0.16	0.24	0.20	0.24	0.16	0.20	0.12	0.16
Point 231	0.358	0.16	0.20	0.16	0.20	0.16	0.20	0.12	0.16	0.20	0.28
Point 232	0.360	0.20	0.24	0.20	0.24	0.16	0.20	0.16	0.20	0.16	0.20
Point 233	0.362	0.16	0.20	0.20	0.20	0.20	0.24	0.16	0.20	0.20	0.24
Point 234	0.364	0.16	0.20	0.16	0.20	0.16	0.20	0.16	0.20	0.16	0.20
Point 235	0.366	0.16	0.20	0.16	0.20	0.16	0.16	0.16	0.20	0.16	0.20
Point 236	0.368	0.12	0.20	0.16	0.20	0.16	0.20	0.16	0.24	0.16	0.16
Point 237	0.370	0.16	0.24	0.20	0.24	0.20	0.24	0.20	0.24	0.20	0.24
Point 238	0.372	0.16	0.20	0.16	0.20	0.16	0.20	0.16	0.20	0.16	0.20
Point 239	0.374	0.20	0.24	0.16	0.20	0.20	0.24	0.16	0.20	0.20	0.20
Point 240	0.376	0.16	0.20	0.16	0.20	0.16	0.20	0.16	0.24	0.16	0.16
Point 241	0.378	0.12	0.20	0.16	0.24	0.20	0.24	0.16	0.20	0.16	0.20
Point 242	0.380	0.16	0.20	0.20	0.20	0.20	0.24	0.16	0.20	0.16	0.24
Point 243	0.382	0.16	0.20	0.20	0.24	0.16	0.20	0.16	0.20	0.12	0.20
Point 244	0.384	0.20	0.24	0.16	0.20	0.16	0.20	0.12	0.20	0.16	0.20
Point 245	0.386	0.16	0.20	0.20	0.24	0.16	0.20	0.16	0.20	0.16	0.20
Point 246	0.388	0.16	0.20	0.20	0.20	0.20	0.24	0.20	0.24	0.16	0.20
Point 247	0.390	0.16	0.20	0.16	0.20	0.20	0.24	0.16	0.20	0.12	0.20
Point 248	0.392	0.16	0.20	0.16	0.20	0.16	0.24	0.20	0.24	0.16	0.20
Point 249	0.394	0.20	0.20	0.20	0.20	0.16	0.24	0.20	0.24	0.16	0.20

Modified Port 0.100" lift N_2 (cont.)

		Run 1		Run 2		Run 3		Run 4		Run 5	
	Time	V_{high}	V_{low}	V_{high}	V_{low}	V_{high}	V_{low}	V_{high}	V_{low}	V_{high}	V_{low}
Point 250	0.396	0.16	0.20	0.20	0.24	0.20	0.24	0.16	0.24	0.16	0.20
Point 251	0.398	0.16	0.20	0.20	0.20	0.20	0.24	0.16	0.24	0.16	0.24
Point 252	0.400	0.12	0.16	0.20	0.24	0.16	0.20	0.16	0.20	0.16	0.20
Point 253	0.402	0.16	0.20	0.16	0.20	0.20	0.24	0.20	0.24	0.16	0.20
Point 254	0.404	0.16	0.20	0.20	0.20	0.16	0.20	0.20	0.24	0.16	0.20
Point 255	0.406	0.20	0.24	0.20	0.24	0.20	0.24	0.16	0.20	0.16	0.24
Point 256	0.408	0.16	0.24	0.20	0.24	0.16	0.20	0.16	0.20	0.16	0.20
Point 257	0.410	0.16	0.20	0.16	0.20	0.16	0.24	0.20	0.24	0.16	0.20
Point 258	0.412	0.16	0.20	0.16	0.20	0.20	0.24	0.20	0.24	0.16	0.20
Point 259	0.414	0.20	0.24	0.20	0.24	0.16	0.20	0.16	0.20	0.16	0.20
Point 260	0.416	0.16	0.20	0.16	0.20	0.20	0.24	0.16	0.20	0.20	0.24
Point 261	0.418	0.16	0.20	0.16	0.20	0.20	0.20	0.20	0.24	0.16	0.20
Point 262	0.420	0.16	0.24	0.16	0.20	0.16	0.20	0.16	0.20	0.16	0.20
Point 263	0.422	0.20	0.24	0.16	0.20	0.16	0.20	0.16	0.20	0.12	0.20
Point 264	0.424	0.16	0.20	0.16	0.20	0.16	0.24	0.16	0.20	0.20	0.24
Point 265	0.426	0.16	0.20	0.16	0.20	0.16	0.20	0.16	0.20	0.20	0.24
Point 266	0.428	0.20	0.24	0.16	0.20	0.16	0.20	0.12	0.20	0.20	0.20
Point 267	0.430	0.16	0.20	0.20	0.24	0.20	0.24	0.12	0.16	0.16	0.20
Point 268	0.432	0.16	0.20	0.16	0.20	0.16	0.20	0.16	0.20	0.16	0.20
Point 269	0.434	0.16	0.20	0.16	0.20	0.16	0.20	0.20	0.24	0.16	0.20
Point 270	0.436	0.16	0.24	0.16	0.20	0.16	0.20	0.12	0.16	0.16	0.20
Point 271	0.438	0.16	0.20	0.16	0.20	0.16	0.20	0.20	0.24	0.16	0.20
Point 272	0.440	0.20	0.20	0.16	0.20	0.16	0.20	0.16	0.20	0.16	0.20
Point 273	0.442	0.16	0.20	0.20	0.20	0.20	0.24	0.16	0.20	0.16	0.20
Point 274	0.444	0.16	0.20	0.16	0.20	0.16	0.20	0.16	0.24	0.12	0.16
Point 275	0.446	0.16	0.20	0.16	0.20	0.16	0.20	0.16	0.20	0.16	0.16
Point 276	0.448	0.16	0.20	0.16	0.20	0.20	0.20	0.16	0.20	0.16	0.20
Point 277	0.450	0.16	0.20	0.16	0.24	0.12	0.16	0.20	0.24	0.16	0.20
Point 278	0.452	0.12	0.16	0.20	0.24	0.20	0.24	0.16	0.20	0.20	0.20
Point 279	0.454	0.16	0.20	0.20	0.24	0.16	0.20	0.20	0.24	0.16	0.16
Point 280	0.456	0.16	0.20	0.16	0.20	0.16	0.24	0.20	0.24	0.20	0.24
Point 281	0.458	0.16	0.20	0.16	0.24	0.16	0.20	0.20	0.24	0.16	0.20
Point 282	0.460	0.16	0.16	0.16	0.20	0.16	0.20	0.16	0.20	0.16	0.20
Point 283	0.462	0.16	0.20	0.16	0.20	0.12	0.16	0.16	0.20	0.16	0.20
Point 284	0.464	0.20	0.24	0.20	0.24	0.16	0.24	0.20	0.24	0.20	0.24
Point 285	0.466	0.12	0.16	0.20	0.20	0.16	0.20	0.20	0.24	0.16	0.20
Point 286	0.468	0.16	0.20	0.16	0.20	0.20	0.24	0.16	0.24	0.16	0.20
Point 287	0.470	0.16	0.20	0.20	0.24	0.16	0.20	0.20	0.24	0.12	0.20
Point 288	0.472	0.20	0.24	0.16	0.20	0.16	0.20	0.16	0.20	0.16	0.20
Point 289	0.474	0.16	0.20	0.20	0.20	0.16	0.20	0.20	0.24	0.12	0.16
Point 290	0.476	0.16	0.20	0.16	0.20	0.20	0.24	0.16	0.24	0.16	0.20
Point 291	0.478	0.16	0.20	0.20	0.24	0.20	0.20	0.16	0.20	0.16	0.20
Point 292	0.480	0.20	0.24	0.16	0.20	0.12	0.20	0.16	0.20	0.16	0.20
Point 293	0.482	0.20	0.24	0.20	0.20	0.16	0.20	0.20	0.20	0.16	0.24
Point 294	0.484	0.20	0.24	0.16	0.24	0.20	0.24	0.16	0.24	0.12	0.16
Point 295	0.486	0.16	0.20	0.20	0.24	0.20	0.24	0.16	0.20	0.20	0.24
Point 296	0.488	0.16	0.20	0.16	0.20	0.12	0.16	0.20	0.24	0.16	0.20
Point 297	0.490	0.20	0.24	0.20	0.24	0.16	0.20	0.20	0.24	0.12	0.16
Point 298	0.492	0.20	0.24	0.16	0.20	0.20	0.24	0.16	0.20	0.20	0.24
Point 299	0.494	0.16	0.20	0.16	0.20	0.16	0.20	0.16	0.20	0.16	0.16
Point 300	0.496	0.16	0.20	0.16	0.20	0.16	0.20	0.16	0.20	0.16	0.20

Original Port 0.050" lift N_2

		Run 1		Run 2		Run 3		Run 4		Run 5	
	Time	V_{high}	V_{low}	V_{high}	V_{low}	V_{high}	V_{low}	V_{high}	V_{low}	V_{high}	V_{low}
Point 1	-0.102	5.04	5.04	4.92	4.96	4.92	4.96	4.92	4.96	5.00	5.04
Point 2	-0.100	5.04	5.04	4.92	4.92	4.96	5.00	4.92	4.96	5.00	5.04
Point 3	-0.098	5.00	5.04	4.92	4.96	5.00	5.00	4.92	4.96	5.00	5.04
Point 4	-0.096	5.00	5.04	4.92	4.92	4.96	5.00	4.96	4.96	5.04	5.04
Point 5	-0.094	5.00	5.00	4.88	4.92	4.92	4.96	4.92	4.96	5.04	5.08
Point 6	-0.092	5.00	5.00	4.88	4.92	5.00	5.00	4.92	4.92	5.00	5.00
Point 7	-0.090	5.00	5.04	4.92	4.92	5.00	5.04	4.96	4.96	5.00	5.04
Point 8	-0.088	5.00	5.04	4.92	4.96	4.96	5.00	4.96	4.96	5.04	5.04
Point 9	-0.086	4.96	5.00	4.88	4.92	4.96	5.00	4.96	5.00	5.00	5.04
Point 10	-0.084	5.00	5.00	4.92	4.92	5.00	5.00	4.96	5.00	5.00	5.04
Point 11	-0.082	5.00	5.00	4.92	4.92	4.96	5.00	4.92	4.92	5.04	5.04
Point 12	-0.080	4.96	5.00	4.92	4.96	5.00	5.04	4.92	4.96	5.00	5.00
Point 13	-0.078	5.04	5.04	4.92	4.96	4.96	5.00	4.92	4.96	5.04	5.08
Point 14	-0.076	5.00	5.04	4.92	4.92	4.96	5.00	4.92	4.96	5.00	5.04
Point 15	-0.074	5.00	5.04	4.92	4.96	5.00	5.00	4.96	5.00	5.00	5.04
Point 16	-0.072	5.00	5.04	4.92	4.96	4.96	5.00	4.92	4.96	5.04	5.04
Point 17	-0.070	5.04	5.08	4.96	4.96	4.96	5.00	4.92	4.96	5.00	5.04
Point 18	-0.068	5.00	5.00	4.92	4.92	4.96	4.96	4.96	5.00	5.00	5.04
Point 19	-0.066	5.00	5.04	4.92	4.96	5.00	5.04	4.96	5.00	5.00	5.04
Point 20	-0.064	5.00	5.04	4.92	4.96	5.00	5.04	4.96	5.00	5.04	5.08
Point 21	-0.062	4.96	5.00	4.96	4.96	4.96	5.00	4.96	5.00	5.00	5.04
Point 22	-0.060	5.00	5.04	4.92	4.92	4.96	5.00	4.92	4.96	4.96	5.00
Point 23	-0.058	5.00	5.00	4.92	4.92	4.96	4.96	4.96	4.96	4.96	5.00
Point 24	-0.056	5.00	5.04	4.92	4.96	4.96	5.00	4.96	5.00	5.04	5.08
Point 25	-0.054	5.04	5.08	4.96	4.96	4.96	5.00	4.92	4.96	5.00	5.04
Point 26	-0.052	5.04	5.08	4.92	4.92	5.00	5.00	4.96	4.96	5.04	5.04
Point 27	-0.050	5.00	5.04	4.92	4.92	5.00	5.04	4.96	5.00	5.00	5.00
Point 28	-0.048	5.00	5.04	4.92	4.96	4.96	5.00	4.92	4.96	5.04	5.08
Point 29	-0.046	5.04	5.04	4.92	4.96	4.96	5.00	4.92	4.96	5.00	5.04
Point 30	-0.044	5.00	5.04	4.92	4.92	4.96	4.96	4.96	5.00	5.04	5.04
Point 31	-0.042	4.96	5.00	4.92	4.96	4.96	5.00	4.96	4.96	5.04	5.04
Point 32	-0.040	5.00	5.04	4.92	4.96	5.00	5.00	4.96	4.96	5.00	5.04
Point 33	-0.038	5.00	5.04	4.92	4.92	4.96	4.96	4.92	4.96	5.00	5.04
Point 34	-0.036	5.00	5.04	4.92	4.92	5.00	5.04	4.92	4.96	5.00	5.04
Point 35	-0.034	5.00	5.04	4.92	4.96	4.96	4.96	4.96	4.96	5.00	5.00
Point 36	-0.032	5.00	5.04	4.92	4.92	5.00	5.00	4.96	4.96	5.04	5.08
Point 37	-0.030	5.00	5.04	4.92	4.96	4.96	5.00	4.92	4.92	5.00	5.04
Point 38	-0.028	5.00	5.04	4.92	4.92	5.00	5.00	4.92	4.96	5.04	5.04
Point 39	-0.026	5.00	5.04	4.92	4.96	5.00	5.04	4.88	4.92	5.04	5.08
Point 40	-0.024	5.00	5.04	4.88	4.92	5.00	5.00	4.92	4.96	5.04	5.08
Point 41	-0.022	5.00	5.00	4.96	4.96	4.96	5.00	4.92	4.96	5.00	5.04
Point 42	-0.020	5.00	5.00	4.92	4.92	4.92	4.96	4.96	4.96	5.00	5.04
Point 43	-0.018	5.00	5.00	4.92	4.96	5.00	5.00	4.96	4.96	5.04	5.04
Point 44	-0.016	5.04	5.08	4.92	4.96	4.96	4.96	4.92	4.96	5.00	5.04
Point 45	-0.014	4.96	4.96	4.88	4.92	4.92	4.96	4.92	4.96	4.96	4.96
Point 46	-0.012	4.92	4.96	4.88	4.88	4.92	4.96	4.96	4.96	4.92	4.96
Point 47	-0.010	4.92	4.92	4.84	4.88	4.92	4.92	4.92	4.92	4.92	4.92
Point 48	-0.008	4.88	4.88	4.84	4.84	4.84	4.84	4.88	4.88	4.88	4.88
Point 49	-0.006	4.84	4.84	4.76	4.76	4.80	4.80	4.80	4.84	4.76	4.80

Original Port 0.050" lift N_2 (cont.)

		Run 1		Run 2		Run 3		Run 4		Run 5	
	Time	V_{high}	V_{low}	V_{high}	V_{low}	V_{high}	V_{low}	V_{high}	V_{low}	V_{high}	V_{low}
Point 50	-0.004	4.72	4.76	4.72	4.72	4.72	4.76	4.80	4.80	4.72	4.72
Point 51	-0.002	4.64	4.68	4.64	4.64	4.64	4.64	4.68	4.72	4.64	4.64
Point 52	0.000	4.56	4.60	4.52	4.52	4.56	4.60	4.60	4.68	4.56	4.60
Point 53	0.002	4.44	4.48	4.44	4.48	4.40	4.48	4.48	4.56	4.40	4.44
Point 54	0.004	4.36	4.40	4.36	4.36	4.40	4.44	4.32	4.40	4.32	4.36
Point 55	0.006	4.28	4.32	4.24	4.32	4.24	4.32	4.24	4.28	4.24	4.28
Point 56	0.008	4.20	4.20	4.12	4.16	4.12	4.20	4.12	4.16	4.16	4.20
Point 57	0.010	4.04	4.08	4.00	4.04	4.00	4.04	3.96	4.00	4.04	4.08
Point 58	0.012	3.92	3.96	3.88	3.92	3.92	3.96	3.88	3.92	3.92	3.96
Point 59	0.014	3.80	3.84	3.80	3.84	3.76	3.84	3.76	3.80	3.76	3.84
Point 60	0.016	3.76	3.80	3.68	3.76	3.68	3.72	3.64	3.64	3.68	3.72
Point 61	0.018	3.60	3.64	3.56	3.60	3.56	3.60	3.56	3.60	3.60	3.60
Point 62	0.020	3.52	3.56	3.52	3.52	3.48	3.52	3.44	3.44	3.52	3.56
Point 63	0.022	3.44	3.44	3.40	3.44	3.40	3.40	3.36	3.36	3.40	3.44
Point 64	0.024	3.36	3.40	3.28	3.32	3.32	3.36	3.28	3.28	3.32	3.36
Point 65	0.026	3.28	3.32	3.16	3.20	3.20	3.24	3.20	3.20	3.20	3.24
Point 66	0.028	3.16	3.16	3.12	3.12	3.12	3.12	3.08	3.12	3.12	3.16
Point 67	0.030	3.08	3.08	3.04	3.08	3.04	3.04	3.04	3.04	3.08	3.08
Point 68	0.032	3.00	3.04	2.96	2.96	2.92	2.92	2.92	2.92	2.96	3.00
Point 69	0.034	2.88	2.92	2.88	2.88	2.84	2.88	2.84	2.84	2.88	2.88
Point 70	0.036	2.88	2.88	2.80	2.84	2.80	2.80	2.76	2.76	2.80	2.80
Point 71	0.038	2.80	2.80	2.72	2.76	2.68	2.72	2.64	2.68	2.76	2.76
Point 72	0.040	2.68	2.68	2.64	2.64	2.60	2.64	2.60	2.60	2.64	2.68
Point 73	0.042	2.60	2.60	2.56	2.56	2.56	2.60	2.52	2.52	2.60	2.60
Point 74	0.044	2.52	2.52	2.48	2.48	2.44	2.44	2.48	2.48	2.52	2.56
Point 75	0.046	2.44	2.44	2.44	2.44	2.44	2.44	2.40	2.40	2.44	2.44
Point 76	0.048	2.36	2.36	2.36	2.36	2.32	2.36	2.28	2.32	2.36	2.36
Point 77	0.050	2.36	2.40	2.28	2.28	2.24	2.28	2.24	2.28	2.32	2.32
Point 78	0.052	2.28	2.28	2.20	2.20	2.20	2.24	2.20	2.20	2.28	2.28
Point 79	0.054	2.24	2.24	2.16	2.16	2.12	2.12	2.16	2.16	2.20	2.20
Point 80	0.056	2.20	2.20	2.08	2.12	2.12	2.12	2.16	2.16	2.12	2.12
Point 81	0.058	2.08	2.08	2.08	2.12	2.08	2.08	2.04	2.04	2.08	2.08
Point 82	0.060	2.08	2.08	2.00	2.00	2.04	2.04	2.00	2.00	2.04	2.08
Point 83	0.062	2.00	2.00	1.96	2.00	1.96	1.96	1.92	1.96	1.96	1.96
Point 84	0.064	1.96	1.96	1.92	1.92	1.92	1.92	1.84	1.88	1.92	1.92
Point 85	0.066	1.88	1.92	1.84	1.84	1.84	1.84	1.80	1.84	1.84	1.88
Point 86	0.068	1.88	1.88	1.76	1.80	1.80	1.84	1.80	1.80	1.84	1.88
Point 87	0.070	1.80	1.84	1.76	1.76	1.76	1.76	1.68	1.72	1.76	1.76
Point 88	0.072	1.76	1.76	1.72	1.72	1.64	1.68	1.64	1.68	1.72	1.76
Point 89	0.074	1.72	1.76	1.68	1.68	1.64	1.68	1.64	1.64	1.72	1.72
Point 90	0.076	1.64	1.64	1.56	1.60	1.60	1.60	1.60	1.60	1.64	1.64
Point 91	0.078	1.60	1.64	1.56	1.56	1.56	1.60	1.56	1.60	1.60	1.60
Point 92	0.080	1.56	1.60	1.52	1.52	1.56	1.56	1.48	1.52	1.52	1.56
Point 93	0.082	1.52	1.52	1.52	1.52	1.44	1.48	1.44	1.48	1.52	1.56
Point 94	0.084	1.44	1.48	1.44	1.44	1.40	1.44	1.44	1.44	1.48	1.48
Point 95	0.086	1.44	1.48	1.40	1.40	1.40	1.40	1.36	1.36	1.44	1.44
Point 96	0.088	1.40	1.44	1.36	1.36	1.36	1.36	1.28	1.32	1.40	1.44
Point 97	0.090	1.36	1.36	1.28	1.32	1.28	1.28	1.32	1.32	1.36	1.40
Point 98	0.092	1.36	1.36	1.28	1.32	1.28	1.28	1.28	1.32	1.32	1.32
Point 99	0.094	1.28	1.32	1.24	1.28	1.20	1.24	1.20	1.24	1.24	1.28

Original Port 0.050" lift N_2 (cont.)

		Run 1		Run 2		Run 3		Run 4		Run 5	
	Time	V_{high}	V_{low}	V_{high}	V_{low}	V_{high}	V_{low}	V_{high}	V_{low}	V_{high}	V_{low}
Point 100	0.096	1.24	1.28	1.20	1.24	1.16	1.20	1.16	1.24	1.24	1.24
Point 101	0.098	1.24	1.24	1.20	1.24	1.16	1.20	1.16	1.20	1.20	1.20
Point 102	0.100	1.16	1.16	1.16	1.20	1.12	1.16	1.12	1.12	1.16	1.20
Point 103	0.102	1.16	1.16	1.08	1.12	1.08	1.12	1.12	1.16	1.16	1.20
Point 104	0.104	1.12	1.16	1.08	1.08	1.04	1.08	1.04	1.08	1.12	1.16
Point 105	0.106	1.12	1.16	1.00	1.04	1.04	1.08	1.04	1.08	1.04	1.08
Point 106	0.108	1.08	1.12	1.04	1.04	1.00	1.04	1.00	1.04	1.04	1.08
Point 107	0.110	1.04	1.04	1.00	1.00	0.96	1.00	1.00	1.04	1.00	1.04
Point 108	0.112	1.04	1.08	1.00	1.04	0.96	1.00	0.92	0.96	0.96	1.00
Point 109	0.114	0.96	1.00	0.92	0.92	0.92	0.96	0.92	0.92	0.92	0.96
Point 110	0.116	0.92	0.96	0.88	0.92	0.88	0.92	0.88	0.92	0.92	0.96
Point 111	0.118	1.00	1.00	0.88	0.92	0.88	0.92	0.84	0.88	0.88	0.92
Point 112	0.120	0.88	0.92	0.88	0.92	0.80	0.84	0.84	0.88	0.88	0.88
Point 113	0.122	0.84	0.88	0.84	0.88	0.80	0.84	0.80	0.84	0.88	0.88
Point 114	0.124	0.84	0.88	0.80	0.84	0.80	0.80	0.76	0.80	0.80	0.84
Point 115	0.126	0.80	0.84	0.76	0.80	0.80	0.84	0.76	0.80	0.80	0.84
Point 116	0.128	0.80	0.80	0.80	0.84	0.76	0.80	0.72	0.76	0.76	0.80
Point 117	0.130	0.76	0.76	0.76	0.80	0.76	0.80	0.76	0.80	0.80	0.80
Point 118	0.132	0.76	0.80	0.72	0.76	0.72	0.76	0.72	0.76	0.72	0.76
Point 119	0.134	0.72	0.72	0.76	0.76	0.72	0.72	0.68	0.72	0.72	0.76
Point 120	0.136	0.68	0.72	0.68	0.76	0.68	0.72	0.68	0.68	0.68	0.72
Point 121	0.138	0.68	0.72	0.64	0.68	0.64	0.68	0.68	0.68	0.64	0.68
Point 122	0.140	0.68	0.72	0.60	0.64	0.60	0.68	0.64	0.68	0.60	0.64
Point 123	0.142	0.64	0.68	0.60	0.64	0.60	0.64	0.60	0.64	0.64	0.68
Point 124	0.144	0.64	0.68	0.60	0.64	0.56	0.60	0.60	0.60	0.64	0.68
Point 125	0.146	0.64	0.68	0.60	0.60	0.56	0.60	0.56	0.60	0.64	0.68
Point 126	0.148	0.56	0.60	0.52	0.56	0.52	0.56	0.60	0.60	0.56	0.60
Point 127	0.150	0.56	0.60	0.52	0.56	0.52	0.56	0.52	0.56	0.56	0.60
Point 128	0.152	0.52	0.56	0.52	0.56	0.48	0.52	0.56	0.60	0.56	0.60
Point 129	0.154	0.56	0.56	0.48	0.52	0.52	0.56	0.52	0.56	0.48	0.56
Point 130	0.156	0.52	0.56	0.44	0.48	0.48	0.52	0.48	0.52	0.52	0.52
Point 131	0.158	0.48	0.52	0.44	0.48	0.44	0.48	0.48	0.52	0.48	0.52
Point 132	0.160	0.48	0.48	0.44	0.48	0.44	0.48	0.44	0.52	0.48	0.52
Point 133	0.162	0.44	0.48	0.44	0.48	0.44	0.44	0.44	0.48	0.48	0.52
Point 134	0.164	0.48	0.52	0.40	0.44	0.36	0.44	0.44	0.48	0.44	0.48
Point 135	0.166	0.44	0.48	0.44	0.48	0.44	0.44	0.44	0.48	0.48	0.52
Point 136	0.168	0.40	0.44	0.40	0.44	0.36	0.40	0.40	0.44	0.44	0.48
Point 137	0.170	0.40	0.44	0.36	0.40	0.40	0.44	0.40	0.44	0.44	0.48
Point 138	0.172	0.36	0.40	0.36	0.40	0.32	0.36	0.36	0.40	0.36	0.40
Point 139	0.174	0.36	0.40	0.32	0.36	0.36	0.40	0.36	0.40	0.36	0.40
Point 140	0.176	0.36	0.40	0.32	0.36	0.36	0.36	0.36	0.36	0.36	0.40
Point 141	0.178	0.36	0.40	0.32	0.40	0.32	0.36	0.32	0.36	0.32	0.36
Point 142	0.180	0.32	0.36	0.32	0.40	0.32	0.36	0.32	0.36	0.32	0.36
Point 143	0.182	0.32	0.36	0.32	0.36	0.28	0.32	0.32	0.36	0.32	0.36
Point 144	0.184	0.32	0.36	0.28	0.32	0.32	0.36	0.28	0.36	0.32	0.36
Point 145	0.186	0.28	0.28	0.28	0.32	0.32	0.36	0.28	0.32	0.32	0.36
Point 146	0.188	0.32	0.32	0.28	0.32	0.28	0.32	0.24	0.28	0.28	0.32
Point 147	0.190	0.24	0.28	0.24	0.28	0.28	0.32	0.28	0.32	0.28	0.32
Point 148	0.192	0.20	0.24	0.24	0.28	0.28	0.32	0.24	0.28	0.24	0.28
Point 149	0.194	0.28	0.32	0.24	0.32	0.24	0.28	0.28	0.32	0.24	0.28

Original Port 0.050" lift N_2 (cont.)

		Run 1		Run 2		Run 3		Run 4		Run 5	
	Time	V_{high}	V_{low}	V_{high}	V_{low}	V_{high}	V_{low}	V_{high}	V_{low}	V_{high}	V_{low}
Point 150	0.196	0.24	0.28	0.24	0.28	0.24	0.28	0.20	0.24	0.24	0.28
Point 151	0.198	0.24	0.28	0.24	0.32	0.24	0.28	0.20	0.24	0.24	0.28
Point 152	0.200	0.24	0.28	0.24	0.28	0.20	0.24	0.20	0.24	0.24	0.28
Point 153	0.202	0.24	0.28	0.24	0.28	0.20	0.24	0.20	0.24	0.20	0.24
Point 154	0.204	0.24	0.28	0.20	0.24	0.16	0.20	0.20	0.20	0.20	0.24
Point 155	0.206	0.20	0.24	0.20	0.24	0.16	0.24	0.20	0.20	0.16	0.20
Point 156	0.208	0.20	0.24	0.16	0.20	0.16	0.20	0.20	0.24	0.16	0.20
Point 157	0.210	0.24	0.24	0.20	0.24	0.16	0.20	0.20	0.20	0.16	0.24
Point 158	0.212	0.20	0.24	0.16	0.20	0.20	0.24	0.20	0.24	0.16	0.24
Point 159	0.214	0.20	0.20	0.16	0.20	0.16	0.20	0.20	0.24	0.16	0.20
Point 160	0.216	0.20	0.24	0.20	0.20	0.16	0.24	0.20	0.20	0.16	0.20
Point 161	0.218	0.16	0.20	0.16	0.20	0.20	0.20	0.20	0.24	0.16	0.20
Point 162	0.220	0.16	0.20	0.16	0.20	0.16	0.20	0.20	0.20	0.16	0.20
Point 163	0.222	0.16	0.20	0.20	0.20	0.16	0.20	0.16	0.24	0.16	0.20
Point 164	0.224	0.16	0.20	0.16	0.20	0.16	0.20	0.16	0.20	0.16	0.16
Point 165	0.226	0.16	0.16	0.16	0.20	0.16	0.20	0.16	0.20	0.12	0.20
Point 166	0.228	0.12	0.16	0.16	0.20	0.16	0.24	0.20	0.24	0.16	0.20
Point 167	0.230	0.16	0.20	0.16	0.20	0.12	0.20	0.16	0.20	0.16	0.20
Point 168	0.232	0.16	0.20	0.12	0.16	0.16	0.20	0.12	0.16	0.16	0.20
Point 169	0.234	0.16	0.20	0.16	0.20	0.16	0.20	0.16	0.20	0.12	0.16
Point 170	0.236	0.12	0.20	0.16	0.20	0.20	0.20	0.12	0.20	0.12	0.16
Point 171	0.238	0.16	0.20	0.16	0.20	0.16	0.20	0.16	0.20	0.16	0.20
Point 172	0.240	0.16	0.20	0.24	0.24	0.16	0.20	0.16	0.20	0.16	0.24
Point 173	0.242	0.16	0.20	0.20	0.24	0.16	0.20	0.16	0.20	0.16	0.16
Point 174	0.244	0.16	0.20	0.16	0.20	0.20	0.20	0.20	0.24	0.12	0.16
Point 175	0.246	0.16	0.20	0.20	0.24	0.16	0.20	0.16	0.20	0.16	0.20
Point 176	0.248	0.12	0.16	0.16	0.24	0.20	0.20	0.16	0.20	0.12	0.20
Point 177	0.250	0.20	0.20	0.20	0.24	0.12	0.16	0.20	0.24	0.16	0.20
Point 178	0.252	0.16	0.20	0.20	0.24	0.16	0.20	0.16	0.16	0.16	0.20
Point 179	0.254	0.16	0.20	0.16	0.20	0.16	0.20	0.16	0.20	0.16	0.20
Point 180	0.256	0.16	0.20	0.16	0.20	0.20	0.24	0.20	0.24	0.16	0.20
Point 181	0.258	0.16	0.16	0.20	0.24	0.20	0.20	0.16	0.20	0.16	0.24
Point 182	0.260	0.16	0.20	0.16	0.20	0.16	0.20	0.16	0.20	0.16	0.20
Point 183	0.262	0.16	0.20	0.12	0.16	0.16	0.20	0.16	0.20	0.12	0.16
Point 184	0.264	0.12	0.16	0.12	0.16	0.16	0.20	0.16	0.20	0.16	0.20
Point 185	0.266	0.16	0.20	0.16	0.20	0.20	0.20	0.16	0.20	0.12	0.16
Point 186	0.268	0.20	0.24	0.20	0.24	0.16	0.20	0.16	0.20	0.16	0.20
Point 187	0.270	0.12	0.16	0.12	0.16	0.16	0.20	0.12	0.16	0.16	0.20
Point 188	0.272	0.16	0.20	0.16	0.20	0.16	0.20	0.16	0.20	0.16	0.20
Point 189	0.274	0.20	0.24	0.16	0.20	0.12	0.16	0.16	0.20	0.12	0.16
Point 190	0.276	0.20	0.24	0.16	0.20	0.12	0.16	0.16	0.20	0.16	0.20
Point 191	0.278	0.16	0.20	0.16	0.20	0.16	0.20	0.16	0.20	0.12	0.16
Point 192	0.280	0.20	0.20	0.20	0.24	0.12	0.20	0.16	0.20	0.16	0.20
Point 193	0.282	0.16	0.20	0.16	0.20	0.16	0.20	0.16	0.20	0.16	0.20
Point 194	0.284	0.16	0.20	0.20	0.24	0.12	0.16	0.16	0.16	0.12	0.16
Point 195	0.286	0.16	0.20	0.20	0.24	0.16	0.20	0.16	0.20	0.16	0.20
Point 196	0.288	0.16	0.20	0.16	0.20	0.12	0.16	0.16	0.20	0.16	0.20
Point 197	0.290	0.16	0.20	0.16	0.20	0.16	0.20	0.20	0.24	0.12	0.16
Point 198	0.292	0.12	0.20	0.16	0.24	0.12	0.16	0.16	0.20	0.16	0.20
Point 199	0.294	0.16	0.20	0.12	0.16	0.16	0.20	0.20	0.24	0.16	0.20

Original Port 0.050" lift N_2 (cont.)

		Run 1		Run 2		Run 3		Run 4		Run 5	
	Time	V_{high}	V_{low}	V_{high}	V_{low}	V_{high}	V_{low}	V_{high}	V_{low}	V_{high}	V_{low}
Point 200	0.296	0.16	0.20	0.16	0.20	0.12	0.20	0.16	0.20	0.16	0.20
Point 201	0.298	0.16	0.20	0.16	0.20	0.16	0.20	0.16	0.20	0.12	0.16
Point 202	0.300	0.16	0.20	0.16	0.20	0.16	0.20	0.20	0.24	0.12	0.16
Point 203	0.302	0.16	0.20	0.12	0.16	0.16	0.20	0.20	0.24	0.16	0.20
Point 204	0.304	0.16	0.20	0.16	0.20	0.16	0.20	0.16	0.20	0.16	0.20
Point 205	0.306	0.20	0.24	0.16	0.20	0.20	0.24	0.16	0.20	0.12	0.16
Point 206	0.308	0.16	0.16	0.20	0.24	0.16	0.20	0.20	0.24	0.12	0.16
Point 207	0.310	0.16	0.20	0.16	0.24	0.16	0.20	0.16	0.20	0.16	0.20
Point 208	0.312	0.16	0.20	0.16	0.20	0.16	0.20	0.16	0.20	0.20	0.24
Point 209	0.314	0.12	0.20	0.16	0.20	0.16	0.20	0.16	0.20	0.12	0.16
Point 210	0.316	0.16	0.20	0.20	0.24	0.20	0.24	0.20	0.24	0.12	0.16
Point 211	0.318	0.16	0.20	0.16	0.20	0.16	0.20	0.16	0.20	0.16	0.20
Point 212	0.320	0.16	0.20	0.16	0.20	0.16	0.16	0.16	0.20	0.12	0.20
Point 213	0.322	0.16	0.24	0.20	0.24	0.16	0.20	0.16	0.20	0.16	0.16
Point 214	0.324	0.20	0.24	0.12	0.20	0.16	0.20	0.16	0.20	0.16	0.20
Point 215	0.326	0.16	0.20	0.16	0.20	0.16	0.20	0.20	0.24	0.16	0.20
Point 216	0.328	0.16	0.20	0.16	0.20	0.12	0.20	0.16	0.20	0.16	0.20
Point 217	0.330	0.20	0.24	0.20	0.24	0.16	0.20	0.16	0.20	0.16	0.20
Point 218	0.332	0.16	0.24	0.16	0.24	0.16	0.20	0.16	0.20	0.20	0.24
Point 219	0.334	0.16	0.20	0.16	0.20	0.16	0.20	0.16	0.20	0.16	0.20
Point 220	0.336	0.16	0.20	0.20	0.24	0.16	0.16	0.16	0.20	0.20	0.24
Point 221	0.338	0.16	0.20	0.16	0.20	0.16	0.20	0.16	0.20	0.16	0.20
Point 222	0.340	0.16	0.20	0.20	0.20	0.16	0.20	0.16	0.16	0.16	0.20
Point 223	0.342	0.16	0.20	0.16	0.20	0.16	0.20	0.16	0.20	0.16	0.20
Point 224	0.344	0.16	0.20	0.16	0.20	0.16	0.20	0.16	0.20	0.12	0.20
Point 225	0.346	0.16	0.16	0.20	0.24	0.20	0.24	0.16	0.20	0.12	0.16
Point 226	0.348	0.16	0.20	0.16	0.20	0.16	0.20	0.12	0.20	0.16	0.20
Point 227	0.350	0.16	0.20	0.16	0.20	0.16	0.20	0.12	0.16	0.16	0.16
Point 228	0.352	0.16	0.20	0.16	0.20	0.16	0.16	0.16	0.20	0.12	0.16
Point 229	0.354	0.20	0.24	0.16	0.20	0.12	0.16	0.12	0.16	0.16	0.20
Point 230	0.356	0.16	0.20	0.20	0.20	0.16	0.20	0.16	0.20	0.08	0.16
Point 231	0.358	0.16	0.20	0.16	0.20	0.20	0.20	0.16	0.16	0.20	0.20
Point 232	0.360	0.20	0.24	0.16	0.20	0.16	0.20	0.20	0.24	0.12	0.16
Point 233	0.362	0.20	0.24	0.20	0.24	0.16	0.20	0.16	0.24	0.16	0.20
Point 234	0.364	0.20	0.24	0.12	0.20	0.16	0.20	0.16	0.24	0.16	0.20
Point 235	0.366	0.16	0.20	0.16	0.20	0.16	0.20	0.16	0.20	0.12	0.20
Point 236	0.368	0.16	0.20	0.16	0.20	0.16	0.20	0.16	0.20	0.12	0.16
Point 237	0.370	0.16	0.24	0.16	0.20	0.16	0.20	0.16	0.24	0.12	0.16
Point 238	0.372	0.20	0.20	0.12	0.16	0.16	0.16	0.16	0.20	0.16	0.20
Point 239	0.374	0.16	0.20	0.20	0.24	0.12	0.20	0.20	0.24	0.12	0.16
Point 240	0.376	0.16	0.20	0.12	0.16	0.12	0.16	0.20	0.20	0.16	0.20
Point 241	0.378	0.20	0.24	0.12	0.16	0.16	0.20	0.20	0.24	0.16	0.20
Point 242	0.380	0.16	0.20	0.16	0.20	0.16	0.20	0.20	0.24	0.16	0.20
Point 243	0.382	0.16	0.20	0.16	0.20	0.16	0.20	0.16	0.20	0.16	0.20
Point 244	0.384	0.20	0.24	0.16	0.24	0.16	0.20	0.16	0.20	0.16	0.20
Point 245	0.386	0.16	0.16	0.16	0.20	0.16	0.20	0.20	0.24	0.16	0.20
Point 246	0.388	0.16	0.20	0.12	0.16	0.16	0.20	0.16	0.20	0.12	0.16
Point 247	0.390	0.16	0.20	0.16	0.20	0.16	0.20	0.24	0.28	0.16	0.20
Point 248	0.392	0.20	0.24	0.20	0.24	0.16	0.20	0.16	0.24	0.16	0.20
Point 249	0.394	0.20	0.24	0.16	0.20	0.16	0.20	0.20	0.24	0.16	0.20

Original Port 0.050" lift N_2 (cont.)

		Run 1		Run 2		Run 3		Run 4		Run 5	
	Time	V_{high}	V_{low}	V_{high}	V_{low}	V_{high}	V_{low}	V_{high}	V_{low}	V_{high}	V_{low}
Point 250	0.396	0.16	0.20	0.16	0.20	0.16	0.20	0.20	0.24	0.20	0.24
Point 251	0.398	0.16	0.20	0.20	0.24	0.16	0.20	0.20	0.24	0.16	0.20
Point 252	0.400	0.12	0.16	0.16	0.20	0.16	0.24	0.16	0.20	0.16	0.20
Point 253	0.402	0.12	0.16	0.12	0.16	0.16	0.20	0.16	0.20	0.12	0.20
Point 254	0.404	0.12	0.16	0.20	0.20	0.16	0.20	0.20	0.24	0.16	0.20
Point 255	0.406	0.20	0.24	0.16	0.20	0.16	0.20	0.16	0.24	0.16	0.20
Point 256	0.408	0.20	0.24	0.16	0.20	0.16	0.20	0.16	0.24	0.12	0.16
Point 257	0.410	0.20	0.20	0.16	0.16	0.16	0.20	0.16	0.20	0.12	0.16
Point 258	0.412	0.16	0.20	0.20	0.20	0.16	0.16	0.16	0.20	0.16	0.20
Point 259	0.414	0.20	0.24	0.16	0.20	0.16	0.20	0.20	0.24	0.12	0.16
Point 260	0.416	0.16	0.20	0.16	0.20	0.20	0.24	0.16	0.20	0.16	0.20
Point 261	0.418	0.12	0.16	0.20	0.24	0.16	0.20	0.16	0.20	0.12	0.20
Point 262	0.420	0.12	0.16	0.20	0.24	0.16	0.20	0.16	0.20	0.12	0.20
Point 263	0.422	0.16	0.20	0.16	0.20	0.16	0.24	0.20	0.20	0.16	0.20
Point 264	0.424	0.16	0.20	0.16	0.20	0.16	0.20	0.12	0.16	0.12	0.16
Point 265	0.426	0.16	0.20	0.16	0.20	0.16	0.20	0.16	0.20	0.12	0.16
Point 266	0.428	0.16	0.20	0.20	0.24	0.16	0.20	0.16	0.20	0.16	0.20
Point 267	0.430	0.12	0.20	0.20	0.24	0.16	0.20	0.12	0.20	0.16	0.20
Point 268	0.432	0.16	0.20	0.20	0.28	0.16	0.20	0.16	0.20	0.16	0.20
Point 269	0.434	0.16	0.20	0.16	0.24	0.16	0.20	0.16	0.20	0.20	0.24
Point 270	0.436	0.12	0.16	0.20	0.20	0.12	0.20	0.20	0.24	0.12	0.16
Point 271	0.438	0.16	0.20	0.16	0.20	0.16	0.20	0.16	0.20	0.16	0.20
Point 272	0.440	0.16	0.20	0.16	0.20	0.16	0.20	0.16	0.20	0.16	0.24
Point 273	0.442	0.12	0.16	0.16	0.20	0.16	0.20	0.16	0.20	0.12	0.20
Point 274	0.444	0.12	0.16	0.20	0.24	0.16	0.20	0.16	0.20	0.16	0.20
Point 275	0.446	0.12	0.20	0.16	0.20	0.20	0.20	0.16	0.16	0.16	0.20
Point 276	0.448	0.16	0.20	0.12	0.16	0.16	0.20	0.16	0.20	0.16	0.24
Point 277	0.450	0.16	0.20	0.20	0.24	0.12	0.16	0.16	0.20	0.16	0.20
Point 278	0.452	0.16	0.16	0.16	0.20	0.16	0.20	0.20	0.24	0.16	0.20
Point 279	0.454	0.16	0.20	0.20	0.24	0.16	0.20	0.20	0.20	0.12	0.16
Point 280	0.456	0.16	0.20	0.16	0.20	0.16	0.20	0.16	0.20	0.12	0.16
Point 281	0.458	0.20	0.20	0.16	0.20	0.16	0.20	0.16	0.20	0.12	0.20
Point 282	0.460	0.16	0.20	0.16	0.20	0.16	0.20	0.16	0.20	0.16	0.20
Point 283	0.462	0.16	0.20	0.16	0.20	0.12	0.16	0.16	0.20	0.12	0.16
Point 284	0.464	0.16	0.20	0.20	0.20	0.16	0.20	0.24	0.24	0.12	0.20
Point 285	0.466	0.16	0.20	0.12	0.16	0.16	0.20	0.20	0.24	0.16	0.20
Point 286	0.468	0.16	0.20	0.16	0.20	0.12	0.16	0.20	0.24	0.16	0.20
Point 287	0.470	0.16	0.20	0.16	0.20	0.16	0.20	0.20	0.24	0.12	0.16
Point 288	0.472	0.16	0.20	0.16	0.20	0.16	0.20	0.16	0.20	0.16	0.20
Point 289	0.474	0.16	0.20	0.16	0.20	0.16	0.20	0.20	0.24	0.12	0.20
Point 290	0.476	0.16	0.20	0.16	0.20	0.12	0.16	0.16	0.20	0.12	0.16
Point 291	0.478	0.16	0.20	0.16	0.20	0.12	0.16	0.24	0.24	0.12	0.16
Point 292	0.480	0.16	0.20	0.20	0.24	0.16	0.20	0.16	0.20	0.12	0.16
Point 293	0.482	0.16	0.20	0.16	0.20	0.16	0.20	0.20	0.24	0.16	0.20
Point 294	0.484	0.16	0.20	0.16	0.20	0.16	0.16	0.20	0.24	0.20	0.24
Point 295	0.486	0.12	0.16	0.16	0.20	0.16	0.20	0.20	0.24	0.16	0.20
Point 296	0.488	0.08	0.12	0.20	0.24	0.20	0.24	0.16	0.20	0.12	0.16
Point 297	0.490	0.12	0.16	0.16	0.20	0.16	0.20	0.20	0.24	0.20	0.24
Point 298	0.492	0.12	0.16	0.16	0.20	0.16	0.20	0.16	0.20	0.16	0.20
Point 299	0.494	0.16	0.20	0.16	0.24	0.16	0.20	0.16	0.24	0.16	0.20
Point 300	0.496	0.12	0.16	0.20	0.24	0.16	0.20	0.16	0.20	0.12	0.16

Original Port 0.100" lift N_2

		Run 1		Run 2		Run 3		Run 4		Run 5	
	Time	V_{high}	V_{low}	V_{high}	V_{low}	V_{high}	V_{low}	V_{high}	V_{low}	V_{high}	V_{low}
Point 1	-0.102	5.00	5.00	5.00	5.00	5.08	5.08	5.00	5.00	5.00	5.04
Point 2	-0.100	5.00	5.04	5.00	5.04	5.04	5.04	5.04	5.04	5.00	5.04
Point 3	-0.098	5.04	5.04	5.00	5.04	5.04	5.08	5.00	5.00	5.00	5.00
Point 4	-0.096	5.04	5.04	4.96	5.00	5.04	5.08	5.00	5.04	5.00	5.00
Point 5	-0.094	5.00	5.04	5.00	5.00	5.00	5.04	5.00	5.04	5.04	5.04
Point 6	-0.092	5.00	5.04	5.00	5.00	5.04	5.04	5.00	5.04	5.00	5.04
Point 7	-0.090	5.04	5.04	5.00	5.04	5.04	5.08	5.00	5.04	5.00	5.00
Point 8	-0.088	5.04	5.04	5.00	5.04	5.04	5.08	4.96	5.00	5.00	5.04
Point 9	-0.086	5.00	5.04	5.00	5.00	5.08	5.08	5.00	5.04	5.00	5.04
Point 10	-0.084	5.04	5.08	5.00	5.00	5.04	5.04	5.00	5.00	5.04	5.08
Point 11	-0.082	5.00	5.00	5.00	5.04	5.04	5.08	5.00	5.04	5.00	5.00
Point 12	-0.080	4.96	5.00	4.96	5.00	5.00	5.04	5.04	5.04	5.00	5.04
Point 13	-0.078	5.00	5.04	5.00	5.04	5.04	5.04	4.96	5.00	5.00	5.04
Point 14	-0.076	5.00	5.04	5.00	5.00	5.04	5.04	5.00	5.00	5.00	5.04
Point 15	-0.074	5.00	5.00	4.96	4.96	5.00	5.04	4.96	5.00	5.00	5.04
Point 16	-0.072	5.00	5.04	5.00	5.04	5.00	5.04	5.00	5.04	5.00	5.00
Point 17	-0.070	5.04	5.08	4.96	5.00	5.00	5.04	5.00	5.04	5.04	5.04
Point 18	-0.068	5.00	5.04	5.00	5.00	5.04	5.04	5.00	5.00	5.00	5.04
Point 19	-0.066	5.00	5.00	4.96	4.96	5.04	5.04	5.04	5.08	5.00	5.04
Point 20	-0.064	5.00	5.00	4.96	5.00	5.08	5.08	5.00	5.04	5.04	5.04
Point 21	-0.062	5.00	5.04	5.00	5.04	5.04	5.08	5.00	5.00	5.04	5.04
Point 22	-0.060	5.00	5.04	5.00	5.00	5.04	5.04	5.00	5.00	5.00	5.04
Point 23	-0.058	5.04	5.04	4.96	5.00	5.00	5.04	5.00	5.00	5.00	5.04
Point 24	-0.056	5.00	5.04	4.96	5.00	5.00	5.04	4.96	5.00	5.00	5.04
Point 25	-0.054	5.00	5.04	5.00	5.00	5.00	5.04	5.00	5.04	4.96	5.00
Point 26	-0.052	5.00	5.00	5.00	5.00	5.04	5.04	5.00	5.00	5.00	5.04
Point 27	-0.050	5.04	5.08	5.00	5.00	5.04	5.04	5.00	5.00	5.00	5.00
Point 28	-0.048	5.04	5.04	4.96	5.00	5.04	5.08	5.00	5.04	5.00	5.00
Point 29	-0.046	5.00	5.04	5.04	5.04	5.00	5.00	5.00	5.04	5.00	5.04
Point 30	-0.044	5.00	5.04	5.00	5.00	5.04	5.08	5.00	5.00	5.00	5.00
Point 31	-0.042	5.04	5.04	4.96	5.00	5.00	5.04	5.00	5.04	5.00	5.00
Point 32	-0.040	5.00	5.04	5.00	5.00	5.04	5.08	5.04	5.04	5.00	5.04
Point 33	-0.038	5.04	5.08	5.00	5.04	5.04	5.04	4.96	5.00	5.00	5.04
Point 34	-0.036	5.04	5.08	5.00	5.04	5.08	5.08	5.00	5.00	5.00	5.00
Point 35	-0.034	5.04	5.04	4.96	5.00	5.04	5.08	5.00	5.00	5.04	5.04
Point 36	-0.032	5.00	5.04	4.96	5.00	5.04	5.08	4.96	5.00	5.04	5.04
Point 37	-0.030	5.00	5.00	5.00	5.00	5.04	5.08	5.00	5.00	5.00	5.04
Point 38	-0.028	5.00	5.00	5.00	5.00	5.04	5.04	5.00	5.04	5.00	5.04
Point 39	-0.026	5.00	5.00	5.00	5.04	5.08	5.08	5.00	5.04	5.04	5.04
Point 40	-0.024	5.04	5.04	5.00	5.00	5.08	5.08	5.00	5.04	5.00	5.04
Point 41	-0.022	5.00	5.00	5.00	5.00	5.04	5.08	4.96	5.00	5.00	5.04
Point 42	-0.020	5.00	5.04	5.00	5.04	5.04	5.04	5.00	5.00	5.00	5.00
Point 43	-0.018	5.00	5.04	5.00	5.04	5.00	5.04	5.00	5.04	5.00	5.04
Point 44	-0.016	5.00	5.00	5.00	5.00	5.00	5.00	5.00	5.04	5.00	5.04
Point 45	-0.014	4.96	5.00	4.96	5.00	4.96	4.96	4.96	5.00	4.96	5.00
Point 46	-0.012	4.92	4.92	4.96	5.00	4.96	4.96	4.96	4.96	4.96	4.96
Point 47	-0.010	4.92	4.92	4.96	4.96	4.92	4.92	4.92	4.92	4.92	4.96
Point 48	-0.008	4.88	4.88	4.88	4.88	4.88	4.88	4.88	4.88	4.84	4.84
Point 49	-0.006	4.80	4.84	4.80	4.84	4.80	4.84	4.80	4.80	4.80	4.80

Original Port 0.100" lift N_2 (cont.)

		Run 1		Run 2		Run 3		Run 4		Run 5	
	Time	V_{high}	V_{low}	V_{high}	V_{low}	V_{high}	V_{low}	V_{high}	V_{low}	V_{high}	V_{low}
Point 50	-0.004	4.76	4.76	4.72	4.76	4.68	4.72	4.72	4.76	4.72	4.76
Point 51	-0.002	4.56	4.60	4.64	4.68	4.56	4.60	4.60	4.64	4.64	4.72
Point 52	0.000	4.52	4.56	4.48	4.52	4.48	4.52	4.52	4.60	4.52	4.56
Point 53	0.002	4.40	4.44	4.32	4.40	4.32	4.44	4.36	4.44	4.44	4.48
Point 54	0.004	4.28	4.32	4.20	4.28	4.16	4.24	4.24	4.32	4.28	4.36
Point 55	0.006	4.08	4.20	4.00	4.12	4.00	4.12	4.08	4.16	4.12	4.20
Point 56	0.008	3.96	4.04	3.76	3.92	3.80	3.92	3.88	3.96	3.96	4.08
Point 57	0.010	3.84	3.92	3.60	3.72	3.64	3.76	3.68	3.80	3.84	3.92
Point 58	0.012	3.60	3.68	3.36	3.48	3.44	3.56	3.52	3.64	3.64	3.76
Point 59	0.014	3.48	3.56	3.20	3.28	3.32	3.40	3.32	3.44	3.52	3.60
Point 60	0.016	3.28	3.36	3.04	3.12	3.12	3.24	3.16	3.28	3.36	3.48
Point 61	0.018	3.12	3.20	2.88	2.96	2.92	3.04	2.96	3.04	3.16	3.24
Point 62	0.020	2.92	3.00	2.76	2.84	2.76	2.84	2.88	2.92	2.96	3.08
Point 63	0.022	2.84	2.88	2.56	2.64	2.64	2.72	2.68	2.72	2.84	2.92
Point 64	0.024	2.64	2.72	2.44	2.52	2.52	2.56	2.56	2.60	2.68	2.72
Point 65	0.026	2.52	2.56	2.32	2.36	2.36	2.40	2.40	2.44	2.52	2.60
Point 66	0.028	2.36	2.40	2.20	2.28	2.24	2.28	2.24	2.32	2.40	2.44
Point 67	0.030	2.28	2.32	2.12	2.16	2.16	2.16	2.20	2.20	2.32	2.36
Point 68	0.032	2.16	2.16	2.00	2.04	2.04	2.12	2.08	2.12	2.20	2.20
Point 69	0.034	2.08	2.12	1.88	1.92	1.96	1.96	1.96	2.00	2.08	2.12
Point 70	0.036	1.92	1.92	1.84	1.88	1.84	1.88	1.88	1.92	2.00	2.00
Point 71	0.038	1.84	1.88	1.72	1.76	1.76	1.76	1.80	1.80	1.88	1.88
Point 72	0.040	1.72	1.76	1.64	1.64	1.60	1.64	1.72	1.76	1.76	1.80
Point 73	0.042	1.64	1.68	1.56	1.56	1.56	1.60	1.64	1.68	1.68	1.72
Point 74	0.044	1.60	1.64	1.44	1.44	1.48	1.48	1.52	1.56	1.56	1.60
Point 75	0.046	1.48	1.52	1.40	1.40	1.44	1.44	1.48	1.48	1.56	1.56
Point 76	0.048	1.44	1.44	1.32	1.32	1.32	1.32	1.36	1.36	1.44	1.44
Point 77	0.050	1.36	1.36	1.24	1.24	1.28	1.28	1.28	1.28	1.36	1.36
Point 78	0.052	1.32	1.32	1.16	1.20	1.20	1.20	1.24	1.24	1.28	1.32
Point 79	0.054	1.20	1.20	1.08	1.08	1.12	1.12	1.16	1.20	1.20	1.20
Point 80	0.056	1.16	1.16	1.00	1.04	1.08	1.08	1.08	1.12	1.12	1.16
Point 81	0.058	1.08	1.08	1.00	1.00	1.00	1.04	1.00	1.00	1.08	1.12
Point 82	0.060	1.00	1.04	0.92	0.92	0.96	0.96	0.92	0.96	1.00	1.00
Point 83	0.062	0.96	0.96	0.84	0.84	0.88	0.88	0.88	0.88	0.96	0.96
Point 84	0.064	0.88	0.88	0.80	0.80	0.88	0.88	0.84	0.88	0.92	0.92
Point 85	0.066	0.88	0.88	0.80	0.80	0.80	0.84	0.84	0.84	0.88	0.88
Point 86	0.068	0.80	0.80	0.72	0.76	0.76	0.80	0.76	0.76	0.84	0.84
Point 87	0.070	0.72	0.72	0.72	0.76	0.72	0.76	0.72	0.72	0.76	0.80
Point 88	0.072	0.68	0.72	0.68	0.68	0.68	0.72	0.64	0.68	0.72	0.76
Point 89	0.074	0.68	0.72	0.60	0.64	0.68	0.68	0.68	0.68	0.64	0.68
Point 90	0.076	0.64	0.64	0.60	0.64	0.64	0.64	0.60	0.64	0.64	0.68
Point 91	0.078	0.60	0.64	0.56	0.56	0.56	0.60	0.56	0.56	0.60	0.64
Point 92	0.080	0.56	0.60	0.52	0.56	0.48	0.52	0.56	0.56	0.56	0.60
Point 93	0.082	0.52	0.52	0.48	0.52	0.52	0.52	0.48	0.52	0.52	0.56
Point 94	0.084	0.48	0.52	0.48	0.52	0.44	0.48	0.48	0.52	0.52	0.56
Point 95	0.086	0.48	0.48	0.44	0.48	0.44	0.48	0.44	0.48	0.44	0.52
Point 96	0.088	0.44	0.48	0.40	0.44	0.36	0.40	0.40	0.44	0.44	0.48
Point 97	0.090	0.40	0.40	0.36	0.40	0.40	0.44	0.40	0.40	0.40	0.40
Point 98	0.092	0.40	0.44	0.32	0.36	0.32	0.40	0.36	0.40	0.36	0.40
Point 99	0.094	0.36	0.36	0.32	0.36	0.32	0.36	0.36	0.36	0.36	0.36

Original Port 0.100" lift N_2 (cont.)

		Run 1		Run 2		Run 3		Run 4		Run 5	
	Time	V_{high}	V_{low}	V_{high}	V_{low}	V_{high}	V_{low}	V_{high}	V_{low}	V_{high}	V_{low}
Point 100	0.096	0.32	0.36	0.28	0.32	0.28	0.32	0.32	0.36	0.32	0.36
Point 101	0.098	0.32	0.36	0.28	0.28	0.32	0.36	0.28	0.32	0.32	0.36
Point 102	0.100	0.32	0.36	0.24	0.28	0.24	0.28	0.24	0.28	0.28	0.32
Point 103	0.102	0.24	0.28	0.20	0.24	0.24	0.28	0.24	0.28	0.28	0.28
Point 104	0.104	0.24	0.28	0.24	0.28	0.24	0.28	0.24	0.28	0.24	0.28
Point 105	0.106	0.20	0.24	0.20	0.24	0.20	0.24	0.20	0.24	0.20	0.24
Point 106	0.108	0.24	0.28	0.24	0.28	0.20	0.24	0.24	0.28	0.20	0.24
Point 107	0.110	0.20	0.24	0.20	0.24	0.20	0.24	0.20	0.24	0.24	0.24
Point 108	0.112	0.20	0.24	0.16	0.20	0.20	0.24	0.16	0.20	0.20	0.24
Point 109	0.114	0.20	0.20	0.20	0.24	0.20	0.20	0.20	0.24	0.16	0.20
Point 110	0.116	0.16	0.20	0.16	0.20	0.16	0.24	0.20	0.24	0.16	0.20
Point 111	0.118	0.16	0.20	0.16	0.16	0.20	0.24	0.24	0.28	0.16	0.20
Point 112	0.120	0.20	0.20	0.16	0.20	0.20	0.24	0.20	0.28	0.16	0.20
Point 113	0.122	0.16	0.16	0.16	0.20	0.16	0.20	0.20	0.24	0.12	0.16
Point 114	0.124	0.20	0.24	0.20	0.24	0.20	0.24	0.20	0.24	0.16	0.20
Point 115	0.126	0.16	0.20	0.20	0.24	0.20	0.24	0.20	0.20	0.16	0.20
Point 116	0.128	0.12	0.20	0.16	0.20	0.16	0.20	0.16	0.20	0.16	0.24
Point 117	0.130	0.16	0.20	0.16	0.20	0.16	0.20	0.16	0.20	0.20	0.20
Point 118	0.132	0.20	0.24	0.20	0.24	0.16	0.20	0.20	0.24	0.20	0.24
Point 119	0.134	0.16	0.20	0.16	0.20	0.16	0.24	0.20	0.24	0.16	0.20
Point 120	0.136	0.20	0.20	0.20	0.24	0.20	0.24	0.16	0.20	0.16	0.20
Point 121	0.138	0.24	0.24	0.16	0.20	0.20	0.24	0.20	0.24	0.16	0.20
Point 122	0.140	0.20	0.24	0.16	0.20	0.20	0.24	0.20	0.24	0.16	0.20
Point 123	0.142	0.12	0.20	0.20	0.24	0.20	0.24	0.20	0.20	0.16	0.20
Point 124	0.144	0.20	0.20	0.16	0.20	0.20	0.24	0.20	0.24	0.12	0.16
Point 125	0.146	0.20	0.20	0.20	0.24	0.20	0.20	0.20	0.24	0.16	0.20
Point 126	0.148	0.20	0.20	0.20	0.20	0.20	0.24	0.20	0.24	0.20	0.24
Point 127	0.150	0.20	0.24	0.16	0.16	0.20	0.24	0.16	0.20	0.20	0.24
Point 128	0.152	0.20	0.24	0.20	0.24	0.20	0.24	0.16	0.20	0.20	0.20
Point 129	0.154	0.20	0.20	0.20	0.20	0.20	0.24	0.20	0.24	0.20	0.24
Point 130	0.156	0.20	0.28	0.20	0.20	0.20	0.24	0.20	0.24	0.16	0.20
Point 131	0.158	0.20	0.24	0.20	0.24	0.20	0.24	0.16	0.24	0.20	0.24
Point 132	0.160	0.20	0.24	0.16	0.20	0.20	0.24	0.20	0.24	0.20	0.24
Point 133	0.162	0.16	0.24	0.20	0.20	0.16	0.20	0.20	0.24	0.20	0.20
Point 134	0.164	0.16	0.20	0.20	0.24	0.20	0.24	0.16	0.20	0.16	0.20
Point 135	0.166	0.20	0.20	0.20	0.24	0.20	0.24	0.16	0.20	0.16	0.20
Point 136	0.168	0.16	0.20	0.16	0.20	0.20	0.24	0.16	0.16	0.20	0.24
Point 137	0.170	0.20	0.20	0.20	0.20	0.20	0.28	0.20	0.24	0.20	0.24
Point 138	0.172	0.16	0.20	0.20	0.24	0.20	0.20	0.16	0.20	0.16	0.20
Point 139	0.174	0.16	0.20	0.20	0.24	0.20	0.24	0.16	0.24	0.16	0.20
Point 140	0.176	0.20	0.20	0.20	0.24	0.20	0.24	0.20	0.24	0.20	0.24
Point 141	0.178	0.16	0.24	0.16	0.20	0.16	0.20	0.20	0.24	0.12	0.20
Point 142	0.180	0.20	0.24	0.20	0.24	0.16	0.20	0.16	0.20	0.16	0.20
Point 143	0.182	0.16	0.20	0.20	0.24	0.20	0.24	0.16	0.24	0.20	0.24
Point 144	0.184	0.20	0.24	0.20	0.24	0.20	0.24	0.12	0.20	0.16	0.20
Point 145	0.186	0.16	0.20	0.20	0.20	0.12	0.16	0.16	0.20	0.20	0.24
Point 146	0.188	0.20	0.24	0.20	0.24	0.16	0.20	0.20	0.24	0.16	0.20
Point 147	0.190	0.16	0.20	0.20	0.24	0.16	0.20	0.16	0.24	0.16	0.20
Point 148	0.192	0.20	0.24	0.16	0.20	0.16	0.20	0.20	0.24	0.20	0.24
Point 149	0.194	0.16	0.20	0.16	0.20	0.20	0.24	0.16	0.20	0.16	0.24

Original Port 0.100" lift N_2 (cont.)

		Run 1		Run 2		Run 3		Run 4		Run 5	
	Time	V_{high}	V_{low}	V_{high}	V_{low}	V_{high}	V_{low}	V_{high}	V_{low}	V_{high}	V_{low}
Point 150	0.196	0.16	0.20	0.20	0.20	0.16	0.24	0.20	0.24	0.16	0.20
Point 151	0.198	0.20	0.24	0.20	0.24	0.16	0.20	0.20	0.24	0.16	0.20
Point 152	0.200	0.20	0.20	0.20	0.24	0.16	0.20	0.16	0.20	0.16	0.24
Point 153	0.202	0.16	0.20	0.16	0.20	0.20	0.20	0.16	0.20	0.16	0.20
Point 154	0.204	0.20	0.24	0.16	0.20	0.20	0.20	0.16	0.20	0.16	0.20
Point 155	0.206	0.20	0.24	0.16	0.20	0.20	0.20	0.20	0.24	0.16	0.20
Point 156	0.208	0.20	0.24	0.20	0.24	0.20	0.24	0.16	0.20	0.20	0.24
Point 157	0.210	0.16	0.20	0.20	0.20	0.20	0.24	0.20	0.24	0.20	0.20
Point 158	0.212	0.16	0.20	0.20	0.24	0.20	0.24	0.16	0.20	0.16	0.20
Point 159	0.214	0.16	0.20	0.16	0.20	0.20	0.24	0.20	0.20	0.20	0.24
Point 160	0.216	0.20	0.20	0.16	0.20	0.20	0.24	0.16	0.20	0.16	0.20
Point 161	0.218	0.20	0.24	0.20	0.24	0.20	0.24	0.16	0.20	0.20	0.20
Point 162	0.220	0.16	0.20	0.20	0.24	0.16	0.20	0.16	0.20	0.16	0.20
Point 163	0.222	0.20	0.24	0.20	0.24	0.20	0.20	0.16	0.20	0.16	0.20
Point 164	0.224	0.12	0.16	0.20	0.24	0.20	0.24	0.20	0.20	0.16	0.20
Point 165	0.226	0.20	0.20	0.16	0.24	0.20	0.24	0.20	0.24	0.20	0.20
Point 166	0.228	0.16	0.20	0.20	0.24	0.16	0.20	0.16	0.20	0.20	0.20
Point 167	0.230	0.20	0.24	0.20	0.24	0.16	0.20	0.16	0.20	0.20	0.24
Point 168	0.232	0.16	0.24	0.16	0.20	0.20	0.24	0.20	0.24	0.20	0.20
Point 169	0.234	0.16	0.20	0.20	0.24	0.20	0.24	0.20	0.24	0.16	0.20
Point 170	0.236	0.20	0.24	0.20	0.24	0.20	0.20	0.20	0.24	0.16	0.20
Point 171	0.238	0.16	0.20	0.20	0.24	0.16	0.24	0.20	0.24	0.20	0.24
Point 172	0.240	0.20	0.20	0.24	0.24	0.12	0.12	0.20	0.24	0.20	0.24
Point 173	0.242	0.16	0.20	0.20	0.24	0.20	0.24	0.20	0.24	0.16	0.24
Point 174	0.244	0.20	0.24	0.20	0.20	0.20	0.20	0.16	0.24	0.16	0.20
Point 175	0.246	0.12	0.20	0.16	0.20	0.16	0.20	0.16	0.20	0.20	0.24
Point 176	0.248	0.16	0.20	0.16	0.20	0.20	0.24	0.20	0.24	0.16	0.20
Point 177	0.250	0.16	0.20	0.20	0.24	0.20	0.24	0.20	0.24	0.16	0.20
Point 178	0.252	0.20	0.24	0.16	0.20	0.16	0.20	0.20	0.24	0.16	0.20
Point 179	0.254	0.16	0.20	0.16	0.20	0.16	0.20	0.20	0.24	0.16	0.20
Point 180	0.256	0.16	0.20	0.16	0.20	0.16	0.20	0.20	0.24	0.20	0.20
Point 181	0.258	0.20	0.20	0.16	0.24	0.20	0.24	0.16	0.20	0.20	0.24
Point 182	0.260	0.20	0.24	0.20	0.24	0.20	0.24	0.20	0.20	0.16	0.20
Point 183	0.262	0.16	0.20	0.20	0.24	0.16	0.20	0.20	0.24	0.20	0.24
Point 184	0.264	0.16	0.20	0.20	0.24	0.16	0.20	0.16	0.20	0.20	0.20
Point 185	0.266	0.20	0.24	0.16	0.20	0.20	0.24	0.20	0.20	0.20	0.24
Point 186	0.268	0.16	0.20	0.16	0.20	0.16	0.20	0.16	0.20	0.20	0.24
Point 187	0.270	0.16	0.20	0.16	0.20	0.20	0.24	0.20	0.24	0.16	0.20
Point 188	0.272	0.16	0.24	0.16	0.20	0.20	0.24	0.16	0.20	0.16	0.20
Point 189	0.274	0.20	0.24	0.16	0.24	0.16	0.20	0.16	0.20	0.20	0.24
Point 190	0.276	0.16	0.20	0.20	0.20	0.16	0.20	0.16	0.24	0.16	0.20
Point 191	0.278	0.16	0.20	0.20	0.24	0.20	0.24	0.20	0.24	0.16	0.24
Point 192	0.280	0.16	0.24	0.16	0.20	0.20	0.24	0.20	0.24	0.16	0.20
Point 193	0.282	0.20	0.24	0.20	0.24	0.20	0.20	0.16	0.20	0.16	0.20
Point 194	0.284	0.16	0.20	0.16	0.20	0.16	0.20	0.20	0.20	0.12	0.16
Point 195	0.286	0.20	0.24	0.20	0.24	0.20	0.24	0.20	0.24	0.16	0.20
Point 196	0.288	0.16	0.20	0.20	0.24	0.20	0.24	0.20	0.24	0.16	0.20
Point 197	0.290	0.20	0.24	0.24	0.28	0.20	0.20	0.20	0.28	0.16	0.20
Point 198	0.292	0.20	0.24	0.20	0.24	0.16	0.24	0.20	0.24	0.16	0.24
Point 199	0.294	0.16	0.20	0.20	0.24	0.16	0.20	0.20	0.24	0.16	0.20

Original Port 0.100" lift N_2 (cont.)

		Run 1		Run 2		Run 3		Run 4		Run 5	
	Time	V_{high}	V_{low}	V_{high}	V_{low}	V_{high}	V_{low}	V_{high}	V_{low}	V_{high}	V_{low}
Point 200	0.296	0.20	0.20	0.20	0.24	0.16	0.20	0.20	0.24	0.16	0.20
Point 201	0.298	0.20	0.24	0.20	0.24	0.16	0.20	0.16	0.24	0.16	0.24
Point 202	0.300	0.20	0.24	0.20	0.28	0.16	0.20	0.20	0.24	0.16	0.20
Point 203	0.302	0.16	0.20	0.20	0.24	0.16	0.20	0.20	0.24	0.16	0.20
Point 204	0.304	0.16	0.24	0.20	0.24	0.20	0.24	0.20	0.24	0.16	0.20
Point 205	0.306	0.20	0.24	0.20	0.24	0.20	0.20	0.16	0.20	0.16	0.20
Point 206	0.308	0.16	0.20	0.16	0.20	0.16	0.20	0.16	0.20	0.20	0.24
Point 207	0.310	0.16	0.20	0.16	0.20	0.16	0.20	0.20	0.24	0.16	0.20
Point 208	0.312	0.20	0.24	0.16	0.20	0.20	0.24	0.20	0.24	0.16	0.20
Point 209	0.314	0.20	0.24	0.16	0.24	0.20	0.24	0.16	0.24	0.16	0.20
Point 210	0.316	0.16	0.20	0.16	0.20	0.20	0.24	0.20	0.24	0.16	0.20
Point 211	0.318	0.16	0.20	0.20	0.24	0.20	0.24	0.20	0.24	0.16	0.20
Point 212	0.320	0.20	0.20	0.20	0.24	0.16	0.24	0.20	0.24	0.16	0.20
Point 213	0.322	0.20	0.20	0.16	0.20	0.20	0.24	0.16	0.24	0.16	0.24
Point 214	0.324	0.20	0.24	0.16	0.20	0.20	0.24	0.16	0.20	0.20	0.24
Point 215	0.326	0.16	0.20	0.16	0.20	0.16	0.20	0.20	0.24	0.16	0.20
Point 216	0.328	0.20	0.20	0.20	0.24	0.20	0.24	0.20	0.24	0.20	0.24
Point 217	0.330	0.20	0.20	0.16	0.20	0.16	0.20	0.16	0.20	0.12	0.20
Point 218	0.332	0.16	0.20	0.16	0.20	0.20	0.20	0.16	0.20	0.20	0.24
Point 219	0.334	0.20	0.24	0.16	0.20	0.16	0.24	0.20	0.24	0.16	0.20
Point 220	0.336	0.20	0.24	0.20	0.24	0.20	0.24	0.20	0.24	0.16	0.20
Point 221	0.338	0.20	0.24	0.20	0.20	0.16	0.20	0.16	0.20	0.20	0.24
Point 222	0.340	0.16	0.20	0.20	0.24	0.16	0.20	0.16	0.20	0.20	0.20
Point 223	0.342	0.20	0.24	0.20	0.24	0.20	0.20	0.16	0.20	0.16	0.20
Point 224	0.344	0.20	0.24	0.20	0.24	0.20	0.24	0.20	0.24	0.16	0.20
Point 225	0.346	0.20	0.24	0.20	0.20	0.16	0.20	0.16	0.20	0.12	0.16
Point 226	0.348	0.20	0.24	0.20	0.24	0.20	0.24	0.16	0.20	0.16	0.20
Point 227	0.350	0.20	0.24	0.20	0.24	0.20	0.24	0.20	0.24	0.20	0.24
Point 228	0.352	0.20	0.24	0.20	0.24	0.20	0.24	0.20	0.24	0.20	0.20
Point 229	0.354	0.20	0.24	0.16	0.20	0.20	0.24	0.20	0.24	0.16	0.24
Point 230	0.356	0.20	0.24	0.16	0.20	0.20	0.20	0.20	0.24	0.16	0.20
Point 231	0.358	0.16	0.24	0.20	0.24	0.20	0.24	0.16	0.20	0.16	0.20
Point 232	0.360	0.20	0.24	0.20	0.24	0.20	0.24	0.16	0.20	0.16	0.24
Point 233	0.362	0.16	0.20	0.16	0.24	0.16	0.20	0.16	0.20	0.20	0.20
Point 234	0.364	0.20	0.20	0.16	0.20	0.20	0.28	0.20	0.24	0.16	0.16
Point 235	0.366	0.16	0.20	0.16	0.20	0.20	0.20	0.20	0.24	0.16	0.20
Point 236	0.368	0.20	0.20	0.20	0.24	0.16	0.20	0.20	0.24	0.16	0.24
Point 237	0.370	0.20	0.24	0.16	0.20	0.20	0.24	0.16	0.20	0.16	0.24
Point 238	0.372	0.16	0.20	0.20	0.24	0.20	0.20	0.20	0.24	0.12	0.16
Point 239	0.374	0.20	0.28	0.16	0.20	0.20	0.24	0.20	0.24	0.16	0.20
Point 240	0.376	0.16	0.24	0.16	0.24	0.16	0.20	0.20	0.24	0.16	0.20
Point 241	0.378	0.20	0.24	0.20	0.20	0.20	0.20	0.20	0.20	0.20	0.24
Point 242	0.380	0.16	0.20	0.16	0.20	0.24	0.28	0.20	0.24	0.16	0.20
Point 243	0.382	0.20	0.24	0.16	0.24	0.20	0.20	0.20	0.20	0.20	0.24
Point 244	0.384	0.12	0.20	0.16	0.24	0.16	0.20	0.16	0.20	0.20	0.20
Point 245	0.386	0.16	0.20	0.16	0.20	0.16	0.20	0.16	0.20	0.12	0.20
Point 246	0.388	0.16	0.20	0.16	0.20	0.20	0.24	0.20	0.24	0.20	0.24
Point 247	0.390	0.16	0.20	0.20	0.24	0.20	0.24	0.20	0.24	0.16	0.20
Point 248	0.392	0.20	0.24	0.20	0.24	0.20	0.24	0.20	0.24	0.12	0.16
Point 249	0.394	0.20	0.20	0.16	0.20	0.20	0.20	0.20	0.24	0.20	0.24

Original Port 0.100" lift N_2 (cont.)

		Run 1		Run 2		Run 3		Run 4		Run 5	
	Time	V_{high}	V_{low}	V_{high}	V_{low}	V_{high}	V_{low}	V_{high}	V_{low}	V_{high}	V_{low}
Point 250	0.396	0.20	0.20	0.16	0.20	0.24	0.28	0.20	0.24	0.16	0.20
Point 251	0.398	0.20	0.24	0.20	0.24	0.20	0.24	0.20	0.24	0.16	0.20
Point 252	0.400	0.20	0.24	0.20	0.24	0.16	0.20	0.16	0.20	0.20	0.20
Point 253	0.402	0.20	0.24	0.20	0.24	0.16	0.20	0.20	0.24	0.20	0.20
Point 254	0.404	0.20	0.28	0.20	0.24	0.20	0.20	0.16	0.16	0.12	0.20
Point 255	0.406	0.20	0.24	0.16	0.20	0.20	0.24	0.20	0.24	0.16	0.20
Point 256	0.408	0.20	0.24	0.20	0.24	0.16	0.20	0.20	0.24	0.16	0.20
Point 257	0.410	0.20	0.24	0.16	0.20	0.16	0.24	0.20	0.24	0.16	0.24
Point 258	0.412	0.20	0.28	0.16	0.24	0.20	0.24	0.16	0.24	0.16	0.20
Point 259	0.414	0.20	0.24	0.16	0.20	0.20	0.24	0.16	0.20	0.16	0.20
Point 260	0.416	0.20	0.24	0.20	0.24	0.20	0.24	0.20	0.20	0.16	0.20
Point 261	0.418	0.16	0.24	0.16	0.20	0.16	0.20	0.16	0.20	0.20	0.24
Point 262	0.420	0.16	0.20	0.20	0.24	0.20	0.24	0.16	0.20	0.16	0.20
Point 263	0.422	0.20	0.24	0.16	0.20	0.20	0.24	0.16	0.20	0.16	0.20
Point 264	0.424	0.16	0.20	0.20	0.24	0.20	0.24	0.16	0.20	0.16	0.16
Point 265	0.426	0.16	0.24	0.16	0.24	0.20	0.20	0.16	0.20	0.20	0.24
Point 266	0.428	0.20	0.20	0.20	0.24	0.20	0.24	0.20	0.24	0.16	0.24
Point 267	0.430	0.20	0.24	0.20	0.24	0.20	0.24	0.20	0.24	0.16	0.20
Point 268	0.432	0.20	0.24	0.16	0.20	0.20	0.24	0.20	0.24	0.16	0.20
Point 269	0.434	0.16	0.20	0.16	0.20	0.16	0.20	0.16	0.20	0.16	0.24
Point 270	0.436	0.20	0.24	0.20	0.24	0.20	0.24	0.16	0.20	0.16	0.24
Point 271	0.438	0.16	0.20	0.20	0.24	0.20	0.24	0.20	0.28	0.16	0.20
Point 272	0.440	0.16	0.20	0.16	0.20	0.20	0.24	0.20	0.24	0.20	0.24
Point 273	0.442	0.20	0.28	0.20	0.20	0.16	0.20	0.20	0.24	0.20	0.24
Point 274	0.444	0.16	0.20	0.20	0.24	0.16	0.24	0.20	0.20	0.16	0.20
Point 275	0.446	0.20	0.24	0.20	0.24	0.20	0.24	0.20	0.24	0.16	0.20
Point 276	0.448	0.20	0.24	0.16	0.20	0.20	0.24	0.20	0.24	0.16	0.20
Point 277	0.450	0.20	0.24	0.24	0.28	0.16	0.20	0.20	0.24	0.20	0.24
Point 278	0.452	0.16	0.20	0.20	0.24	0.16	0.24	0.20	0.20	0.16	0.20
Point 279	0.454	0.20	0.24	0.16	0.20	0.20	0.24	0.20	0.24	0.16	0.20
Point 280	0.456	0.20	0.24	0.16	0.20	0.16	0.20	0.20	0.24	0.16	0.20
Point 281	0.458	0.20	0.24	0.20	0.24	0.20	0.24	0.20	0.24	0.16	0.24
Point 282	0.460	0.20	0.24	0.20	0.24	0.16	0.24	0.20	0.24	0.16	0.20
Point 283	0.462	0.20	0.24	0.20	0.24	0.20	0.24	0.16	0.20	0.20	0.24
Point 284	0.464	0.20	0.24	0.20	0.24	0.20	0.20	0.20	0.20	0.16	0.20
Point 285	0.466	0.16	0.20	0.16	0.24	0.20	0.24	0.20	0.24	0.16	0.20
Point 286	0.468	0.16	0.20	0.20	0.20	0.20	0.20	0.16	0.16	0.16	0.20
Point 287	0.470	0.20	0.24	0.20	0.24	0.20	0.28	0.16	0.24	0.16	0.20
Point 288	0.472	0.24	0.28	0.16	0.20	0.20	0.24	0.20	0.24	0.16	0.16
Point 289	0.474	0.20	0.24	0.20	0.20	0.20	0.24	0.20	0.24	0.16	0.20
Point 290	0.476	0.16	0.20	0.20	0.24	0.20	0.24	0.20	0.24	0.16	0.20
Point 291	0.478	0.20	0.24	0.20	0.24	0.20	0.24	0.16	0.20	0.20	0.24
Point 292	0.480	0.20	0.20	0.20	0.24	0.20	0.24	0.16	0.20	0.20	0.20
Point 293	0.482	0.16	0.20	0.20	0.24	0.20	0.24	0.16	0.20	0.12	0.16
Point 294	0.484	0.20	0.24	0.20	0.24	0.20	0.20	0.16	0.20	0.20	0.24
Point 295	0.486	0.20	0.24	0.20	0.24	0.16	0.20	0.16	0.20	0.16	0.20
Point 296	0.488	0.20	0.24	0.16	0.20	0.20	0.24	0.20	0.24	0.16	0.24
Point 297	0.490	0.16	0.20	0.16	0.24	0.20	0.24	0.16	0.20	0.16	0.20
Point 298	0.492	0.16	0.20	0.20	0.24	0.20	0.24	0.16	0.20	0.16	0.20
Point 299	0.494	0.20	0.24	0.20	0.24	0.16	0.24	0.20	0.24	0.16	0.20
Point 300	0.496	0.16	0.20	0.20	0.24	0.16	0.20	0.16	0.20	0.20	0.24